Natural Product Reports

ROYAL SOCIETY OF CHEMISTRY

REVIEW

View Article Online
View Journal

Published on 09 September 2022. Downloaded by Shanghai Jiaotong University on 10/24/2022 5:38:16 AM.

Check for updates

Cite this: DOI: 10.1039/d2np00046f

Chemistry and biosynthesis of bacterial polycyclic xanthone natural products

Lingxin Kong, Zixin Deng and Delin You *

Covering: up to the end of 2021

Bacterial polycyclic xanthone natural products (BPXNPs) are a growing family of natural xanthones featuring a pentangular architecture with various modifications to the tricyclic xanthone chromophore. Their structural diversities and various activities have fueled biosynthetic and chemical synthetic studies. Moreover, their more potent activities than the clinically used drugs make them potential candidates for the treatment of diseases. Future unraveling of structure activity relationships (SARs) will provide new options for the (bio)-synthesis of drug analogues with higher activities. This review summarizes the isolation, structural elucidation and biological activities and more importantly, the recent strategies for the microbial biosynthesis and chemical synthesis of BPXNPs. Regarding their biosynthesis, we discuss the recent progress in enzymes that synthesize tricyclic xanthone, the protein candidates for structural moieties (methylene dioxygen bridge and nitrogen heterocycle), tailoring enzymes for methylation and halogenation. The chemical synthesis part summarizes the recent methodology for the division synthesis and coupling construction of achiral molecular skeletons. Ultimately, perspectives on the biosynthetic study of BPXNPs are discussed.

Received 3rd July 2022

DOI: 10.1039/d2np00046f

rsc.li/npr

State Key Laboratory of Microbial Metabolism, Joint International Research Laboratory of Metabolic and Developmental Sciences, School of Life Sciences & Biotechnology, Shanghai Jiao Tong University, Shanghai 200240, China. E-mail: dlyou@sjtu.edu.cn; Tel: +86 21 62933765

1. Introduction

The term xanthone refers to the tricyclic 9*H*-xanthen-9-one or dibenzo-γ-pyrone[1] heterocycle skeleton (Fig. 1), which is found in natural products isolated from higher plants, fungi, lichens, and bacteria.[2] Xanthones are typically poly-substituted and occur in various forms such as fully aromatic xanthone (**1**, Fig. 1), dihydroxanthone (**2**, Fig. 1), tetrahydroxanthone (**3** and **4**, Fig. 1), and the relatively rare hexahydroxanthones.[2] Xanthones are described as "privileged" structures because of their pronounced biological activities in a very broad spectrum of disease states, owing to their interactions with the

Published on 09 September 2022. Downloaded by Shanghai Jiaotong University on 10/24/2022 5:38:16 AM.

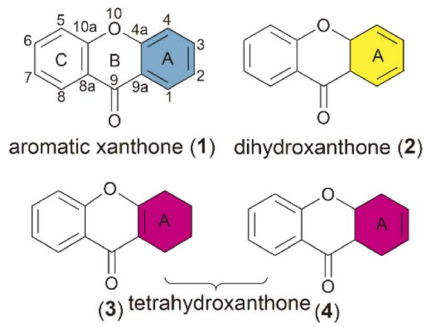

Fig. 1 Structure of xanthones.

corresponding diverse target biomolecules.[2,3] The biological activities of these compounds are associated with the xanthone nucleus, but vary depending on the nature and/or the position of the substituents on the aromatic ring.[1]

Xanthones as a unique moiety are present in numerous natural products and functional molecules. Among them, bacterial polycyclic xanthone natural products (BPXNPs) are considered an important subfamily of natural compounds characterized by a planar fused hexacyclic highly oxygenated skeleton with the xanthone structure.[4] Most of them were isolated from *Actinomycetes*, a group of Gram-positive bacteria known as important secondary metabolite-producing strains. To date, more than 70 members of BPXNPs have been found, which are a subgroup of polyketides assembled by type II polyketide synthases (PKSs) (Fig. 2), according to previous feeding experiments with isotope-labeled precursors[5–8] and current biosynthetic studies.[4] The great interest that BPXNPs have elicited from the scientific community can be explained by their attractive molecular architectures, in conjunction with their wide and various biological activities, including antibacterial (mainly Gram-positive bacteria), antifungal (*e.g.*, yeasts and dermatophytes), antimalarial, antimycoplasmal, anticoccidial, anticancer and cytotoxic activities (*e.g.*, HeLa cells).[2,9]

Some general reviews on xanthones can be found in the recent literature; however, only a few mentioned limited types of BPXNPs,[2,9–12] and no systematic collections and classifications have been performed to date. In this review, we systematically summarize the bacterial-originating BPXNPs, exploring their structural diversities and various biological activities and introducing the pharmacological interest in their cytotoxic and antitumor activities through related structure–activity research. In particular, we discuss the *in vivo* biosynthetic machinery, focusing on the recent important findings on the enzymatic construction of important structural moieties. Finally, we briefly discuss the representative chemical synthesis of BPXNPs.

2. Structural diversity

As is illustrated in Fig. 1, four types of tricyclic xanthones have been found in BPXNPs. To date, about 60% of BPXNPs contain fully aromatic xanthone (**1**), 40% contain tetrahydroxanthone (**3** or **4**) and only one compound carries dihydroxanthone (**2**). Alternatively, no BPXNPs with hexahydroxanthone have been found to date. The difference in the tricyclic xanthone structure

Dr. Lingxin Kong received her PhD in 2016 from Shanghai Jiao Tong University, and then started her postdoctoral fellowship until 2020. Currently, she is working in Shanghai Jiao Tong University as an Assistant Researcher in Prof. You*'s lab. Her interest lies in the biosynthesis of polycyclic xanthones and conducting in-depth investigation on the enzymatic mechanism and molecular machinery of xantholipin biosynthesis.*

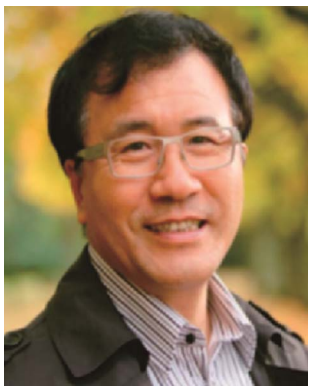

Prof. Zixin Deng received his PhD in Microbial Genetics from the University of East Anglia (1987) while working in the Streptomyces *group at the John Innes Centre. He is the Dean of the School of Life Sciences and Biotechnology, Shanghai Jiao Tong University and School of Pharmaceutical Sciences, Wuhan University and is a Member of the Chinese Academy of Sciences, Fellow of the American Academy of Microbiology, and Fellow of The Royal Society of Chemistry. His research interests center around synthetic biology,* Streptomyces *genetics, biochemistry and molecular biology of antibiotic biosynthesis, and phosphorothiolation of DNA.*

Prof. Delin You received his PhD in 2001 from Jilin University. After a two-year Postdoctoral Fellowship at Peking University, he began his research career at Shanghai Jiao Tong University in 2003. From 2010 to 2011, he worked with Prof. Peter C. Dedon as a Research Scientist at the Massachusetts Institute of Technology. His research interests center around the biosynthesis of natural products (including xantholipin, piericidin, chlortetracycline, tetramycin, echinomycin and anisomycin) and phosphorothioate modifications of DNA.

This journal is © The Royal Society of Chemistry 2022

Published on 09 September 2022. Downloaded by Shanghai Jiaotong University on 10/24/2022 5:38:16 AM.

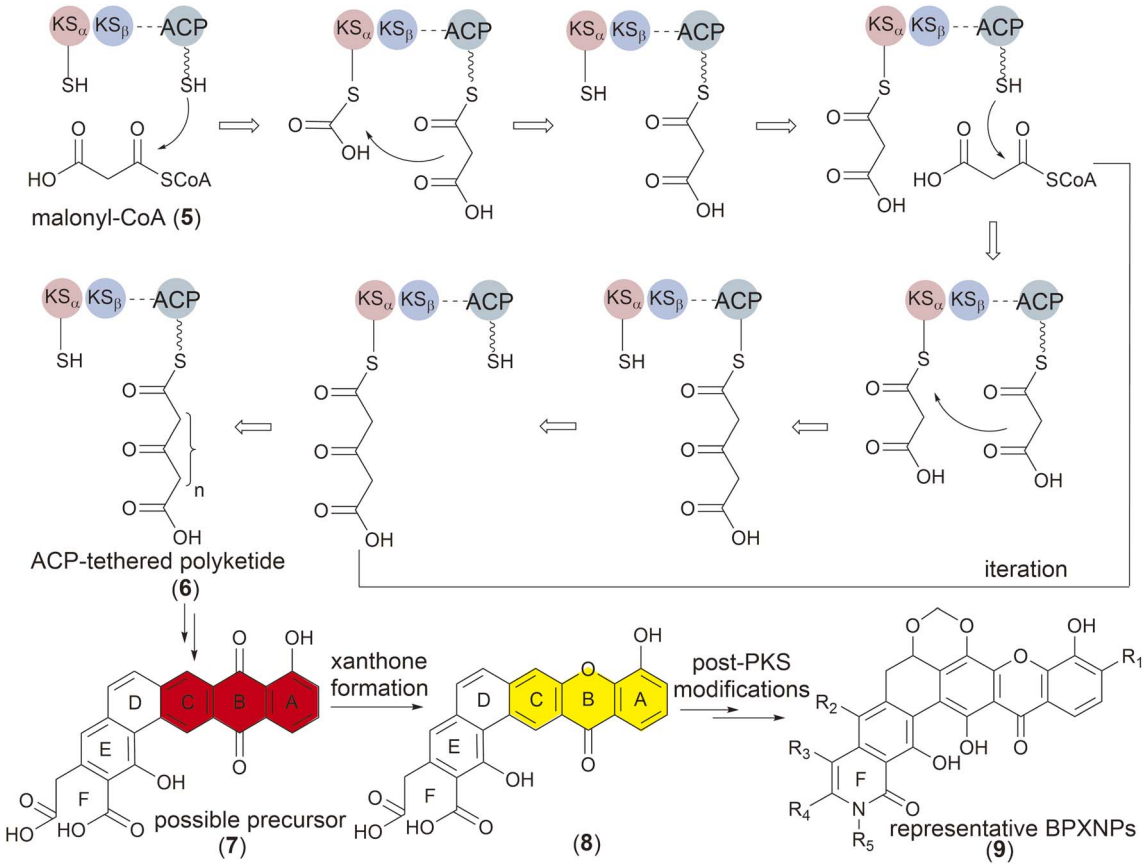

Fig. 2 Schematic biosynthetic machinery of BPXNPs.

may result from varying degrees of redox reactions during the biosynthesis of BPXNPs. Considering the structural diversity of BPXNPs, they cannot be classified only based on structure of ring A within tricyclic xanthone. In this review, we classify BPXNPs according to their core skeleton structures (ring A–G) and post modifications (glycosylation, acylation and halogenation). These compounds with different ring systems are presented in Table 1, including their classification, compound name, source organisms and related references.

During the screening of BPXNPs, physical methods including thin-layer chromatography (TLC), infrared absorption spectroscopy (IR), and ultraviolet-visible absorption spectroscopy (UV-Vis) have been employed for the primary identification of the polycyclic xanthone skeleton. BPXNPs exhibit a characteristic absorption profile in the range of 210–600 nm (Table 2). Also, other technologies used for the molecular structure and absolute configuration determinations of BPXNPs are included.[9]

2.1 BPXNPs with tetrahydrobenzene ring A

Kibdelones A–C (**10–12**, Fig. 3)[13] and their corresponding oxidized analogues, including 13-oxokibdelone A (**13**), 25-hydroxy-24-oxokibdelone C (**14**) and 25-methoxy-24-oxokibdelone C (**15**), respectively, represent BPXNPs containing tetrahydrobenzene ring A (Fig. 3). Among them, the different oxidation states of ring E, the hydroxylation at C25 and the chlorination or carbonyl at C24 (Fig. 3) may result from selective redox modifications during biosynthesis.

2.2 BPXNPs with (hydro)-quinone ring C

Among the hexacyclic skeletons, diverse BPXNPs exist based on their ring oxidation state. One example is the structural diversity among cervinomycins (**16–25**, Fig. 4). Cervinomycins A1 (**16**) and A2 (**17**)[15–17] share the same polycyclic skeleton but differ in ring C (Fig. 4). Ring C in **16** is hydroquinone *versus* the oxidized benzoquinone in **17**. This phenomenon can be found between cervinomycin B_1 (**18**) and B_2 (**20**),[18] cervinomycin B_3 (**19**) and B_4 (**21**),[18] cervinomycin C_1 (**22**) and C_2 (**24**),[19] and cervinomycin C_3 (**23**) and C_4 (**25**)[19] (Fig. 4). Moreover, cervinomycins also differ in nitrogen-containing heterocyclic ring F and oxazolidine ring G. This structural diversity can be attributed to the diverse activities of biosynthetic enzymes *in vivo*.

2.3 BPXNPs with different coupling types of ring D

As can be seen in Fig. 1, rings A, B and C are comprised of a tricyclic xanthone nucleus. In the majority of BPXNPs (such as kibdelones (**10–12**, Fig. 3)), ring D couples with xanthone to form benzoxanthone, resulting in the folding of their molecular skeleton in the "4 + 2" or "4 + 3" type. However, in isokibdelones A–C (**26–28**, Fig. 5)[14] and citreamicins θ A and B (**30** and **31**, Fig. 5),[20] respectively, the coupling of ring D is different from

Published on 09 September 2022. Downloaded by Shanghai Jiaotong University on 10/24/2022 5:38:16 AM.

Table 1 BPXNPs isolated from bacteria

Classification	Entries	Compound names	Isolation source	Methods	Ref.
BPXNPs with tetrahydrobenzene ring A	1	Kibdelone A–C and analogues	*Actinomycetes Kibdelosporangium* sp. MST-108-465	UV, MS, NMR, CD	13 and 14
BPXNPs with (hydro)-quinone ring C	1	Cervinomycin A1, A2	*Streptomyces cervinus* strain AM-5344	TLC, UV, NMR, IR, MS	15–17
	2	Cervinomycin B_{1-4}	*Streptomyces* CPCC 204980	UV, MS, NMR	18
	3	Cervinomycin C_{1-4}		UV, MS, NMR	19
BPXNPs with different coupling type of ring D	1	Isokibdelone A–C	*Actinomycetes Kibdelosporangium* sp. MST-108-465	UV, MS, NMR, CD	13 and 14
	2	Citreamicin θ A and θ B	*Streptomyces caelestis*	UV, MS, NMR, CD, SCXRD	20
BPXNPs with heterocyclic lactam ring F	1	Sch56036	*Actinoplanes* sp. SCC 2314	UV, IR, MS, NMR	21
	2	Xantholipin	*Streptomyces flavogriseus* SIIA-A02191	MS, IR, NMR	22
	3	MDN-0185	*Micromonospora* sp. CA-256353	UV, MS, IR, NMR	23
	4	Ukixanthomycin A	*Streptomyces* sp. HGMA004	UV, MS, NMR	24
	5	Sattahipmycin	*Streptomyces* sp. GKU 257-1	UV, IR, MS, NMR	25
BPXNPs with heterocyclic oxazolidine ring G	1	Arixanthomycin A–C	Uncultured bacteria	UV, MS, NMR	26
	2	Kigamicin A–E	*Amycolatopsis* sp. ML630-mF1	UV, IR, MS, NMR	27 and 28
	3	Citreamicin α, β, γ, η, ζ	*Micromonospora citrea*	UV, IR, MS, NMR	29
	4	Citreamicin εA, εB	*Streptomyces caelestis* AW9-9C	UV, MS, NMR, SCXRD	30
BPXNPs with methylene dioxygen bridge ring H	1	Xantholipin B	*Streptomyces flocculus* WJN-1	MS, UV, NMR	31
	2	Sch42137	*Actinoplanes* sp. SCC1906	TLC, CD, UV, IR, MS, NMR	32
	3	CBS40	Genetic DNA heterologous expression in *Streptomyces albus*	MS, NMR	33
	4	Simaomicin α, β	*Actinomadura madurae* ssp. simaoensis	UV, NMR, MS, SCXRD	34
	5	Actinoplanone A–G	*Actinoplanes actinoplanaceae* sp. R-304	TLC, UV, IR, NMR, CD, MS	35 and 36
Glycosylated BPXNPs	1	Neocitreamicin I, II	*Micromonospora citrea*	UV, MS, NMR	37
	2	IB-00208	*Actinomadura* sp. BL-42-PO13-046 strain CECT-5318	UV, IR, TLC, MS, NMR	38
	3	FD-594	*Streptomyces* sp. TA-0256	TLC, UV, IR, MS, NMR, SCXRD	8
	4	BE-13793X	*Streptomyces tanasiensis* 3007-H1	MS, NMR	39
	5	MS901809	*Streptomyces* sp. Y-90	MS, NMR	40
	6	Calixanthomycin A	eDNA heterologous expression in *Streptomyces albus*	MS, IR, NMR	41
Acylated BPXNPs	1	Turbinmicin	*Micromonospora* sp. WMMC-415	MS, NMR, SCXRD	42
	2	Actinomadurone	*Actinomadura* sp. BCC 35430	MS, NMR, CD, IR	43
Halogenated BPXNPs	1	(Chloro)-/albofungin	*Actinomyces albus* var. fungatus	UV, MS, CD, NMR	44 and 45
			Streptomyces chrestomyceticus BCC24770	UV, IR, NMR, MS, SCXRD	46 and 47
	2	Sch54445	*Actinoplanes* sp. SCC 2314	CD, UV, IR, MS, NMR	48
	3	Lysolipin X, I	*Streptomyces violaceoniger* strain Tü 96 and *S. tendae* Tü 4042	UV, IR, CD, NMR, MS, SCXRD	49–52

This journal is © The Royal Society of Chemistry 2022

Published on 09 September 2022. Downloaded by Shanghai Jiaotong University on 10/24/2022 5:38:16 AM.

Table 2 Characteristic HR-ESI-MS data and UV-Vis absorption of the known BPXNPs

Classification	Entries	Compound names	Molecular formula	HR-ESI-MS	λ_{max} (nm)	Ref.
BPXNPs with tetrahydrobenzene ring A	1	Kibdelone A	$C_{29}H_{24}ClNO_{10}$	604.0996 $[M + Na]^+$	214, 254, 311, 420, 447	13
	2	Kibdelone B	$C_{29}H_{26}ClNO_{10}$	606.1128 $[M + Na]^+$	208, 258, 308, 402, 444	13
	3	Kibdelone C	$C_{29}H_{28}ClNO_{10}$	608.1259 $[M + Na]^+$	217, 272, 308, 339, 396	13
BPXNPs with (hydro)-quinone ring C	1	Cervinomycin A1	$C_{29}H_{23}NO_9$	529.135 $[M + H]^+$	303, 376, 385	15
	2	Cervinomycin A2	$C_{29}H_{21}NO_9$	527.124 $[M + H]^+$	260, 329, 375, 420	15
	3	Cervinomycin B_1	$C_{29}H_{25}NO_9$	532.1596 $[M + H]^+$	240, 299, 326, 389	18
	4	Cervinomycin B_2	$C_{29}H_{23}NO_9$	530.1441 $[M + H]^+$	232, 298, 324, 411	18
	5	Cervinomycin B_3	$C_{28}H_{23}NO_9$	518.1447 $[M + H]^+$	240, 299, 325, 401	18
	6	Cervinomycin B_4	$C_{28}H_{21}NO_9$	516.1290 $[M + H]^+$	232, 298, 324, 421	18
	7	Cervinomycin C_1	$C_{28}H_{24}NO_9$	518.1443 $[M + H]^+$	241, 283, 323, 370	19
	8	Cervinomycin C_2	$C_{28}H_{22}NO_9$	516.1280 $[M + H]^+$	241, 314, 502	19
	9	Cervinomycin C_3	$C_{26}H_{20}NO_8$	474.1192 $[M + H]^+$	240, 282, 320, 368	19
	10	Cervinomycin C_4	$C_{26}H_{18}NO_8$	472.1035 $[M + H]^+$	240, 290, 502	19
BPXNPs with different coupling type of ring D	1	Isokibdelone A	$C_{29}H_{24}ClNO_{10}$	604.0986 $[M + Na]^+$	239, 271, 319, 404, 442	14
	2	Isokibdelone B	$C_{29}H_{26}ClNO_{10}$	606.1143 $[M + Na]^+$	203, 244, 266, 326, 447, 583	14
	3	Isokibdelone A rhamnoside	$C_{35}H_{34}ClNO_{14}Na$	750.1569 $[M + Na]^+$	210, 229, 271, 410, 442	14
	4	Citreamicin θ A	$C_{30}H_{25}NO_{11}$	576.1508 $[M + H]^+$	237, 278, 323, 441	20
	5	Citreamicin θ B	$C_{30}H_{25}NO_{11}$	576.1500 $[M + H]^+$	237, 278, 323, 441	20
BPXNPs with heterocyclic lactam ring F	1	Albofungin	$C_{27}H_{24}N_2O_9$	520 $[M]^+$	228, 240, 255, 305, 375	44,53
	2	Chloroalbofungin	$C_{27}H_{23}ClN_2O_9$	554 $[M]^+$	231, 250, 300, 337, 360	53
	3	Sch5445	$C_{30}H_{29}N_2O_9Cl$	597.1609 $[M + H]^+$	215, 251, 270, 326, 393	48
	4	Lysolipin I	$C_{29}H_{24}ClNO_{11}$	598.2024 $[M + H]^+$	273, 310, 349, 408	51
	5	Sch56036	$C_{30}H_{31}NO_8$	534.2102 $[M + H]^+$	260, 290, 315, 354, 365	21
	6	Xantholipin	$C_{27}H_{18}ClNO_{10}$	552.0549 $[M + H]^+$	240, 274, 310, 388	54
	7	MDN-0185	$C_{26}H_{22}NO_{10}$	508.1243 $[M + H]^+$	220, 270, 380	23
	8	Sattahipmycin	$C_{26}H_{20}NO_8$	474.1180 $[M + H]^+$	212, 256, 324, 353, 369, 410	25
	9	Ukixanthomycin A	$C_{29}H_{23}NO_{11}$	562.1351 $[M + H]^+$	260, 304, 330, 356, 372, 438	24
BPXNPs with heterocyclic oxazolidine ring G	1	Arixanthomycin A	$C_{37}H_{38}NO_{14}$	720.2300 $[M + H]^+$	287, 327, 346, 403	26
	2	Arixanthomycin B	$C_{29}H_{24}NO_{10}$	546.1379 $[M + H]^+$	285, 331, 399	26
	3	Arixanthomycin C	$C_{28}H_{22}NO_{10}$	532.1246 $[M + H]^+$	287, 324, 347, 399	26
	4	Kigamicin A	$C_{34}H_{35}NO_{13}$	688.2055 $[M + Na]^+$	277, 236, 254, 280, 341	27
	5	Kigamicin B	$C_{40}H_{45}NO_{15}$	802.2647 $[M + Na]^+$	277, 236, 254, 280, 341	27
	6	Kigamicin C	$C_{41}H_{47}NO_{16}$	832.2763 $[M + Na]^+$	277, 236, 254, 280, 341	27
	7	Kigamicin D	$C_{48}H_{59}NO_{19}$	976.3531 $[M + Na]^+$	277, 236, 254, 280, 341	27
	8	Kigamicin E	$C_{55}H_{71}NO_{22}$	1120.4357 $[M + Na]^+$	277, 236, 254, 280, 341	27
	9	Citreamicin α	$C_{36}H_{31}NO_{12}$	672.2117 $[M + 3H]^+$	223, 255, 320, 384, 410	29
	10	Citreamicin β	$C_{35}H_{29}NO_{12}$	658.1925 $[M + 3H]^+$	223, 255, 320, 384, 410	29
	11	Citreamicin λ	$C_{33}H_{25}NO_{12}$	630.1596 $[M + 3H]^+$	223, 255, 320, 384, 410	29
	12	Citreamicin ξ	$C_{35}H_{29}NO_{12}$	656.1778 $[M + H]^+$	223, 255, 320, 384, 410	29
	13	Citreamicin η	$C_{31}H_{23}NO_{11}$	588.1479 $[M + 3H]^+$	223, 255, 320, 384, 410	29
	14	Citreamicin δ	$C_{30}H_{21}NO_{11}$	594.1001 $[M + Na]^+$	228, 252, 332, 432	55
	15	Citreamicin ε	$C_{30}H_{26}NO_{11}$	576.1525 $[M + H]^+$	236, 274, 347, 437	55
BPXNPs with methylene dioxygen bridge ring H	1	Xantholipin B	$C_{27}H_{18}ClNO_9$	536.0713 $[M + H]^+$	250, 270, 310, 340, 380	31
	2	Simaomicin α	$C_{28}H_{25}NO10$	536.1537 $[M + H]^+$	253, 320, 379, 395	34
	3	Simaomicin β	$C_{27}H_{23}NO_{10}$	522.1400 $[M + H]^+$	253, 320, 379, 395	34
	4	Actinoplanone A	$C_{28}H_{25}N_2O_{10}Cl$	585.1342 $[M + H]^+$	229, 253, 306, 366, 382	36
	5	Actinoplanone B	$C_{28}H_{24}NO_{10}Cl$	570.1091 $[M + H]^+$	226, 252, 336, 363, 377	36
	6	Actinoplanone C	$C_{28}H_{26}N_2O_{10}$	551 $[M + H]^+$	228, 253, 336, 360, 375	36
	7	Actinoplanone D	$C_{28}H_{25}NO_{10}$	536 $[M + H]^+$	221, 249, 298, 312, 328, 372	36
	8	Actinoplanone E	$C_{31}H_{29}N_2O_{10}Cl$	625 $[M + H]^+$	233, 253, 308, 342, 370, 386	36
	9	Actinoplanone F	$C_{32}H_{29}N_2O_{10}Cl$	653.1480 $[M + H]^+$	231, 254, 308, 346, 386	36
	10	Actinoplanone G	$C_{32}H_{30}N_2O_{11}$	619 $[M + H]^+$	207, 253, 304, 340, 380	36
Glycosylated BPXNPs	1	Neocitreamicin I	$C_{36}H_{31}NO_{11}$	654.1993 $[M + H]^+$	223, 255, 320, 384	56
	2	Neocitreamicin II	$C_{44}H_{43}NO_{15}$	826.2714 $[M + H]^+$	223, 255, 320, 384	56
	3	IB-00208	$C_{36}H_{34}O_{10}$	693.2194 $[M + 3H]^+$	225, 255, 325, 385	57
	4	FD-594	$C_{47}H_{56}O_{20}$	939.6 $[M - H]^-$	214, 233, 276, 363, 420	58
	5	Calixanthomycin A	$C_{36}H_{38}O_{14}$	695.2327 $[M - H]^+$	226, 295, 329	41
Acylated BPXNPs	1	Turbinmicin	$C_{34}H_{30}NO_{11}$	628.1809 $[M + H]^+$	241, 289, 383	42
	2	Actinomadurone	$C_{34}H_{31}NO_{10}$	614.2032 $[M + H]^+$	261, 316, 393	43
Halogenated BPXNPs	1	Albofungin	$C_{27}H_{24}N_2O_9$	520 $[M]^+$	228, 240, 255, 305, 375	44,53
	2	Chloroalbofungin	$C_{27}H_{23}ClN_2O_9$	554 $[M]^+$	231, 250, 300, 337, 360	53
	3	Sch5445	$C_{30}H_{29}N_2O_9Cl$	597.1609 $[M + H]^+$	215, 251, 270, 326, 393	48
	4	Lysolipin I	$C_{29}H_{24}ClNO_{11}$	598.2024 $[M + H]^+$	273, 310, 349, 408	51

Published on 09 September 2022. Downloaded by Shanghai Jiaotong University on 10/24/2022 5:38:16 AM.

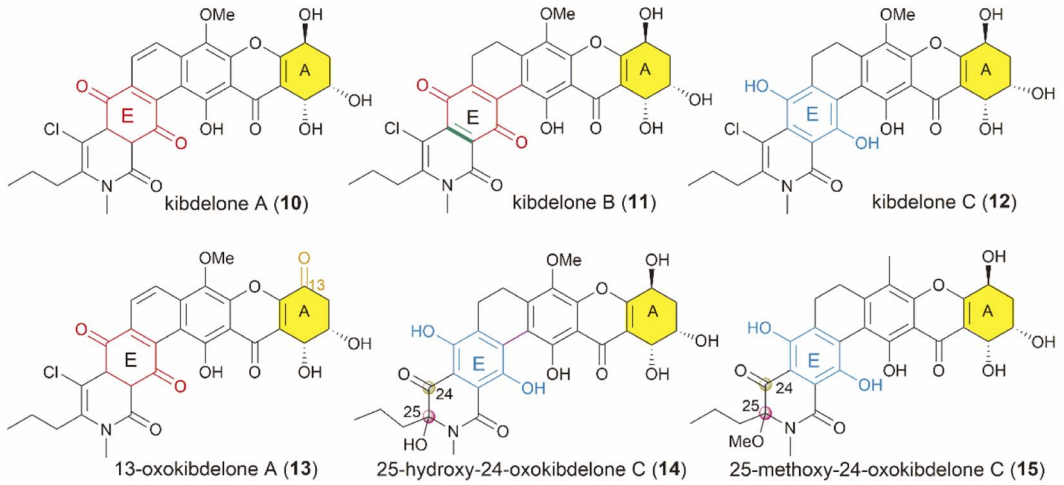

Fig. 3 Kibdelones and analogues with tetrahydrobenzene ring A.

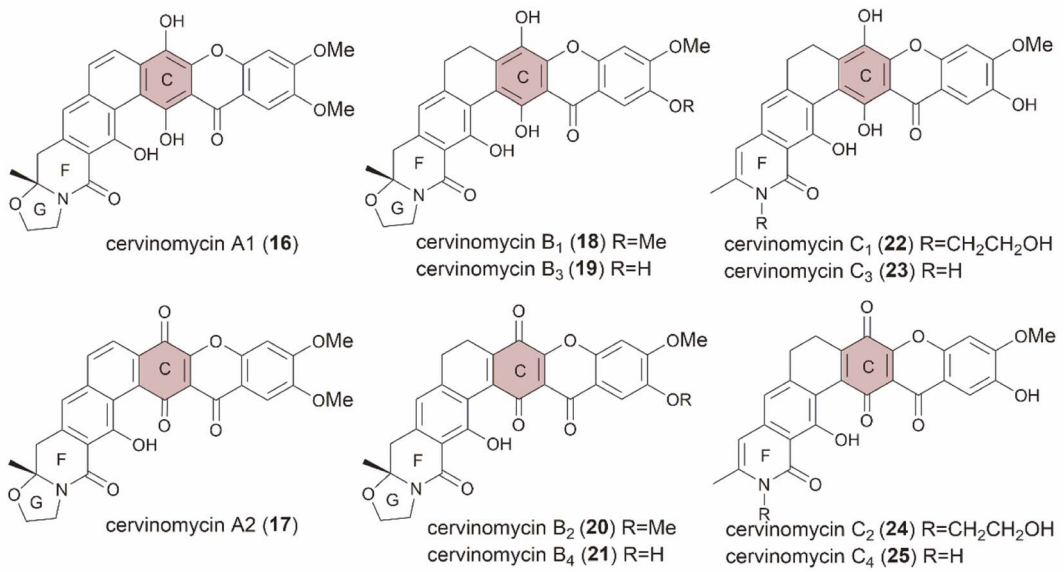

Fig. 4 Structural diversity of cervinomycins.

that in kibdelones (**10–12**, Fig. 3), leading to the formation of isobenzoxanthone. This difference contributes to the different types of molecular folding in the "3 + 3" type. Moreover, the isokibdelone A rhamnoside (**29**, Fig. 3) was also isolated from the wheat fermentation culture of the same strain. The co-production of these BPXNPs by the same strain suggests the divergence and complexity of their biosynthetic pathway.[14]

2.4 BPXNPs with heterocyclic lactam ring F

BPXNPs carrying heterocyclic lactam F ring firstly vary in the substituents on their amide nitrogen atom, such as methyl group in Sch56036 (**32**, Fig. 6)[21] and 1-hydroxypropionic acid group in ukixanthomycin (**36**, Fig. 6).[24] Secondly, these compounds contain different substituents on the δ-position (C_{25}) next to the amide, such as a methyl group existing in major compounds (xantholipin (**33**),[22] MDN-185 (**34**),[23] dehydroxanthomycin (**35**)[59] and sattahipmycin (**37**, Fig. 6)),[25] and a butyryl group in Sch56036 (**32**).

2.5 BPXNPs with heterocyclic oxazolidine ring G

In some BPXNPs, the substituents on the nitrogen atom of amide ring F can be further involved in the construction of heterocyclic oxazolidine ring G, such as arixanthomycin A–C (**38–40**)[26] and kigamicin A–E (**41–45**)[27,28] (Fig. 7), respectively. The C4′ of the carboxylated oxazolidine ring G in **38–40** is simultaneously substituted by a carboxy group. Moreover, oxazilidone ring G with a carbonyl group at C5′ can be found in citreamicins (**46–53**)[29] (Fig. 7). The citreamicins (**46–51**) are further diversified by the various modifications of ring A and ring G. Meanwhile,

 This journal is © The Royal Society of Chemistry 2022

Published on 09 September 2022. Downloaded by Shanghai Jiaotong University on 10/24/2022 5:38:16 AM.

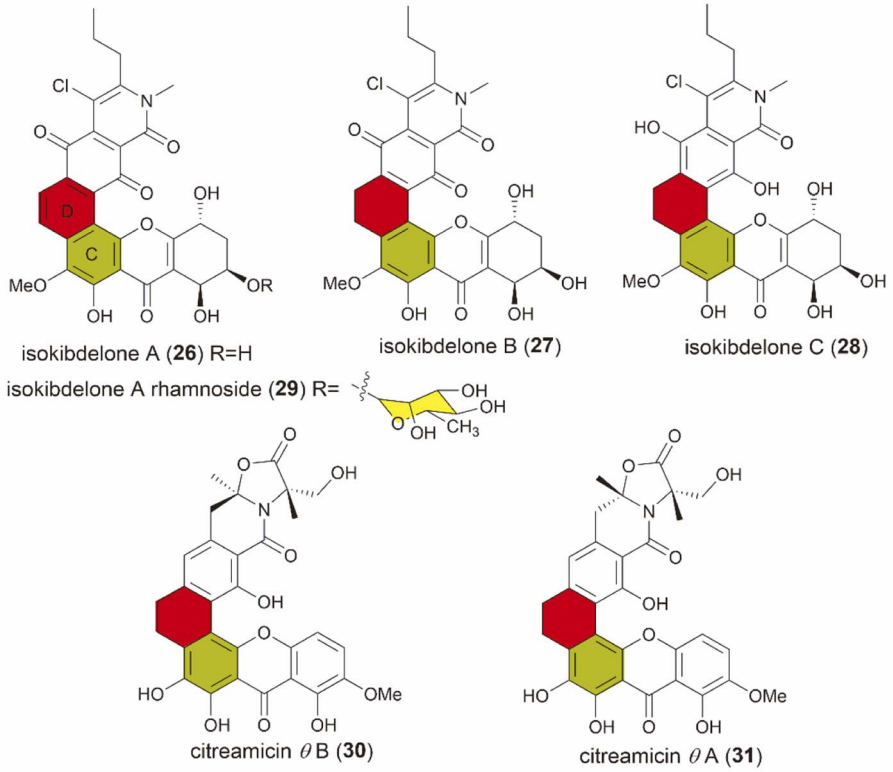

Fig. 5 BPXNPs with "3 + 3" molecular skeleton folding type resulting from different coupling types between ring D and xanthone.

citreamicin εA and εB (**52** and **53**, Fig. 7)[29] differ from each other in the configuration of the methyl group at C2′, respectively.

2.6 BPXNPs with methylene dioxygen bridge ring H

Xantholipin B (**54**),[31] Sch42137 (**55**),[32] CBS40 (**56**),[33] simaomicins[34] (**57** and **58**) and actinoplanones A–G (**59–65**),[35,36] respectively (Fig. 8), feature an unprecedented ring H containing a methoxyl group fused with a hydroxy group. This moiety is known as the methylene dioxygen bridge reported in plant-originating alkaloids[60] and is a rare skeleton in microbial metabolites. Moreover, the formation of this moiety occurs between ring C and ring D in **54**, **56** and **59–65**, while it exists between ring D and E in **55** and **57** and **58**.

2.7 Glycosylated BPXNPs

Multiple oxidization is one outstanding characteristic of BPXNPs, and the presence of a hydroxyl group allows other modifications such as *O*-glycosylation. Glycosylated BPXNPs

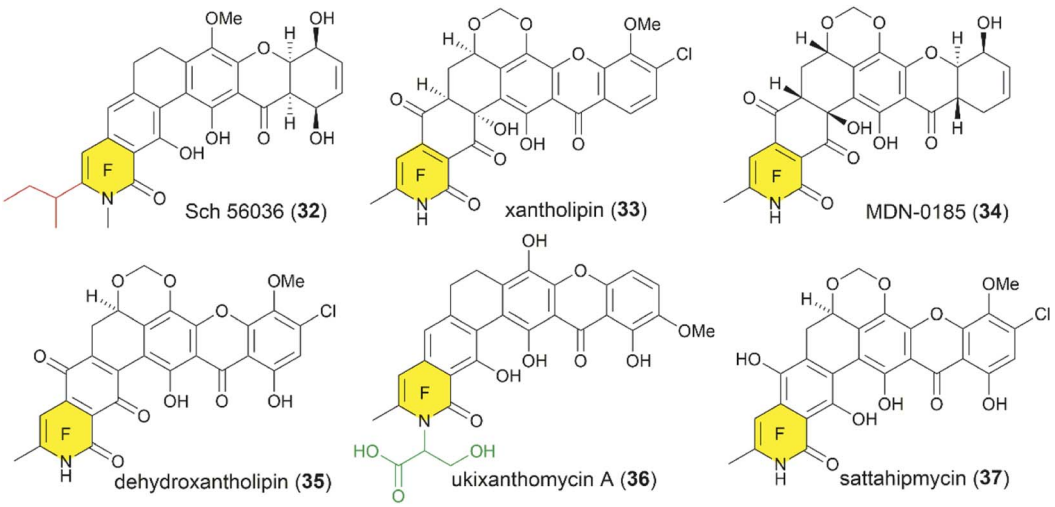

Fig. 6 Structures of BPXNPs with lactam ring F.

Published on 09 September 2022. Downloaded by Shanghai Jiaotong University on 10/24/2022 5:38:16 AM.

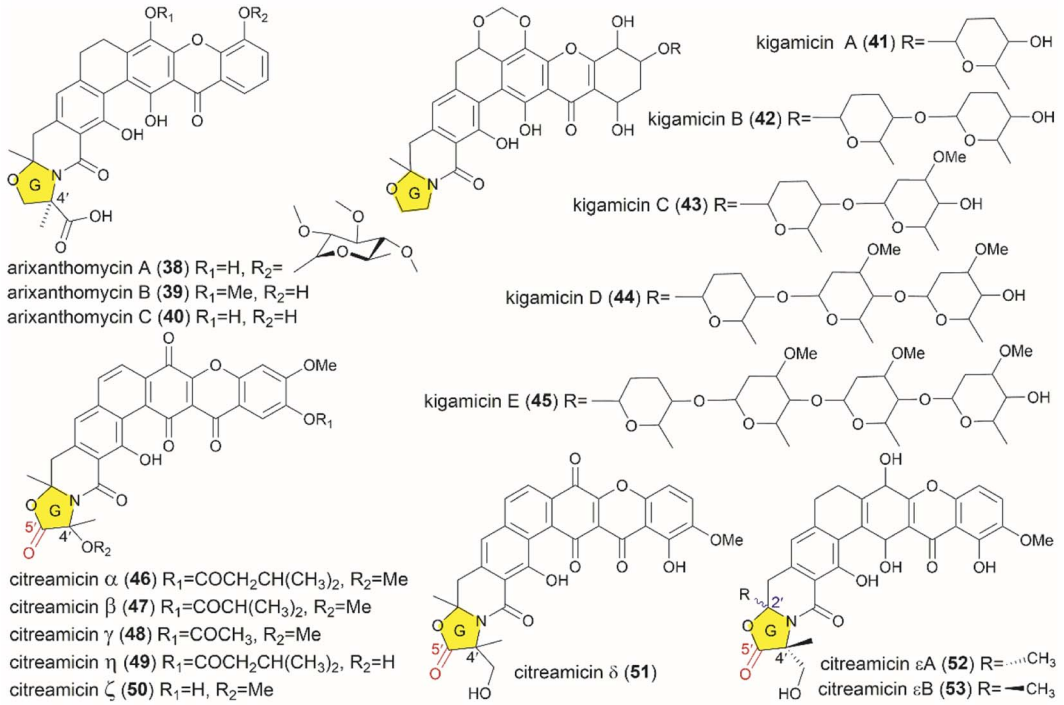

Fig. 7 BPXNPs with complicated heterocyclic oxazole ring G.

vary in the type of sugar groups, the number of sugars and the position where the sugar is located. IB-00208 (**66**, Fig. 9),[38,57] neocitreamicin II (**68**, Fig. 9),[37] kibdelone rhamnosides (**69–71**, Fig. 9)[13] and calixanthomycin A (**72**, Fig. 9)[61] are glycosylated BPXNPs with one sugar group. In **66** and **72**, the trimethyldeoxypyranose hexose is attached to the *p*-hydroxyl group at C22 of ring E. In **69–71**, the glucose is loaded on C11 of ring A. In **68**, an acetylated oliose is attached to C12 of ring A.[37] An acetylated oliose is attached to C12 of ring A in **68**.[37] However, compared with neocitreamicin I (**67**), the glycosylation in **68** did not exhibit an obvious effect on the antibacterial activity.[37] MS 901809 (**73**, Fig. 9), BE-13793X[39] (**74**, Fig. 9) and FD-594 (**75**, Fig. 9)[8] are glycosylated with a trisaccharide sugar chain. Similarly, the trisaccharide is composed of two D-olivoses and one D-oleandrose, but it is loaded onto different positions of ring A.

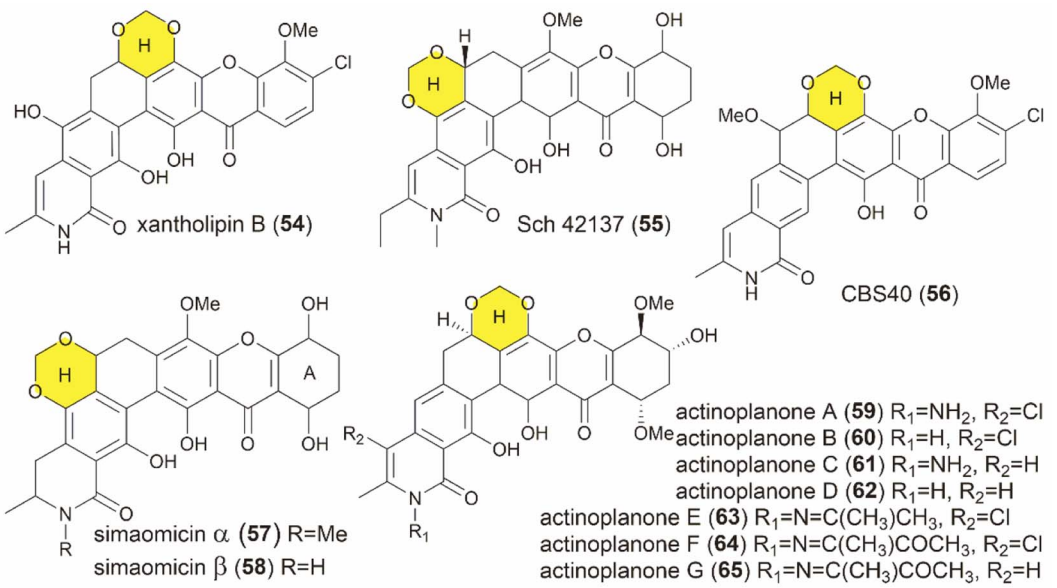

Fig. 8 BPXNPs with methylene dioxygen bridge ring H.

 This journal is © The Royal Society of Chemistry 2022

Published on 09 September 2022. Downloaded by Shanghai Jiaotong University on 10/24/2022 5:38:16 AM.

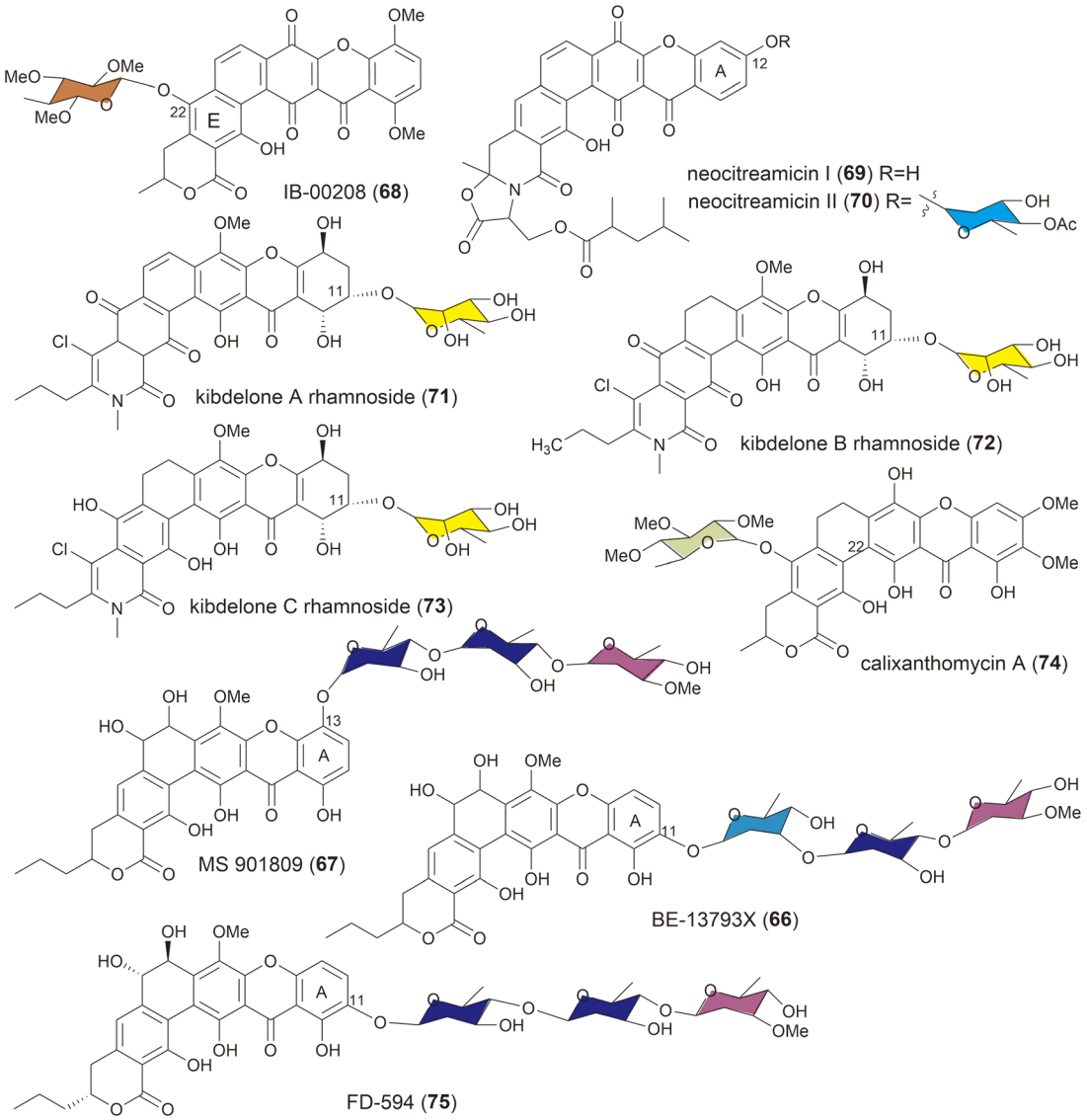

Fig. 9 Glycosylated BPXNPs.

2.8 Acylated BPXNPs

Actinomadurone[43] (**76**, Fig. 10) and turbinmicin[42] (77, Fig. 10) are the only two BPXNPs with a polyene chain at ring A. These two compounds share a similar molecular structure except for the oxidation state of ring E. Meanwhile, **76** and 77 exhibit opposite configurations at C9 and C14. The different number of double bonds in the polyene chain suggest different selectivities of acyltransferases on acyl group donors involved in biosynthetic machineries.

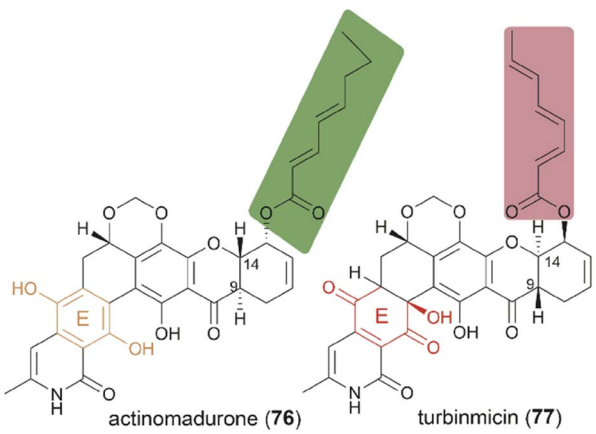

Fig. 10 Structures of turbinmicin and actinomadurone.

2.9 Halogenated BPXNPs

Another structural characteristic of some BPXNPs is halogenation. Chloroalbofungin (**79**, Fig. 11),[44–46] Sch54445 (**80**, Fig. 11)[48] and lysolipins[49–52] (**81** and **82**, Fig. 11) are chlorinated BPXNPs. Among them, chlorination occurs in the different rings. In **81** and **82** and **80**, the chlorinations occur in aromatic rings A and E, respectively. But in **79**, the chlorination is found in

Published on 09 September 2022. Downloaded by Shanghai Jiaotong University on 10/24/2022 5:38:16 AM.

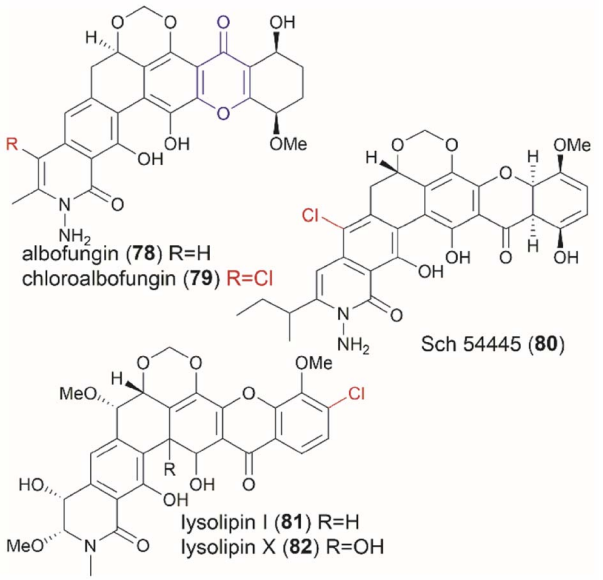

Fig. 11 Halogenated BPXNPs.

heterocyclic lactam ring F. This phenomenon may be due to the regioselectivity of halogenase during the biosynthesis process *in vivo*.

Since their discovery, the orientation of the ether oxygen atom (O15) in the tricyclic xanthone nucleus in albofungins (**78** and **79**, Fig. 11)[44,53] has been proposed to be different from that in other BPXNPs, such as simaomicins (**50** and **51**)[34] (Fig. 6) and CBS40 (**49**)[33] (Fig. 6). Recently, these two compounds have been isolated again from the fermentation cultures of *Streptomyces chrestomyceticus* BCC 24770. Based on the SCXRD data, rings A and B in albofungin (**78**) and chloroalbofungin (**79**) rotated 180°, leading to the same orientation of O15 with all the other known BPXNPs (Fig. 12).[47] Moreover, the NMR and CD spectra of chrestoxanthones A–C (**83–85**),[46] respectively, and albofungin A (**86**)[62] coproduced by the same strain supported this finding (Fig. 12).

Taken together, the structures of BPXNPs are complex, where one molecule can possess more than two characteristics simultaneously. Considering the complex tricyclic skeleton and existence of chiral substituents, the structural determination of BPXNPs is challenging. In addition, other factors (such as solvent-dependent atropisomerism of FD-594 (**75**)[8,58]) may perturb their stable forms, which requires the use of multiple methods and technologies. Bacteria provide a rich source of natural products with potential therapeutic applications, and screening of bacterial extracts has contributed to the discovery of natural products with diverse structures and biologically active compounds. Modern 'omics'-based technologies have revealed the potent potential of *Actinobacteria* for encoding diverse natural products. To avoid the re-isolation of known compounds, the "genetic dereplication" strategy[63] and OSMAC (one strain many compounds) approach[64] have been successfully used during large-scale culture for discovering natural products with novel skeletons. Guided by efficient metatranscriptomic, metatranscriptomic and computational strategies, more BPXNPs will be identified from versatile bacteria with diverse ecology. The information provided here can be beneficial for the screening of BPXNPs from the rich reservoir of extensive natural products.

3. Various biological activities

BPXNPs exhibit diverse biological activities such as antibacterial (mainly Gram-positive bacteria), anti-fungal, antiparasitic and antitumor activities.[4] In this review, their biological activities are presented in Table 3, and then discussed separately. Moreover, some pioneering studies on the plausible biological mechanism are summarized.

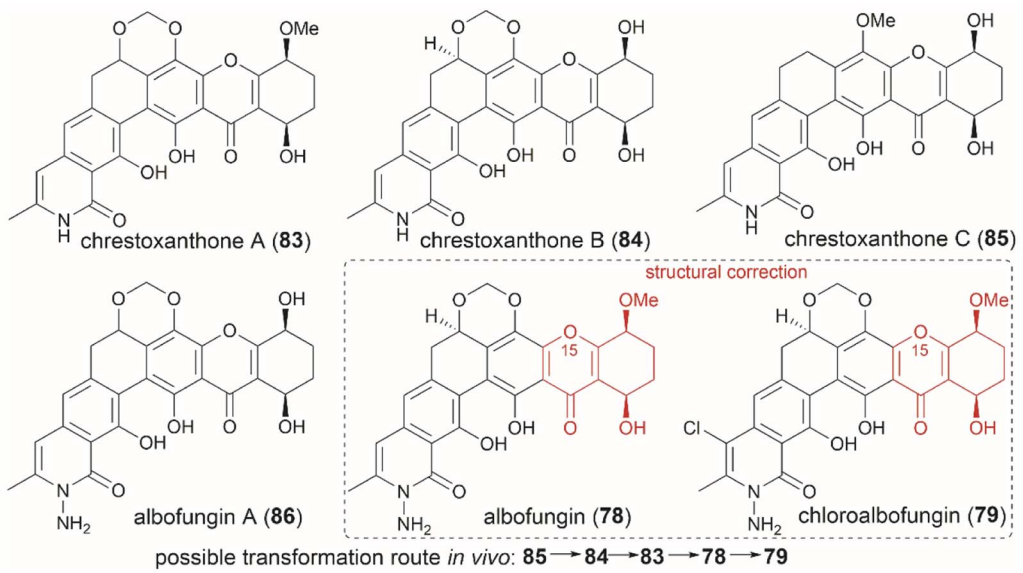

Fig. 12 Structures of albofungin derivatives.

 This journal is © The Royal Society of Chemistry 2022

Published on 09 September 2022. Downloaded by Shanghai Jiaotong University on 10/24/2022 5:38:16 AM.

Table 3 Biological activities of BPXNPs[a]

Classification	Entries	Compound names	Antibacterial		Antifungal	Antiparasitic	Antitumor	Antimycoplasmal
			G^+	G^-				
BPXNPs with tetrahydrobenzene ring A	1	Kibdelones	***	##	x	√	+++++	N
BPXNPs with (hydro)-quinone ring C	1	Cervinomycin A	***	—	—	√	N	
	2	Cervinomycin B_{1-4}	***	x	N	N	+++++	
	3	Cervinomycin C_{1-4}	***	x	N	N	++++	N
BPXNPs with different coupling type of ring D	1	Isokibdelones	N	N	N	N	++	N
	2	Citreamicin θ A and B	***	N	N	N	++	N
BPXNPs with heterocyclic lactam ring F	1	Sch56036	N	N	$$$	N	N	N
	2	Xantholipins	**	—	$$$	N	++	N
	3	MDN-185	N	N	N	√	N	N
BPXNPs with heterocyclic oxazolidine ring G	1	Arixanthomycins	**[c]	—	√[$]	N	√	N
	2	Kigamicins	***	x	N	N	+	N
	3	Citreamicins	***	##	N	N	+++++	N
BPXNPs with methylene dioxygen bridge ring H	1	CBS40	****	√[##]	N	N	N	N
	2	Simaomicins	***	x	√	√	√	N
	3	Actinoplanones	****	—	$$$$	N	++++	N
Glycosylated BPXNPs	1	Neocitreamicins	***	—	N	N	N	N
	2	IB00208	***	—	N	N	+++	N
	3	FD-594	***	—	—	N	++	N
Acylated BPXNPs	1	Turbinmicin	N	N	$$$	N	N	N
	2	Actinomadurone	N	N	$$$$	N	++++	N
Halogenated BPXNPs	1	Albofungins	**	###[a]	$$$	√	+++++[b]	N
	2	Sch54445	N	N	$$	N	N	N
	3	Lysolipins	****	###	√	N	√	N

[a] '√' indicates biological activity, 'x' indicates inactive, 'N' indicates absence of test, and '—' indicates no obvious or weak activity (MIC > 50 μg mL^{-1}). Known biological activity assays were performed against different strains and these comparisons should be viewed as indicative not quantitative. **** indicates the activity against G^+ bacteria with MIC < 10 ng mL^{-1}, *** indicates activity against G^+ bacteria with MIC < 1 μg mL^{-1}, ** indicates activity against G^+ bacteria with MIC < 10 μg mL^{-1}, ### indicates activity against G^- bacteria with MIC < 1 μg mL^{-1}, and ##indicates activity against G^- bacteria with MIC < 10 μg mL^{-1}. [a]Albofungin A (**86**) showed strong activity against G^- bacteria.[62] [b]Albofungin (**78**) and albofungin A (**86**) showed strong antitumor activity with IC_{50} < 0.01 ng mL^{-1}.[62] [c]Only arixanthomycins (**38–40**) showed strong activity against selected G+ bacteria with MIC < 10 μg mL^{-1}. +++++ indicates an IC_{50} < 0.01 ng mL^{-1}, ++++ indicates an IC_{50} < 0.1 ng mL^{-1}, +++ indicates an IC_{50} < 0.01 μg mL^{-1}, ++ indicates an IC_{50} < 0.1 μg mL^{-1}, and + indicates an IC_{50} < 1 μg mL^{-1}. $$$$ indicates antifungal activity with MIC < 0.1 μg ml^{-1}, $$$ indicates antifungal activity with MIC < 1 μg ml^{-1}, $$ indicates antifungal activity with MIC < 50 μg ml^{-1}, $ indicates antifungal activity with MIC > 50 μg ml^{-1}.

3.1 Biological activities

3.1.1 Antibacterial activity. Most of the BPXNPs listed in Table 3 showed potent antibacterial activities and many of them exhibited dramatic activity against Gram-positive (G^+) bacteria. Especially, the MIC values of citreamicin η (**49**, Fig. 7) against several G^+ strains were reported to be <0.015 μg mL^{-1}. Likewise, citreamicins δ and ε (**51–53**, Fig. 7) displayed exceptional activity against several pathogens including many resistant strains (such as *Staphylococcus aureus* MRSA) with MIC < 0.06 μg mL^{-1}. Compared with the current commercially available G^+ antibiotics daptomycin and linezolid, their activities were very favorable.[55] However, they showed less activity against Gram-negative (G^-) pathogens than meropenem.[55] Kigamicins (**41–45**, Fig. 7) inhibited the growth of G^+ bacteria including *Staphylococcus aureus* MRSA with MICs of 0.1–0.78 μg mL^{-1}, but were not active against G^- bacteria. Several BPXNPs possess activity against both G^+ and G^- bacteria, such as actinoplanone A (**59**, Fig. 8). **59** is highly active against G^+ bacteria (MIC < 0.7 ng mL^{-1}), and is also very effective against G^- bacteria (MIC of 0.05–12.5 μg mL^{-1}). However, actinoplanone B (**60**) and F (**64**) were inactive against G^- species (MIC > 50 μg mL^{-1}).[36] Their only structural difference lies in the substituents of the nitrogen atom in heterocycle F, and then the NH_2 substituent in **59** is proposed to enhance the activity.[36] However, the detailed mechanism is still under debate.

Possible biological mechanisms have been proposed. Triacetylcervinomycin A1 showed higher solubility, lower toxicity and more potent antimicrobial activity than cervinomycin A1 (**16**, Fig. 3). The addition of triacetylcervinomycin A1 with a final concentration of 1.0 μg mL^{-1} at the time of inoculation obviously inhibited the growth of the tested organism. When it was added to a logarithmic phase culture (even with the concentration of 10.0 μg mL^{-1}), a negligible effect was detected.[65] It was found to inhibit the incorporation of labeled precursors of cell wall peptidoglycan (*N*-acetylglucosamine), RNA (uridine), DNA (thymidine) and protein (L-leucine) in both whole cell and acid-insoluble macromolecular fractions.[65] Meanwhile, it stimulated the leakage of amino acids and potassium ions from the resting cells. The use of phospholipids could partially reverse its

Published on 09 September 2022. Downloaded by Shanghai Jiaotong University on 10/24/2022 5:38:16 AM.

inhibitory activity. All these findings suggest that triacetylcervinomycin A1 may interact with phospholipids in the cytoplasmic membrane, interfering with the membrane transport system.[65]

Lysolipins (**81** and **82**, Fig. 11) were highly active against both growing and dormant microbial cells and their sphaeroplasts.[51] They showed high affinity for lipids and the binding could be decreased by several lipids (such as sphingolipids and phosphoglycerides).[51] It is postulated that **81** and **82** may work as glycopeptide synthesis inhibitors by interacting with the C55-lipid carrier bactoprenol, and thus interfere with cell-wall biosynthesis.[49,52] However, this hypothesis cannot be used to explain the selective specific activity of BPXNPs (such as simaomycins (**57** and **58**, Fig. 8) and kigamicins (**41–45**, Fig. 7)) against only some of G^+ bacteria. Thus, the authentic target molecules and a possible general antibacterial mechanism still need to be discovered.

3.1.2 Antiparasitic activities. The antiparasitic activity of BPXNPs is attractive. Albofungins (**78** and **79**, Fig. 11) showed activity against helminths and nematocida (LD_{99} < 1.2 nM)[13] in humans, and preferably in companion and meat-producing animals. **78** and **79** could reduce, inhibit or retard the growth, viability and egg fecundity of helminths and ameliorate the symptoms of helminth infection.[66] Cervinomycins A1 and A2 (**16** and **17**, Fig. 4)[15] and kibdelones (**10–12**, Fig. 3)[13] also exerted modest antiparasitic activity. Simaomicin α (**57**, Fig. 8) is the only BPXNP proven to have anticoccidial activity against all the commercially important chicken coccidia species (such as *Eimeria tenella*, *E. acervulina*, *E. brunetti*, *E. necatrix*, and *E. maxima*) with an optimal dosage of 1 ppm in the diet of chickens.[67] Meanwhile, **57** exhibited remarkably strong antimalarial activities *in vitro*. It showed considerably more potent antimalarial activity against *Plasmodium falciparum* strains K1 (drug-resistant) and FCR3 (drug-sensitive) (IC_{50} of 0.045 and 0.0097 ng mL^{-1} for strain K1 and FCR3, respectively) than the clinically-used antimalarial drugs (such as triacsin C (IC_{50} 6.0 ng mL^{-1} against strain K1 and 8.0 ng mL^{-1} against strain FCR3)).[68] Additionally, MDN-0185 (**34**, Fig. 6) exhibited potency comparable to **57** against *P. falciparum* 3D7 parasites (IC_{50} of 9 nM).[23] **17** and **50** provide an alternative starting point for further mechanism studies and development of antiplasmodial chemotherapy candidates.

3.1.3 Antitumor activity. Cytotoxicity is the second prevalent biological activity of BPXNPs. Albofungin A (**86**, Fig. 12), albofungin (**78**, Fig. 11) and chloroalbofungin (**79**, Fig. 11) displayed significant antitumor activities against HeLa (cervical carcinoma), MCF 7 (breast carcinoma), and HepG2 (hepatocellular carcinoma) cells (IC_{50} ranging from 0.003 μM to 0.9 μM).[62] Terminal deoxynucleotidyl transferase (dUTP) nick-end labeling and flow cytometry analysis verified that **86** could induce cellular apoptosis. Xantholipin (**33**, Fig. 6) was found to have extremely high activity against the oral squamous carcinoma cell line KB (IC_{50} < 2 nM) and leukemia cell line HL60 (IC_{50} < 0.3 μM) and it was even 10-fold more effective than doxorubicin against a lung cancer cell line and 3-fold more affective against a colon cancer line.[69] The IC_{50} values of citreamicin εA and εB (**52** and **53**, Fig. 7) against HeLa were 0.032 and 0.031 μM, respectively.[70] Kibdelone A (**10**, Fig. 3) had potent activity against the SR (leukemia) tumor cell line (GI_{50} of 1.2 nM) and SN12C (renal) cell carcinoma cell (GI_{50} < 1 nM).[13] Under the nutrient-dependent condition, kigamicins A–E (**41–45**, Fig. 7), respectively, were discovered to selectively kill human pancreatic cancer cells (PANC-1) (IC_{50} of 1 μg mL^{-1}),[27] indicating that they may be new candidates for "anti-austerity" strategy treatment. "Anti-austerity" is a new strategy to repress cancer *via* the elimination of nutrient deprivation tolerance. The elimination makes cancer cells sensitive to the microenvironment characteristic of oxygen and nutrient insufficiency.[71,72] BPXNPs with potent cytotoxicity provide potential drug reserve for cancer treatment.

3.1.4 Antifungal activity. In the last two decades, owing to the rapid increase in common and rare fungal infections, the demand for novel more effective and safe antifungal agents gave impetus to the discovery of Sch42137 (**55**, Fig. 8),[32] Sch54445 (**80**, Fig. 11)[48] and Sch56036 (**32**, Fig. 6).[21] All of them possessed broad spectrum antifungal activity. **55** showed very strong activity against yeasts (MICs < 0.125 μg mL^{-1}) and dermatophytes, which was similar to albofungin (**78**, Fig. 11) but slightly more active than simaomicin α (**57**, Fig. 8) and slightly weaker than **32**. However, the antifungal activity of **80** against various yeasts and dermatophytes was superior to that of **57** with an MIC of 0.38 ng mL^{-1}.[48] Compared with **55** and **32**, **80** demonstrated the strongest activity against *Aspergillus*, a clinically important pathogen of fungal infections.[48] Additionally, actinoplanones (**59–65**, Fig. 8) showed antifungal activity against the rice blast fungus *P. oryzae* with IC_{50} values of 0.0016–0.106 μg mL^{-1} and their activities followed the order of **59** > **63** > **65** > **61** > **64** > **62** > **60**. The comparative structural analysis suggested that the substituents at the nitrogen atom of ring F contributed to the more potent activity.[36] Turbinmicin (**77**, Fig. 10) showed potent *in vitro* activities against a wide range of fungi including pan-resistant *Candida auris*, echinocandin- and triazole-resistant *Candida glabrata*, and triazole-resistant *Aspergillus fumigatus* (MICs of 0.03–0.5 μg mL^{-1}).[42] **77** exhibited a dose-dependent reduction of fungal burden in a fumigatus-infected mouse model. According to the membrane trafficking analysis of *Saccharomyces cerevisiae*, **77** was proposed to impair vesicle-mediated trafficking by inhibiting Sec14p. Sec14p is a fungus-specific target, against which there are no approved antifungal agents.[73] The hydrolysis of the polyene tail of **77** resulted in reduced antifungal activity, and the tail was proposed to extend into a hydrophobic pocket left vacant by Sec14p based on the molecular docking.[42] However, exploitation of Sec14p as a target is under debate for further preclinical development. The therapeutic potential of **77** suggests the importance of BPXNPs as potential sources for antifungal candidate drug discovery. Accordingly, comparative antifungal activity assays of BPXNPs should be conducted to give more insight into the structure activity relationships (SAR), which will benefit the combinatorial biosynthesis of novel derivatives.

3.1.5 Other activities. The activities of BPXNPs are not limited to those listed in Table 3. Cervinomycins A1 and A2 (**16** and **17**, Fig. 4), respectively, are the only two BPXNPs that have been tested for activity against mycoplasma.[15] Xantholipin (**33**,

 This journal is © The Royal Society of Chemistry 2022

Published on 09 September 2022. Downloaded by Shanghai Jiaotong University on 10/24/2022 5:38:16 AM.

Fig. 6) inhibited the gene expression of HSP47 (IC_{50} of 0.20 μM) and could inhibit collagen production induced by treatment with TGF-β (IC_{50} of 27 nM).[22] HSP47 plays an essential role as a molecular chaperone for collagen maturation.[74] The induced expression of HSP47 is a novel universal biomarker to identify phenotypically altered collagen-producing cells during fibrosis.[75,76] Thus, HSP47 is a potential target for fibrotic diseases.[77] Therefore, **33** can be developed as a modulator or inhibitor of HSP47 gene expression for the treatment of some fibrotic diseases. As can be seen in Table 3, not all BPXNPs have been tested for all the listed biological activities, and thus more work on the evaluation of their activity should be done. Nevertheless, these excellent activities have excited academic interest in the synthetic and biosynthetic studies of BPXNPs.

3.2 SAR studies for cytotoxicity

The potent cytotoxicity of BPXNPs indicates that they may be potential chemotherapeutic anti-cancer agents. However, systematic studies on the cytotoxic mechanism of BPXNPs have not been conducted. Recently, we have gotten clues from exploratory studies.

Actinoplanone A (**59**, Fig. 8) exhibited 10^2 to 10^3 times stronger cytotoxicity than mitomycin C and doxorubicin.[36] It was found to dominantly inhibit DNA synthesis than protein and RNA syntheses.[36] The anthracycline daunorubicin (**87**, Fig. 13) affects various biochemical processes including DNA and RNA synthesis inhibition.[78] X-ray analysis of the daunorubicin-d(CpGpTpApCpG) complex revealed an intercalating action between **87** and DNA base pairs.[79] Based on the structural analogy, the possible interaction of **59** with DNA was proposed by Dreiding models. In the model, the planar B–D ring system of **59** is almost superimposable on the B–D rings in **87** and the substituents with an axial configuration on ring A of **59** (OH and OMe at C12 and C13, respectively) oriented similarly to the oxygen atoms at C9 and C13 on ring A in **87**. Therefore, the B–D ring system of **59** was speculated to insert into the DNA base pairs and the substituents on the A ring interact with the oxygen and nitrogen atoms of DNA bases *via* hydrogen bonds (Fig. 13). This was the first and only proposal on the interaction between BPXNPs and DNA.

In 2004, simaomicin α (**57**, Fig. 8) was firstly suggested to be a cell cycle regulator due to the DNA damage-induced G_2 arrest abrogation in Jurkat cells.[80] Subsequently, in 2008, **57** was reported to affect stage development of the malaria parasite *Plasmodium falciparum* in a time- and concentration-dependent manner.[81] When T-cell leukemia Jurkat cells were treated with **57** of 3 nM, the number of cells in the G1 phase increased and those in G2-M phase decreased with an induced increase in cellular caspase-3 activity and DNA fragmentation. The latter phenomenon indicated the promotion of apoptosis. The lower retinoblastoma protein phosphorylation level in the **57**-treated cells indicated that it may target the upstream pathway of retinoblastoma protein phosphorylation. Similarly, when treated with cervinomycin A1 (**16**, Fig. 4), the cells in the G1 phase accumulated.[82] It is known that the abnormal proliferation of tumor cells can be attributed to cell cycle regulation aberrations resulting from the expression of oncogenes or mutations in tumor-suppressor genes in the G1 phase.[82] Furthermore, the genes associated with the progression of the G1 phase and the transition from the G1 to S phase have been found to be involved in various physio-pathological processes.[83] Therefore, **16** and **57** can be developed as chemotherapeutic anticancer drugs targeting the inhibition of cell cycle progression at the G1 phase.

Apoptosis plays a fundamental role in normal animal development and tissue homeostasis. The abnormal regulation of apoptosis is associated with various human diseases,

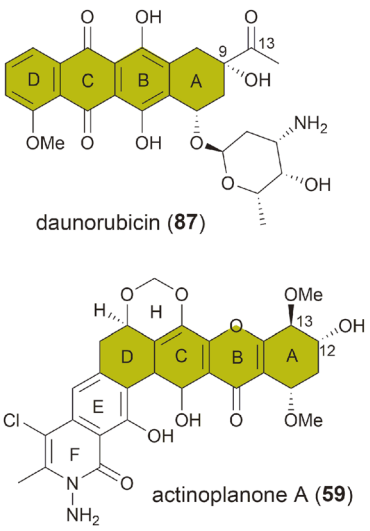

Fig. 13 Structural comparison of daunorubicin and actinoplanone A.

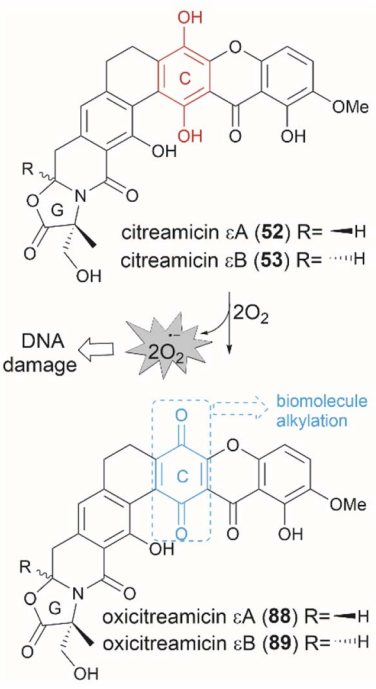

Fig. 14 Proposed cytotoxic mechanism of citreamicin ε.

Published on 09 September 2022. Downloaded by Shanghai Jiaotong University on 10/24/2022 5:38:16 AM.

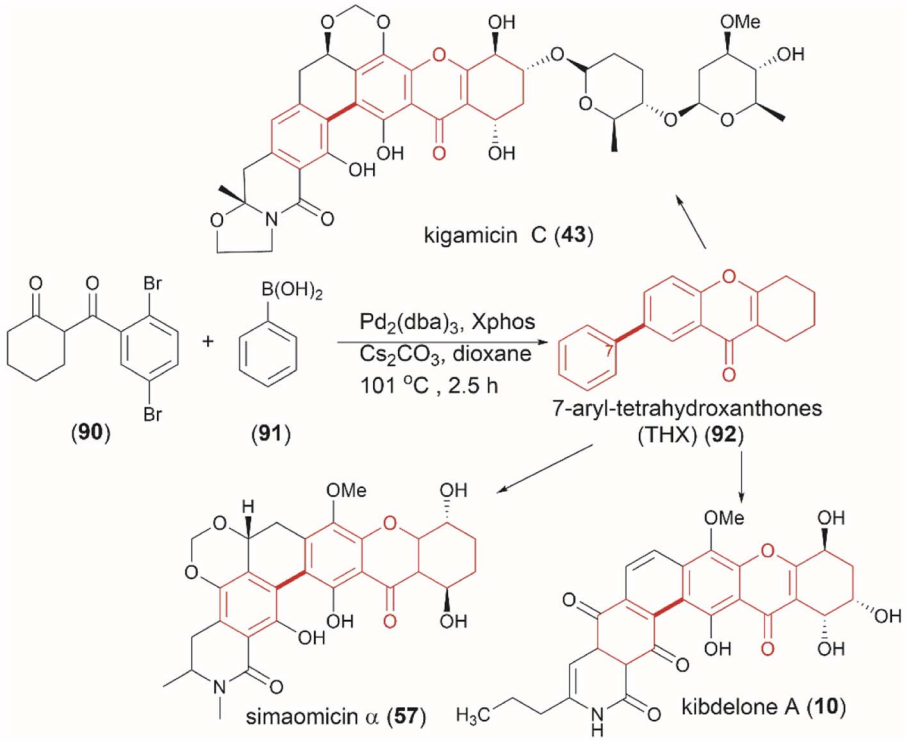

Fig. 15 Identification of the minimal pharmacophore 7-aryl-tetrahydroxanthone.

including immunological and developmental disorders, neurodegeneration, and cancers.[84] Caspases act as key executioners responsive to apoptosis,[84] where their activation is one of the important biomarkers of cell apoptosis.[85] Treatment of HeLa cells with citreamicins ε A and B (**52** and **53**, Fig. 7) resulted in the downregulation of full-length caspase-3 and upregulation of its cleaved form and cleaved PARP-1.[30] Moreover, **52** and **53** could increase the level of intracellular reactive oxygen species (ROS). The corresponding oxidized products oxicitreamicin ε (**88** and **89**, Fig. 14) exhibited reduced capacity to increase the intracellular ROS concentration and exhibited more than 15-fold weaker cytotoxicity against HeLa cells than that of **52** and **53**, respectively.[70] This finding suggests the importance of the *p*-hydroxyl group on ring C in **52** and **53** for their biological activities. It was proposed that the *p*-hydroxyl group of ring C can be oxidized into *p*-benzoquinone group (Fig. 14), and the resultant ROS could damage DNA directly. Alternatively, the *p*-benzoquinone group can induce apoptosis through covalent binding with cellular nucleophiles such as the nucleophilic amino groups present on proteins and DNA.[86] Meanwhile, similar to oxazolines, the five-membered oxazolidone ring G (Fig. 14) might also contribute to the cytotoxic activity by inhibiting protein biosynthesis.[87]

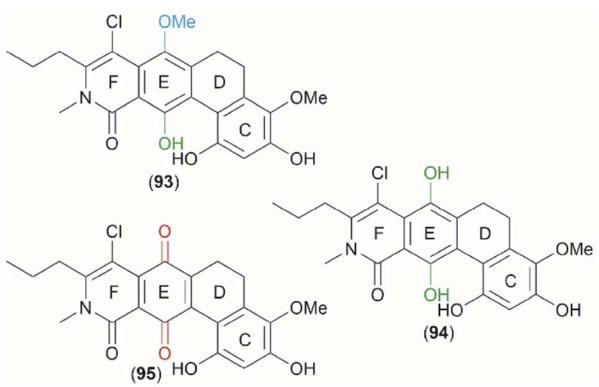

Fig. 16 Truncated kibdelones tested in the biological activity assays.

Prior to drug development, SAR and mode of action (MOA) studies need to be performed. Accordingly, the following examples are worth mentioning. Simaomicin α (**57**), kigamicin C (**43**) and kibdelone A (**10**) all display potent anticancer activities and share the common 7-aryl-tetrahydroxanthones (THX, **92**) nucleus (Fig. 15). To ascertain whether **92** is responsible for the "anti-austerity" effects of the kigamicins, Shipman *et al.* synthesized **92** *via* a Pd-catalyzed ring closure/cross-coupling reaction (Fig. 15). The synthesized **92** displayed cytotoxicity against human pancreatic cancer (PANC-1) cells but was less active than **43**, which was used as a positive control. These results suggested that **92** is the minimal pharmacophore for "anti-austerity" and other structural elements of BPXNPs also play an important role in strengthening the biological response.[88]

The kibdelones (**10–12**, Fig. 3) displayed potent and selective cytotoxicity against a range of human tumor cell lines. However, the isomeric isokibdelones (**26–28**, Fig. 5) did not display significant antitumor activity. The discovery of **26–28** represented an ideal opportunity to expand the structure activity

 This journal is © The Royal Society of Chemistry 2022

Published on 09 September 2022. Downloaded by Shanghai Jiaotong University on 10/24/2022 5:38:16 AM.

relationship investigations into BPXNPs. During the chemical synthesis of kibdelone C (**12**), the antitumor activities of truncated tetracyclic (ring C-F) intermediates (**93–95**, Fig. 16) with varying oxidation states and substitutions on the ring E were evaluated.[89] Based on the result of the growth-inhibitory activity assay, **90** (Fig. 16) was inactive, while compounds **94** and **95** exhibited weak activity (GI_{50} of 4.5 μM). The structural comparison suggested that the hydroquinone and benzoquinone ring E in **94** and **95** was important for their activity. However, the activities of **94** and **95** were still much weaker than that of **12**. Therefore, the tetrahydroxanthone rings A and B were speculated to be highly associated with the potent cytotoxicity.

Among the kibdelones, kibdelones A–C (**10–12**, Fig. 3), respectively, vary in the oxidation state of ring E (benzoquinone *vs.* hydroquinone) and ring D (saturated *vs.* unsaturated). Enantiomers of kibdelone C (**12**) and different kibdelone congeners (Fig. 17) were synthesized to unveil the possible MOA.[90,91] **12** could not bind DNA or inhibit topoisomerase, but caused morphological changes in human cancer cells by affecting the actin cytoskeleton indirectly. (+)- and (−)-**12** showed similar potent toxicity, suggesting that the absolute configuration of ring A does not affect activity. Nevertheless, methyl-(+)-kibdelone C (**96**) exhibited comparable activity to that of (+)-kibdelone C. The activity of dimethyl-(+)-kibdelone C (**97**) decreased substantially, suggesting the essentiality of the hydroxyl group in ring C. Meanwhile, the unaffected activities of the de-chlorinated derivatives (**99–101**, Fig. 17) suggested that the chloride of ring F is dispensable and the hydroxylations around ring A were apparently not required for activity (**101** with an aryl A ring lacking hydroxylation is fully active).[90] Considering the importance of ring A for activities,[89] the polycyclic ring system was proposed to act as scaffolding to present the carbonyls (rings B and F) and phenols (rings C and E) in a defined orientation. This common structure suggests

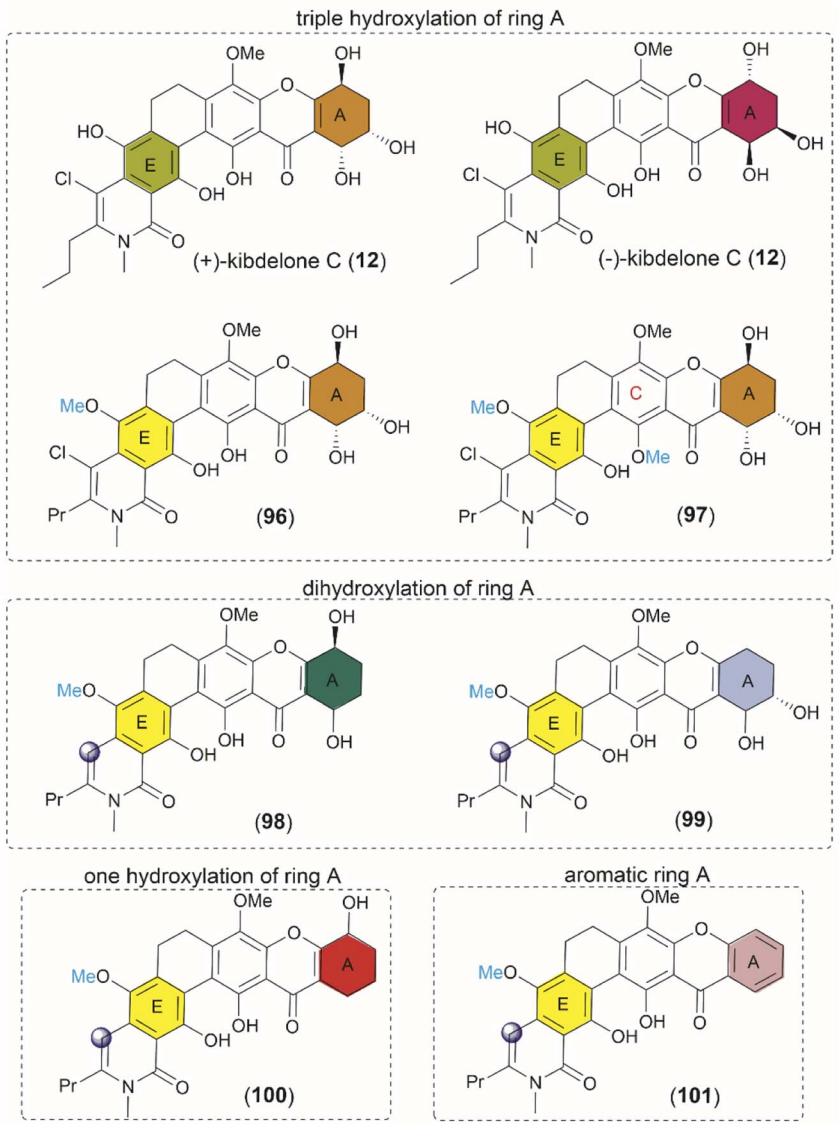

Fig. 17 Synthesized congeners of kibdelone C.

Published on 09 September 2022. Downloaded by Shanghai Jiaotong University on 10/24/2022 5:38:16 AM.

a similar biological mechanism for BPXNPs. Moreover, the phenols of rings C and E were proposed to bind metal, but this possibility remains speculative at present.

Other substituents have also been proposed to be associated with biological activities. Glycosylated arixanthomycin A (**38**, Fig. 7) showed particularly more potent antiproliferative activity than non-glycosylated arixanthomycins B and C (**39** and **40**, Fig. 4). The glycosylation was proposed to be important for the antiproliferative activity. However, most BPXNPs without glycosylation also show potent activity. Thus, further studies are needed to determine whether **38** has a distinct MOA from other BPXNPs or the sugar is needed to improve the bioavailability.

To meet the ever-increasing demand of novel drugs against life-threatening infections and diseases, new agents with innovative chemistry and MOA are desperately needed. The remarkable antifungal activities and more potent antitumor activities of BPXNPs than clinical drugs make them potential candidates for medical development. However, their precise mechanisms of function need to be confirmed first. The proposed SAR here will benefit future comprehensive investigation toward mode-of-function of BPXNPs.

4. Biosynthetic studies

Considering their diverse biological activities, BPXNPs may be potential candidates for drug development. Accordingly, it is necessary to understand their biosynthetic machinery before combinatorial biosynthesis of derivatives with higher activities. Herein, we focus on the natural biosynthesis of BPXNPs. During biosynthesis studies, answers for two important questions still need to be discovered. One is the biosynthetic origin of the carbon skeleton of BPXNPs, while the other is the construction mechanism of tricyclic xanthone nucleus.

4.1 Isotope incorporation studies

In the case of the first question, BPXNPs were firstly proposed to be aromatic polyketides synthesized by type II PKSs (Fig. 2). However, the xanthone nucleus can't be derived from the simple folding of a single polyketide chain. Regarding the second question, the tricyclic xanthone was proposed to be formed either by condensation of two independent units (Fig. 18I) or by oxidative cleavage of a carbocyclic intermediate derived from a single polyketide chain with decarboxylation of the carbonyl atom and insertion of a new oxygen atom (Fig. 18II).[5] ^{13}C-NMR analysis of simaomicin α (**57**) isolated from culture feeding with ^{13}C-labeled acetates supported the single acetate-derived polyketide molecular frameworks with interruptions at the xanthone ring. Based on this finding, a single polyketide chain (**106**) was proposed to be firstly derived from oxidative condensation of thirteen acetates (**105**) in a head-to-tail fashion, and then it underwent cyclization and

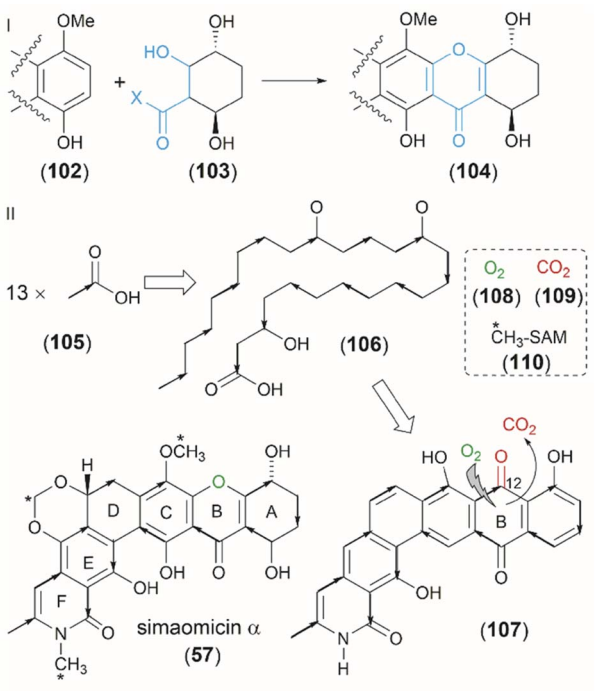

Fig. 18 Two hypotheses for xanthone ring formation.

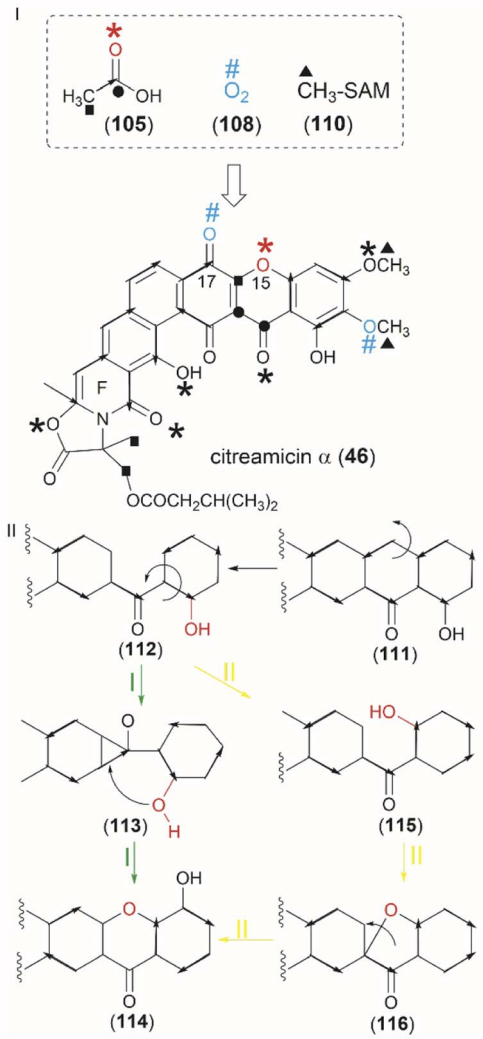

Fig. 19 Proposed xanthone biosynthesis in citreamicin α.

This journal is © The Royal Society of Chemistry 2022

Published on 09 September 2022. Downloaded by Shanghai Jiaotong University on 10/24/2022 5:38:16 AM.

oxidation. For the formation of the xanthone ring, a consecutive set of reactions including the oxidative cleavage of benzoquinone ring B, decarboxylation of the carbonyl carbon (C12) and reclosure with an atmospheric oxygen atom (O_2, **108**) were proposed (Fig. 18II). However, the symmetrical and freely rotating benzophenone intermediate was not observed for **57**, and thus the possibility of the condensation of two independently formed units still cannot be absolutely ruled out. Additionally, three methyl groups substituted on two oxygen atoms and a nitro atom were suggested to be derived from ^{13}C-labeled *S*-methyl of methionine (SAM, **110**) by methyltransferases (Fig. 18II).

To provide further biosynthetic support for BPXNPs, Carter's group conducted similar isotope-labeled feeding experiments on citreamicin α (**46**) with [1,2-$^{13}C_2$]-**105**, [1-^{13}C]-**105**, [2-^{13}C]-**105**, [1-^{13}C,$^{18}O_2$]-acetic acid and $^{18}O_2$ (**108**).[6] The incorporation of labeled atoms clearly confirmed the single acetate-originating polyketide chain. The ^{13}C-**105** and ^{18}O-**108** feeding experiments showed that the oxygen atoms at C25, C14, C12, C8, C3, and C1 were derived from **105**, whereas the oxygen atoms at C17 and C11 were isotopically enriched upon exposure to **108**. It is worth noting that in **46**, C14 and C9 were derived from one acetate unit but C8 and C7 were derived from two separate acetate units. Taken together, these carbon arrangements suggested a more complex rearrangement route for the construction of xanthone, rather than simple decarboxylation and oxygen addition. Meanwhile, the acetic acid-originating oxygen at C15 contradicts the proposed mechanism of simaomicin α (**57**), in which the corresponding atom originated from oxygen. Therefore, two different xanthone ring construction routes were proposed for **46** (Fig. 19). Each of these processes begins with the excision of a single carbon *via* oxidative decarboxylation, leading to the formation of a reactive intermediate (**112**) (Fig. 19). Then, the resultant intermediate **112** is rearranged into the xanthone ring system *via* a spiro intermediate (**113**) or a cyclopropyl alternative (**116**) (Fig. 19). The two rearrangement processes depicted in Fig. 19 lead to the observed incorporation of the acetate-originating oxygen atom in the xanthone ring.

These different isotope incorporations in xanthone attracted research interest in lysolipin X[7] (**82**, Fig. 20I). The isotopic atmospheric oxygen atom was incorporated into the xanthone ring, suggesting a similar xanthone formation pathway to that of **57**. Meanwhile, an intact malonate (**117**) moiety was recruited as the three-carbon starter unit and eleven other malonate units were used as two carbon building blocks for the construction of the polyketide skeleton. Most of the oxygen atoms of **82** were derived from molecular oxygen, suggesting that one more reduction occurred to the backbone before aromatization (Fig. 20I). Eventually, two hypotheses for the construction of the xanthone ring involving Baeyer–Villiger (BV) oxidation were proposed (Fig. 20II). In these two processes, one oxygen atom is inserted in the proposed anthraquinone intermediate (**118**) by BV oxidation, leading to the formation of a lactone intermediate (**119**). Then, the rearrangement of **119** results in the formation of a xanthone ring either *via* decarbonylation (Fig. 20IIa) or by lactone opening, intramolecular OH-attack, resulting in decarboxylation and ring reclosure (Fig. 20IIb).

Nevertheless, different from the simple lactone opening and reclosure mechanism (Fig. 20IIb), other more complex mechanisms for the formation of the xanthone ring were suggested based on the carbon–carbon connectivities in the aglycon part of FD-594 (**122**).[8] The incorporation and the connection of labeled acetate absolutely corroborated that the type II PKSs synthesized the polyketide skeleton (Fig. 21I). According to the typical type II PKS enzymatic machinery,[92] the oxidative condensation of fourteen acetate units (**105**) led to the formation of a polyketide chain, and then aromatic cyclization and oxidations resulted in the formation of an anthraquinone intermediate (**124**). The classical BV oxidation resulted in the opening of **124** for the construction of the xanthone ring. However, the two-carbon unit arrangements of ring A in **122** were different from that of MS 901809 aglycon (**123**). Therefore, the xanthone ring was postulated to be formed through decarbonylation and reclosure with (Fig. 21IIb) or without ring A rotation (Fig. 21IIa).

Answers for these two questions could be found through isotope feeding data; however, other possibilities still cannot be excluded. Genetic manipulation of BPXNP-producing strains and biochemical characterization of relevant biosynthetic enzymes will provide more direct proof. Owing to the development of molecular cloning and molecular sequencing, many FAD-dependent monooxygenases (FMO) have been proven to catalyze BV oxidation during the biosynthesis of natural products.[93–98] Therefore, identification of the genes encoding relevant

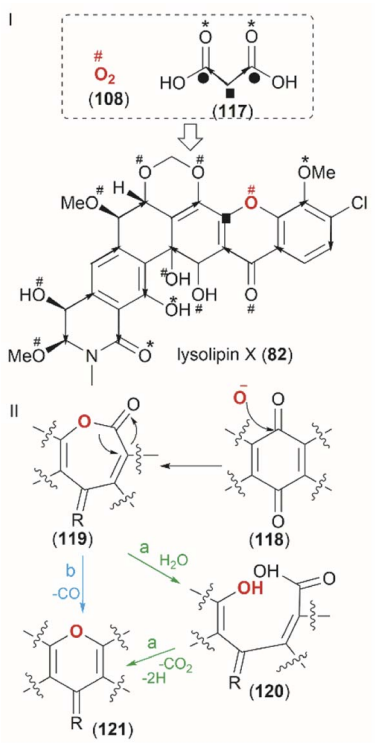

Fig. 20 Proposed construction of xanthone ring in lysolipin X.

Published on 09 September 2022. Downloaded by Shanghai Jiaotong University on 10/24/2022 5:38:16 AM.

enzymes in the biosynthetic gene clusters (BGCs) of BPXNPs is crucial for unveiling the xanthone ring formation enigma.

4.2 Cloning of BGCs

The available genomic sequences and analysis of DNA sequences are increasingly being used to guide the discovery of BGCs. To date, BGCs for lysolipins (**81** and **82**),[52] FD-594 (**75**),[99] xantholipin (**33**),[47] arixanthomycins (**38–40**),[26] cervinomycin B and C (**18–25**),[18] albofungins (**78** and **79**),[18] calixanthomycin A (**72**)[61] and sattahipmycin (**37**)[25] have been reported. The existence of genes for type II PKSs in the BGCs confirmed the previously proposed polyketide biosynthetic pathway. Meanwhile, the consistency between the large proportion of oxidoreductase-encoding genes and the highly oxidative molecular structure of BPXNPs make them the most highly modified aromatic polyketides known to date. These microbial metabolites arise biosynthetically from multiple cyclizations occurring in a single polyacetate chain, accounting for the high degree of oxygenation on the aromatic and heteroaromatic rings.

The first BGC was the *llp* cluster for lysolipins (**81** and **82**), which was cloned using ketosynthase and halogenase gene probes.[42] In total, 42 genes in the 42 kb of the *llp* cluster were proposed to be responsible for the biosynthesis of **81** and **82** (Fig. 22I). Among them, three genes encode the typical minimal type II PKSs. Gene *llp*D encodes the acyl carrier protein (ACP), *llp*E encodes the ketosynthase-β (KSβ) subunit and *llp*F encodes the ketosynthase-α (KSα) subunit. The existence of these three genes suggested that this BGC is responsible for bacterial aromatic polyketide. Three putative cyclase-encoding genes (*llp*CI, *llp*CII, and *llp*CIII) were presumed to be co-transcribed with these minimal PKSs genes. The sequence similarities of these cyclases to other known cyclases revealed that LlpCI may catalyze B-ring cyclization between C-7 and C-16, LlpCIII may be involved in the cyclization of ring D and/or E and LlpCII is also involved in the formation of the polyketide backbone. In the case of the nitrogen in ring F of **81** and **82**, a putative amide synthase LlpA (with high amino acid similarity to OxyD[100] and FdmV[101]) was proposed to amidate malonyl-CoA (**5**) into malonamyl-CoA (**126**) or amidate a polyketide intermediate (Fig. 22II).[42] Then, the polyketide precursor (**127** or **129**) undergoes multistep post-modifications, including reduction, oxidation, halogenation, and methylation. According to the reported enzymatic mechanism in the biosynthesis of stylopine,[102–107] one of the three putative cytochrome-P450-dependent monooxygenases (LlpOIV, LlpOVI, and LlpOVII) may be responsible for the methylene dioxygen bridge in ring H (as shown in compound **130** (Fig. 22II)). The isotopic feeding data suggested that BV oxidation is necessary for the synthesis of xanthone; however, none of the three candidate FMOs (LlpOI, LlpOV, and LlpOVIII) possess the conserved fingerprint motif sequence FXGX3HX3(Y/F) of Baeyer–Villiger monooxygenases (BVMOs).[52] Unfortunately, it was difficult to conduct

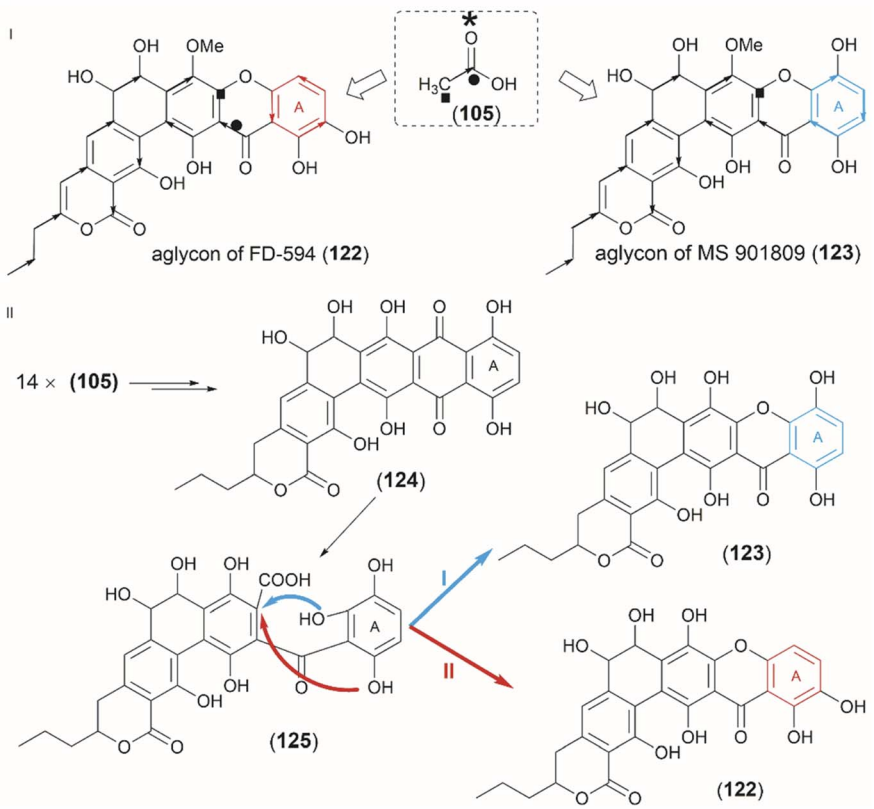

Fig. 21 Proposed xanthone ring formation in FD-594 and MS 901809.

 This journal is © The Royal Society of Chemistry 2022

Published on 09 September 2022. Downloaded by Shanghai Jiaotong University on 10/24/2022 5:38:16 AM.

manipulations of the producing strain, and thus more detailed biosynthetic information still need to be discovery.

The second BGC was the *pnx* cluster for FD-594 (**75**) reported by Kudo *et al.* (Fig. 23I).[99] The sequence analysis revealed that three genes (*pnxA*, *pnxB*, and *pnxC*) encode type II minimal PKS proteins homologous to LlpF, LlpE and LlpD, respectively. PnxU (ketosynthase III, KSIII), PnxV (ACP) and PnxJ (acyltransferase, AT) showed high sequence similarity to the PKS-priming enzymes ZhuH (KSIII), ZhuG (ACP) and ZhuC (AT), respectively.[108] These three proteins (PnxU, PnxV and PnxJ) were proposed to act as similar priming KS to catalyze the biosynthesis of the butyrate starter unit (Fig. 23). Together, the six proteins (PnxA, PnxB, PnxC, PnxU, PnxV, and PnxJ) were proposed to catalyze the synthesis of the polyketide chain (**137**), and three other putative cyclases (PnxD, PnxK and PnxL) apparently are responsible for the cyclization and aromatization for the construction of the presumed pentangular intermediate (**138**).[108] One of the two proteins (PnxF or PnxM) may be responsible for the removal of the reduced hydroxyl group at C11. Among the thirteen oxidoreductases, two FMOs (PnxO4 and PnxO6) were speculated to catalyze the construction of xanthone through a ring-opening process *via* epoxidation and BV-type oxidation. PnxO6 exhibits high sequence similarity with PokO2 (46%)[109] and MtmOII (45%).[110] These two proteins were proposed to be involved in the epoxidation of the tetracyclic aromatic polyketide intermediates in the biosynthesis of polyketomycin and mithramycin, respectively. PnxO4 shows sequence similarity to GrhO5 (54%)[111] and TcmG (57%).[112] GrhO5 was proposed to be a key enzyme for the formation of the unique spiroketal in the biosynthesis of griseorhodin and TcmG was suggested for the triple hydroxylation of tetracenomycin A2 to tetracenomycin C. Meanwhile, PnxO4 shows 43% sequence similarity with LlpOVIII. This finding suggested that the PnxO4 and LlpOVIII may be responsible for the construction of the shared xanthone ring in FD-594 (**75**) and lysolipins (**81** and **82**), respectively. In the proposed machinery, PnxO6 catalyzes the epoxidation reaction of **138**, and then PnxO4 is presumed to catalyze the BV-type oxidation of the epoxide intermediate **139**, leading to the formation of lactone epoxide intermediate **140**.[99] Subsequently, two putative hydrolases PnxN and PnxP may be responsible for the lactone ring hydrolysis, and thus initiate the epoxide ring rotation, ring opening and decarboxylation,

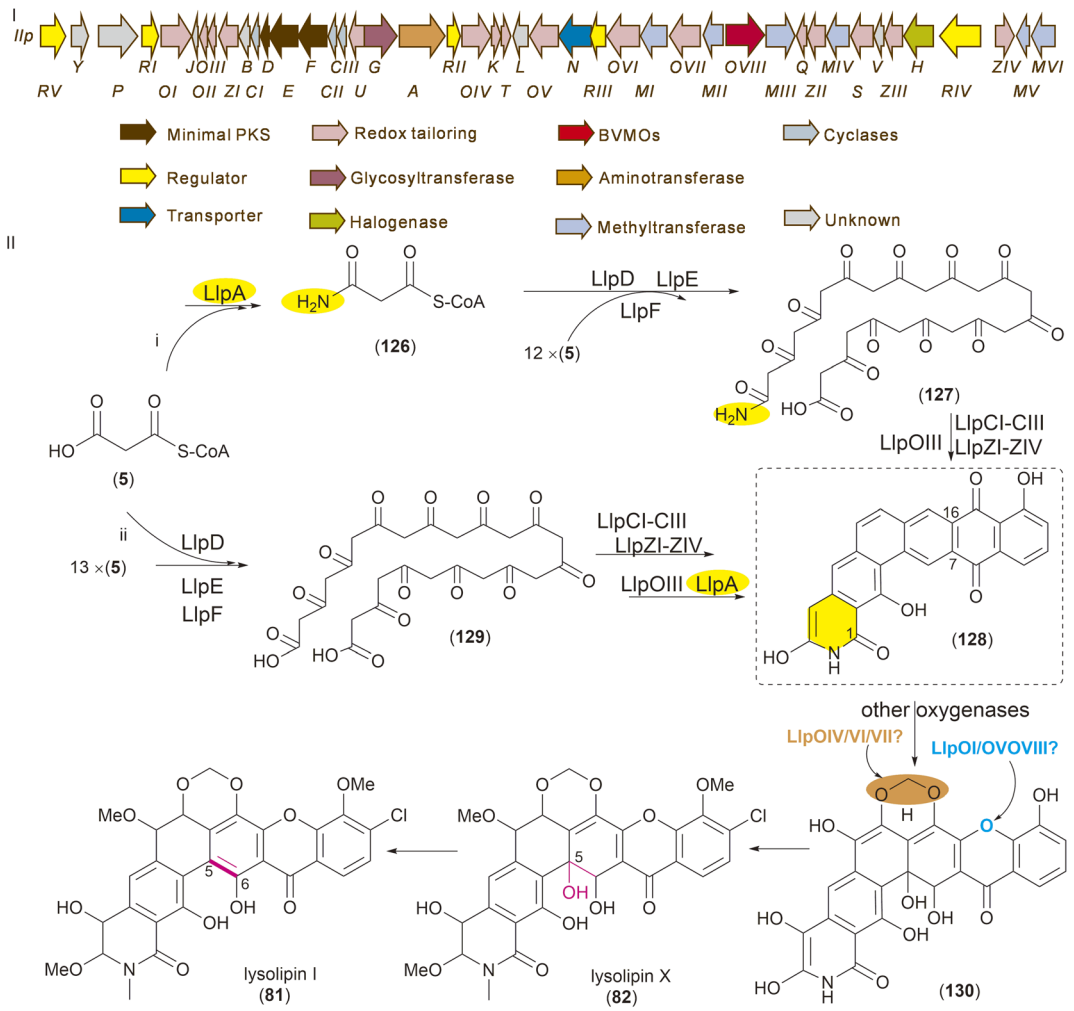

Fig. 22 BGC and the proposed biosynthetic pathway of lysolipin.

Published on 09 September 2022. Downloaded by Shanghai Jiaotong University on 10/24/2022 5:38:16 AM.

leading to the construction of the xanthone ring in **143** (Fig. 23II).[99] Two glycosyltransferases PnxGT1 and PnxGT2 are encoded in the *pnx* cluster. PnxGT1 was proposed to catalyze three olivose transfers to the FD-594 aglycon (**122**) from TDP-olivose and methyltransferase PnxMT2 methylates the hydroxy group of the terminal olivose into oleandrose (Fig. 23II). However, the role of another iterative glycosyltransferase (GT1) and the glycosylation mechanism of PnxGT2 for contiguous iterative glycosylation remain unclear. Meanwhile, no direct biochemical evidence supporting the proposal of the four-enzyme-catalyzed xanthone formation has been reported.

The third biosynthetic BGC (*xan* cluster) was reported in 2012 for xantholipin (**33**) (Fig. 24I).[113] The structural similarity of **33** to lysolipins suggested that the conserved sequence of *llpH* may be used as primers for amplification of the halogenase gene *xan*H. Using the sequence of *xanH* as a probe, the *xan* cluster was identified.[113] XanY1–Y5 were proposed for the recycling of *S*-adenosyl methionine (SAM), and XanB1–B3, probably acetyl-CoA carboxylases, catalyze the carboxylation of acetyl-CoA to form the building unit malonyl-CoA (**5**). For these eight genes, no orthologs genes could be found in the *llp* and *pnx* cluster. Three type II minimal PKS enzymes (XanD-ACP, XanE-KSβ, and

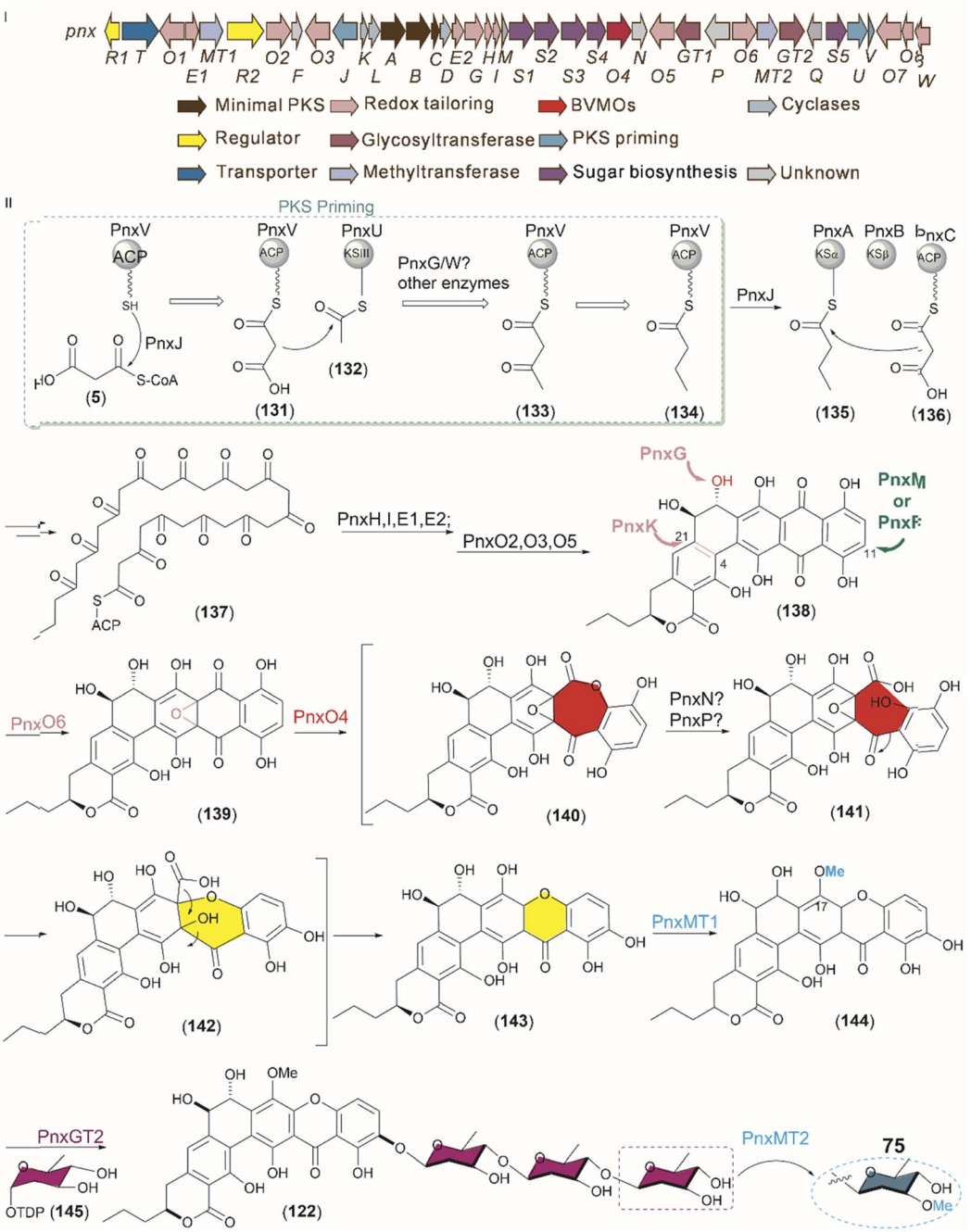

Fig. 23 BGC and the proposed biosynthetic pathway of FD-594.

 This journal is © The Royal Society of Chemistry 2022

Published on 09 September 2022. Downloaded by Shanghai Jiaotong University on 10/24/2022 5:38:16 AM.

XanF-KSα) were proposed to catalyze the oxidative condensation of 13 malonate units (**5**), giving rise to the hypothetical ACP-tethered fully oxidized polyketide **146**, and then two 3-oxoacyl-ACP reductases (XanZ3 for C19 reduction and XanZ4 for C11 reduction) with three cyclases (XanC1–C3, C1 for the cyclization between C9 and C14; XanC2 for cyclization between C5 and C18; and XanC3 for coupling between C4 and C21, and also C2 and C23) contributing to the formation of the ACP-tethered pentacyclic compound **148** (Fig. 24II). Consistent with the highly oxidized structure of **33**, 19 redox genes were identified within the *xan* cluster. Based on the NMR and LC-MS analysis of the biosynthetic intermediates (**138**, **139**, **141** and **144**) accumulated in gene interruption mutant strains, a possible biosynthetic pathway was proposed[113] (Fig. 24II).

Among the minimal PKS complexes, KS_β genes have been shown to be robust phylogenetic markers for structural differences in the natural products encoded by type II PKS BGCs.[114] The functional characterization of DNA extracted directly from environmental samples (environmental DNA and eDNA) provides a means of exploring PKS systems for structurally diverse metabolites with novel carbon skeletons.[114] In 2014, Brady's group found that the phylogenetic divergence of the pentangular polyphenol KS_β gene was strongly correlated with the structural differences in the final products. Using the eDNA-derived KS_β sequence from archived soil eDNA libraries, they found the *arx* cluster for arixanthomycins (**38–40**) (Fig. 25I).[26] 35 genes within *arx* cluster were predicted to be involved in the biosynthesis, regulation, and resistance of **38–40**. Based on the comprehensive functional analysis of BGC,[115] a plausible biosynthetic pathway was proposed (Fig. 25II). The hexacyclic naphthaxanthone core was predicted to arise from a pradimicin-type anthraquinone intermediate (**156**) by the oxidation of BVMO Arx30 (high sequence similarity with XanO4). The oxazolidine (ring G) may be formed spontaneously upon the incorporation of serine (**158**) into the terminal carboxylate by aminotransferase Arx5. One of the glycosyltransferases Arx9 was

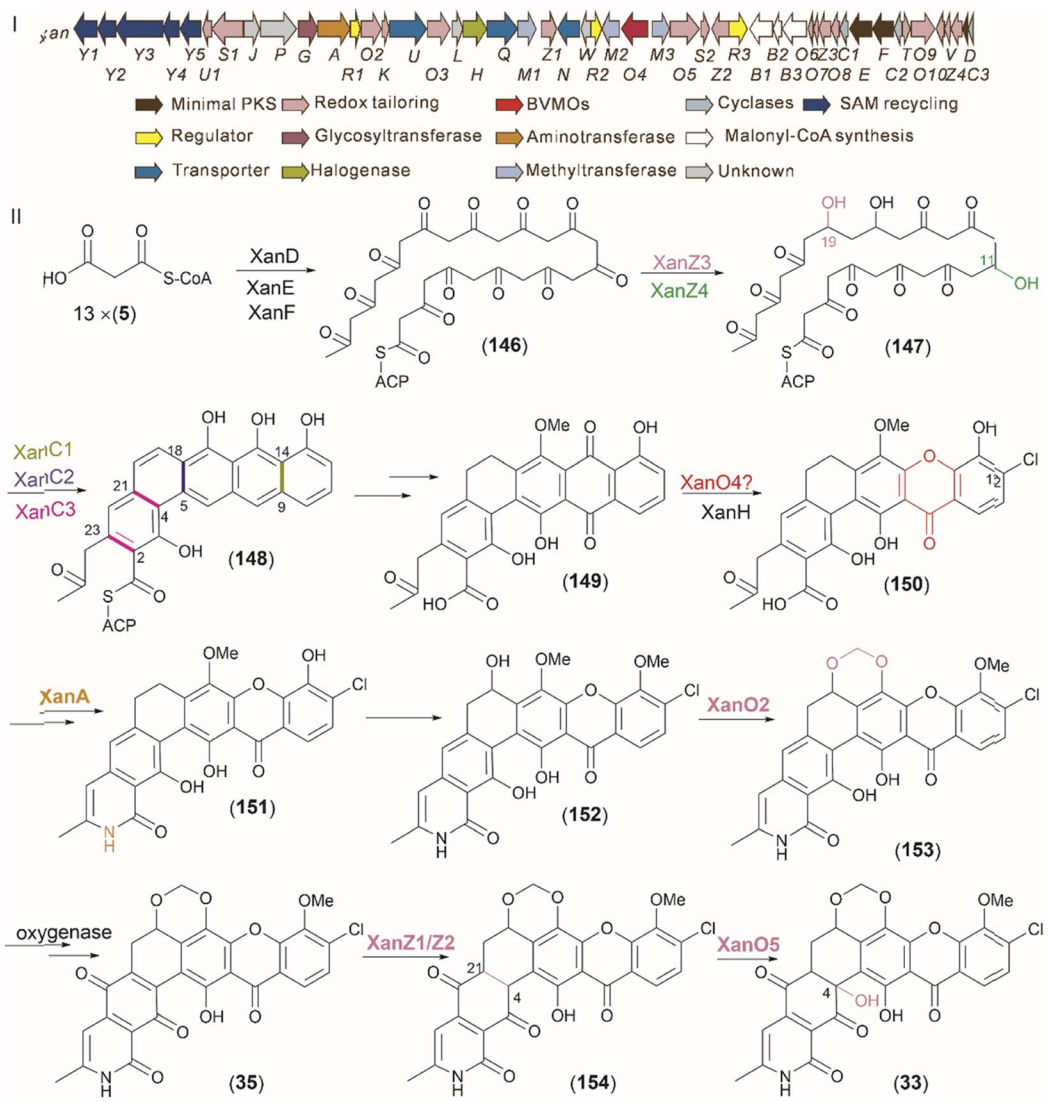

Fig. 24 BGC and proposed biosynthetic pathway of xantholipin.

Published on 09 September 2022. Downloaded by Shanghai Jiaotong University on 10/24/2022 5:38:16 AM.

proposed to transfer the quinovose sugar. *O*-methyltransferases Arx6, Arx12 and Arx32 may methylate the attached quinovose (Fig. 25II).

Another successful example of mining aromatic polyketides through the sequence-based metagenomic strategy is the discovery of calixanthomycin A (**72**) (Fig. 26I).[61] The minimal PKS system composed of Clx10 (KS_β), Clx11 (KS_α) and Clx9 (ACP) and three cyclases (Clx8, 30 and 31) were proposed to catalyze the generation of a benzo-naphthacene quinone intermediate (**162**) (Fig. 26II). Clx4 and Clx27 were proposed to be responsible for the formation of xanthone from the anthraquinone precursor (**163**), in a similar machinery involved in PnxO6 and PnxO4.[99] The hydroxyl group at C11 can be found in FD-594 (**75**) and **72**, and two cytochrome-P450 hydroxylases PnxO5 and Clx28 with 61% sequence identity suggested their role in hydroxylation at C11. The resultant hydroxyl groups at C11 and C12 were possibly methylated by the *O*-methyltransferase candidates Clx2 and Clx43. The *D*-quinovose sugar was proposed to be derived from glucopyranose-1-phosphate (**167**), which was transformed into *D*-quinovose (**170**) by the consecutive set of reactions catalyzed by glucose-1-phosphate thymidylyltransferase Clx14, dTDP-glucose 4,6-dehydratase Clx13 and UDP-glucose 4-epimerase Clx12. Clx21 was a homologous OMT of Arx12 and was proposed to methylate the hydroxy groups in **170** (Fig. 26II). Meanwhile, one or more OMT candidates (Clx2, Clx23 and Clx 38) may be involved in the multiple methylations.

It has been reported that each genome of *Actinomycetes* contains 20–40 distinct BGCs encoding specialized metabolites, but only a few of them have been chemically explored.[116] This means *Actinomycetes* may have potential to biosynthesize more

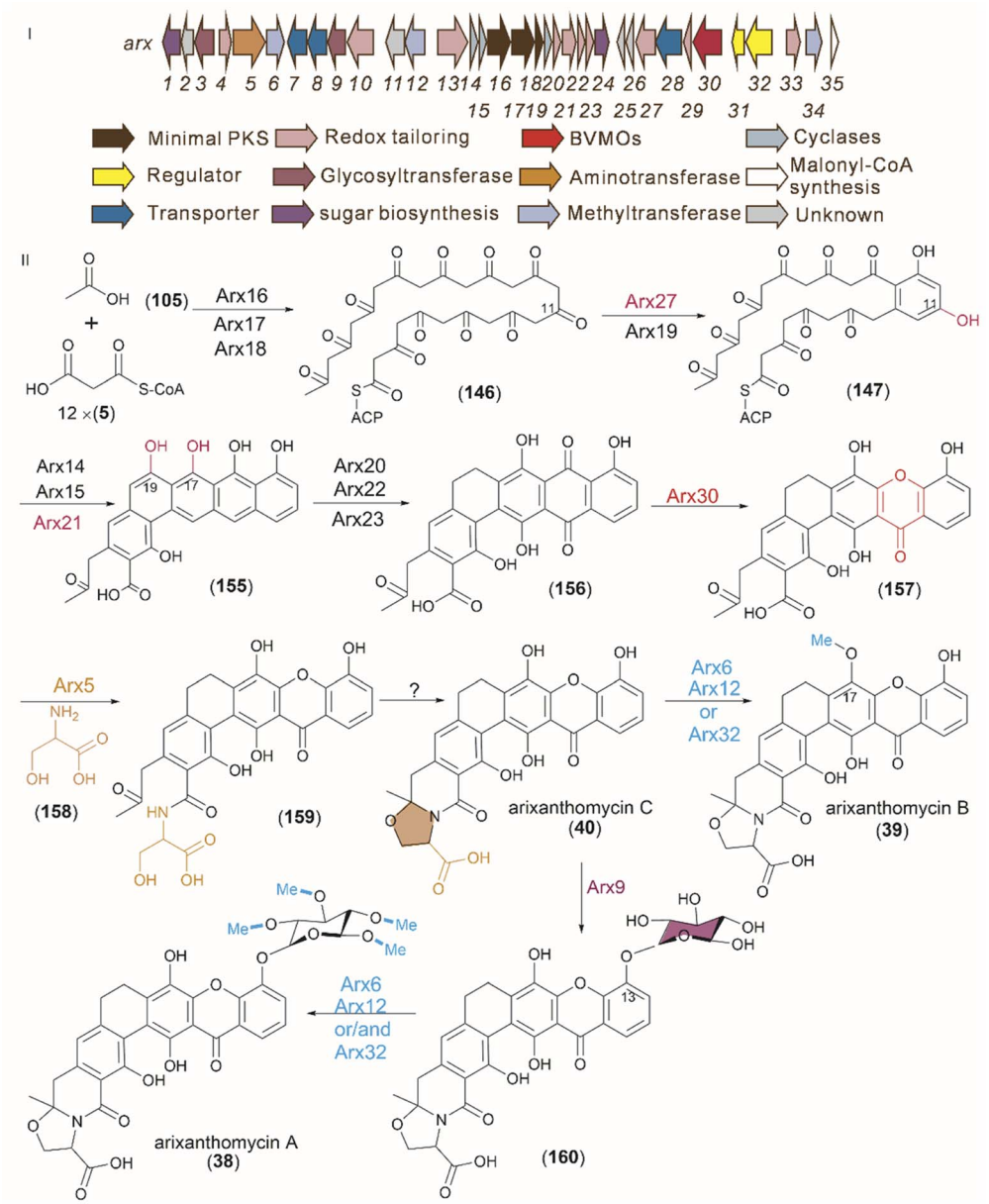

Fig. 25 BGC and the presumed biosynthetic pathway of arixanthomycins.

 This journal is © The Royal Society of Chemistry 2022

Published on 09 September 2022. Downloaded by Shanghai Jiaotong University on 10/24/2022 5:38:16 AM.

secondary metabolites than have been discovered (evolution-guided). Advances in genome sequencing, bioinformatic tools and computational approaches have accelerated the exploration of the biosynthetic gene clusters (BGCs) encoding natural products. AntiSMASH analysis of *Streptomyces* CPCC 204980 (CPCC 204980) has led to the discovery of a possible BGC (*cer* cluster) for cervinomycin A2 (**38**), cervinomycins B_{1-4} (**39–41**)[18] and C_{1-4} (**43–46**)[19] (Fig. 27I). Genes within this BGC show significant similarity to that reported from the *arx* cluster. Considering that genes with high sequence similarity may have similar function, a biosynthesis pathway for ten cervinomycins was proposed (Fig. 27II). A similar consecutive set of reactions involved in type II minimal PKSs, cyclase, and redox proteins contributed to the construction of a possible pradimicin-type anthraquinone (**173**). Two possible BVMOs Cer1 and Cer5 may be involved in the construction of the xanthone system in **174**. Two of the three monooxygenases and one of the three methyltransferases may be responsible for the hydroxylation and methylation of ring A in **177**. **177** may be the common precursor of all cervinomycins. The possible selectivity on the nitrogen donors of aminotransferases Cer2, Cer4 and Cer33 may be the main reason for the production of **23**, **19** and **22**, respectively, with heterocyclic ring F and G (Fig. 27II). Moreover, oxygenases (Cer7 and Cer14) and methyltransferases (Cer3 and Cer15) may contribute to the divergence of the ten cervinomycins. However, all these proposals await future comprehensive biosynthetic studies.

Similarly, the antiSMASH analysis of the genome sequence contributed to the identification of BGCs for dehydroxantholipin (**35**)[59] and albofungins.[62] With the increasing number of available BGCs, the biosynthetic machinery responsible for the production of BPXNPs will be illustrated.

4.3 Biosynthetic studies of xantholipin

Since the discovery of BPXNPs, biosynthetic studies of BPXNPs were retarded owing to the difficulties in genetic manipulations of the producing strain. Detailed biosynthetic studies of BPXNPs have not been conducted, other than xantholipin (**33**, Fig. 6). Since the cloning of the *xan* cluster, You's group conducted a long-term and systematic investigation, which provided important references for biosynthetic studies of other BPXNPs.

4.3.1 Tricyclic xanthone construction in xantholipin. One important contribution by You's group is the successful *in vitro* enzymatic construction of the xanthone ring. Based on the aforementioned bioinformatic analysis and genetic manipulations of the genes probably responsible for specific structure moieties, *xanO4* was regarded as the most possible candidate for the construction of tricyclic xanthone. The *ΔxanO4* mutant did not produce **33**, and instead accumulated the methylated

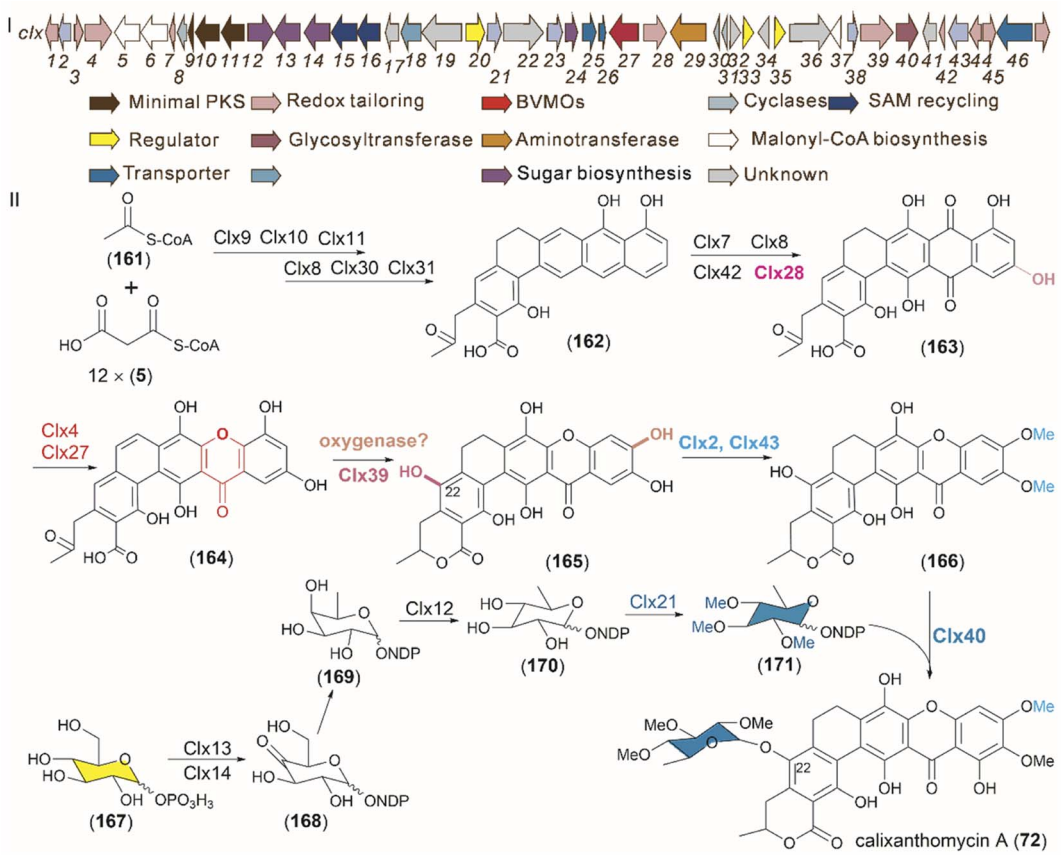

Fig. 26 BGC and proposed biosynthetic pathway of calixanthomycin A.

Published on 09 September 2022. Downloaded by Shanghai Jiaotong University on 10/24/2022 5:38:16 AM.

anthraquinone compound **149** (ref. 113) (Fig. 28). The discovery of **149** was consistent with the previous proposal that xanthone may be derived from the anthraquinone precursor. Whether XanO4 can catalyze the presumed BV oxidation still needs to be answered. XanO4 contains two conserved domains, *i.e.*, a monooxygenase (Pfam01360) domain and FAD binding (Pfam01494) domain.[4] Meanwhile, XanO4 exhibits significant homology to the reported class A FMOs MtmOIV (30% identity)[117] and GrhO5 (42% identity).[111] Typically, MtmOIV is referred to as a representative-type 'O' BVMO[118] responsible for the BV-type oxidative cleavage of the polycyclic scaffold in the biosynthesis of mithramycin. Type 'O' BVMOs is encoded by a single gene and belongs to class A FMOs without the typical "BVMO" fingerprint sequence FXGXXXHXXXWP. The typical "BVMO" sequence was

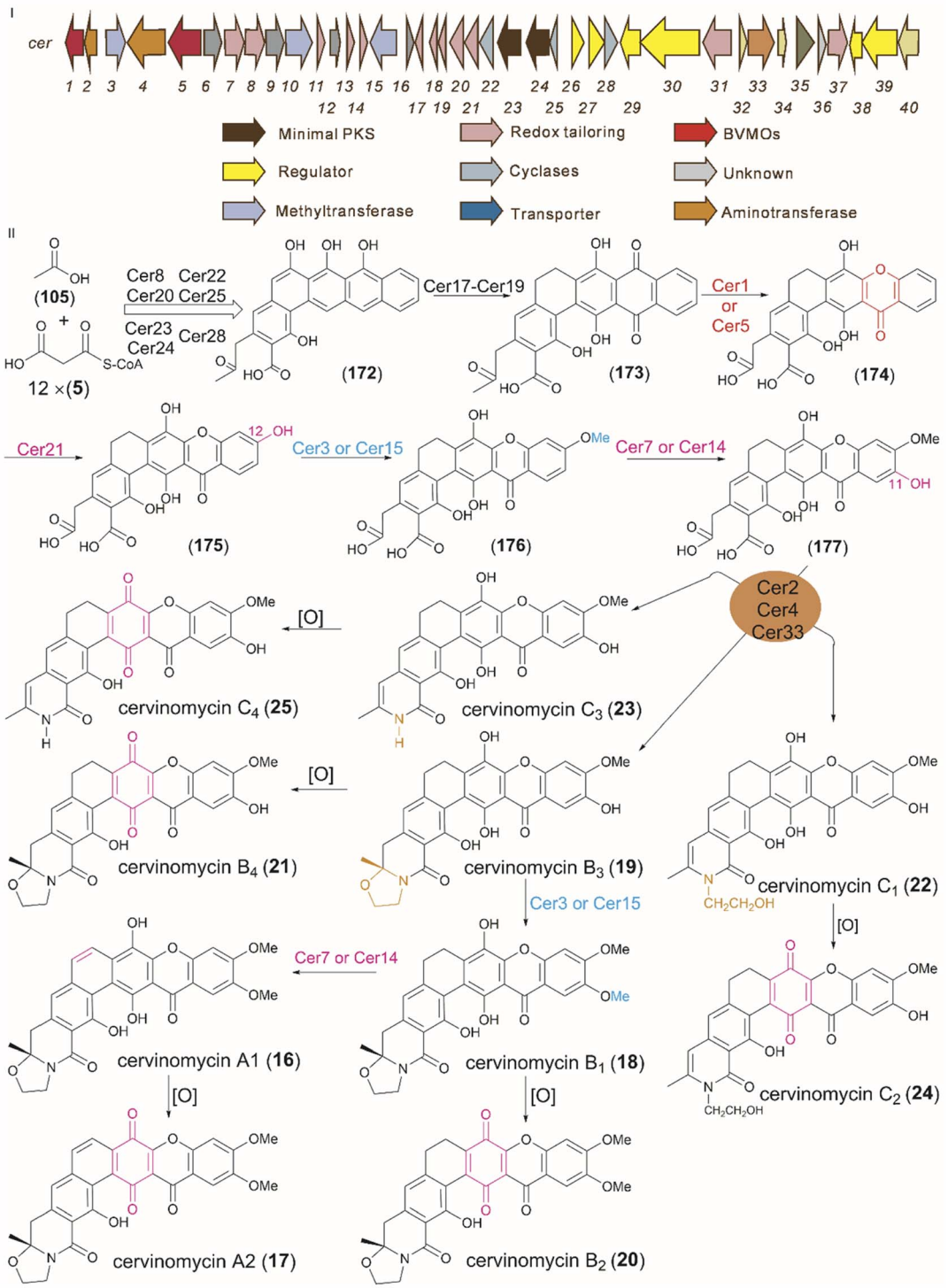

Fig. 27 BGC and the proposed biosynthesis pathway of cervinomycins.

 This journal is © The Royal Society of Chemistry 2022

Published on 09 September 2022. Downloaded by Shanghai Jiaotong University on 10/24/2022 5:38:16 AM.

not found in XanO4, but the conserved FAD-binding motif GXGXXG and typical NAD(P)H binding motif have been identified.[4] Moreover, XanO4 exhibits high sequence identity with other FMOs including LlpOVIII (70% identity), PnxO4 (45% identity), and Arx30 (60% identity) encoded by BGCs of lysolipins (**81** and **82**), FD-594 (**75**), and arixanthomycins (**38–40**), respectively. Moreover, phylogenetic analysis showed that XanO4 clusters into the same clade with MtmOIV and GrhO5 and forms a small well-supported subclade with the FMOs from the BGCs of BPXNPs. This suggests that these FMOs may possess similar function in the biosynthesis of BPXNPs.

To verify whether XanO4 is responsible for the formation of the xanthone nucleus, compound **149** was used as a substrate in an *in vitro* assay.[4] LC-MS analysis of the reaction products suggested a loss of 26 Da (not 12 Da) from **149**, indicating the absence of two carbon atoms and two hydrogen atoms (Fig. 28I). Structural analysis of the reaction product **178** confirmed the formation of xanthone and the removal of the methyl group at C17-hydroxyl group. The loss of a methyl group suggested that the oxidative transformation of anthraquinone **149** to xanthone **178** is accompanied by demethylation. According to the common oxidative demethylation mechanism, the *N*- or *C*-methyl moiety is firstly hydroxylated to a hemiaminal intermediate, and then the methyl group will be spontaneously eliminated in the form of formaldehyde.[119] Sodium bisulfate was reported to form a hydroxymethane sulfonate adduct with formaldehyde, which could be used to detect formaldehyde.[120] However, no mass signal corresponding to the adduct was found in the reaction system of XanO4. To illustrate the origin of the oxygen atoms at C15 and C17, $^{18}O_2$ was used to replace $^{16}O_2$ in the *in vitro* enzymatic reaction systems. LC-MS analysis revealed the incorporation of one and two labeled oxygen atoms (Fig. 28II). Meanwhile, the oxygen atom from H_2O^{18} could not be incorporated in **178**.[4] The incorporation of oxygen atoms was consistent with the label type of lysolipin X[52] (**82**) (Fig. 20I). In particular, the incorporation of an oxygen atom in the positions corresponding to O15 in **82** suggested that the construction of xanthone involves BV oxidation, followed by rearrangement through decarbonylation (Fig. 20IIa) or decarboxylation (Fig. 20IIb). However, the incorporation of oxygen in **157** indicated that besides the expected insertion of oxygen in the tricyclic xanthone, another oxygen atom derived from molecular oxygen is inserted at C17 and the C17 methoxy group in **149** is likely disposed in the form of methanol (**180**) (Fig. 28II).

To unveil the possible enzymatic mechanism, You's group conducted multiple sequence alignments of XanO4 with MtmOIV. The alignments suggested that the conserved arginine residue R45 corresponds to R52 in MtmOIV, which has been suggested to be important for FAD-binding and the BV oxidation reaction in the biosynthesis of mithramycin.[121] Incubation of the XanO4-R45A mutant with **149** did not result in the production of **178**, but yielded another new product **181**. MS analysis of **181** revealed that it is 14 Da less than that of **149**, suggesting the loss of CH_2. Comparative NMR analysis of the signals at C17 and C15 supported the molecular structure of **181** as a demethylated anthraquinone. The 12 Da loss from **149** to

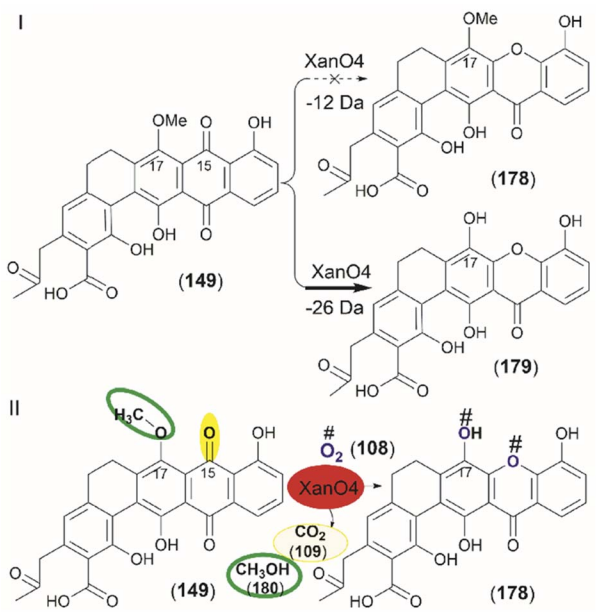

Fig. 28 Xanthone ring formation catalyzed by XanO4.

181 in the *in vitro* assay of XanO4-R45A with $^{18}O_2$ confirmed the demethoxylation activity (Fig. 29).[4]

These works revealed that XanO4 catalyzes the oxidative replacement of the carbonyl group at C15 and methoxy group at C17 in anthraquinone **149**, resulting in the formation of the xanthone ring and demethoxylation (Fig. 29). The unexpected demethoxylation is likely facilitated by methanol as the leaving group. However, the xanthone ring could not be constructed in demethylated anthraquinone **181** (Fig. 29), suggesting the importance of the methoxy group at C17 for the formation of xanthone. Meanwhile, in the mutant XanO4-R45A, the demethoxylation reaction occurred without the formation of xanthone (Fig. 29), suggesting the necessity of R45.

Taking all the findings into account, You's group postulated the enzymatic mechanism for XanO4 (Fig. 30). Firstly, the multifunctional XanO4 was proposed to catalyze the oxidation at C17, potentially *via* epoxide intermediate **183**. The

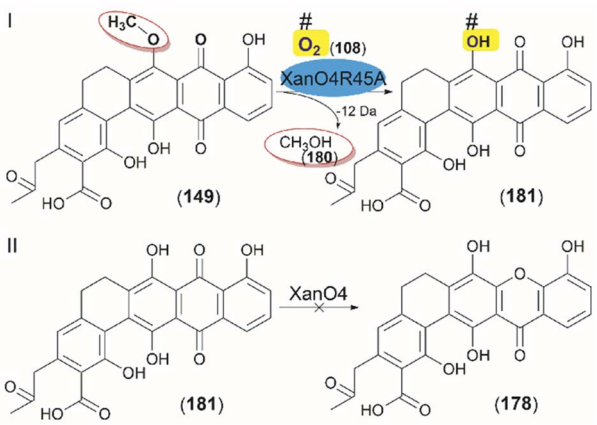

Fig. 29 Demethoxylation reaction catalyzed by XanO4R45A.

Published on 09 September 2022. Downloaded by Shanghai Jiaotong University on 10/24/2022 5:38:16 AM.

epoxidation breaks the ring aromaticity and permits the subsequent BV oxidation for the formation of **185** and ring cleavage (Fig. 30I). The ring cleavage is followed by decarboxylation, disposing the C17 methoxy as methanol (**180**) and leading to the formation of the xanthone ring. This made the reaction a novel type compared to the previously reported BV oxidations. The classic BV oxidative oxygen insertion for the lactone formation in neopentalenolactone D represents a new branch of the pentalenolactone biosynthetic pathway.[93] MtmOIV was reported to catalyze the oxidative C–C bond cleavage *via* BV oxidation and decarboxylation.[117] Moreover, a BVMO tailoring domain within a hybrid acyltransferase-less (AT-less) PKS/nonribosomal peptide synthetase (NRPS) system was characterized to catalyze the BV oxidation of an acyl carrier protein (ACP)-tethered thioester to an ACP-linked thiocarbonate, which represents the first example of BVMOs operating *in cis* in the PKS and NRPS biosynthetic paradigm.[94] Recently, a multifunctional BVMO CcsB was elucidated to catalyze the formation of an in-line carbonate in the macrocyclic portion of cytochalasin E, making FMO a potent potential catalyst for the transformation of ketones into carbonates.[122] The reactions catalyzed by XanO4 expand the inventory of FMO-mediated reactions.

This proposed anthraquinone-to-xanthone conversion catalyzed by XanO4 shows similarity to the three enzyme-catalyzed conversions of anthraquinone versicolorin A to demethylsterigmatocystin. These conversions involve epoxidation, BV-type rearrangement and decarboxylation, and occur in a deduced oxidation-reduction-oxidation sequence.[123] Regarding the formation of the xanthone ring, the enzymatic machineries in fungi (more than three oxidoreductases work together) and plants (cytochrome P450 monooxygenases act on two central intermediates *via* intramolecular oxidative coupling) are different from that of XanO4 (see Section 4.4). In xantholipin (**33**), the reactions required for xanthone ring formation and demethoxylation (BV oxidation, decarboxylation and oxidative demethoxylation) are accomplished by the single multifunctional XanO4 (Fig. 30I). Compared with the more complicated

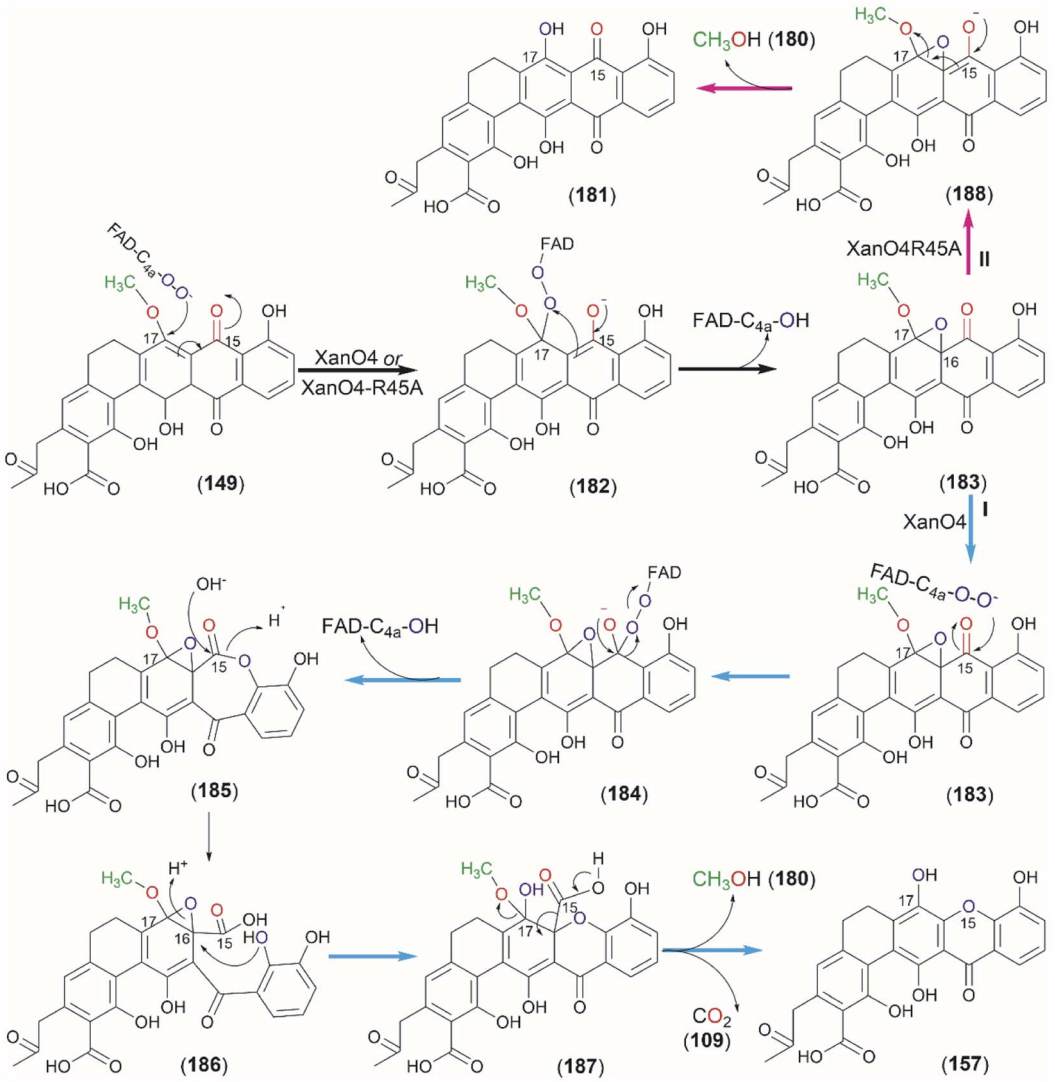

Fig. 30 Proposed mechanism of XanO4.

 This journal is © The Royal Society of Chemistry 2022

Published on 09 September 2022. Downloaded by Shanghai Jiaotong University on 10/24/2022 5:38:16 AM.

xanthone construction machineries in fungi and plants, XanO4-like-mediated xanthone ring formation in bacteria seems to be more economic and efficient. During this process, C17 oxidation was deemed to prime anthraquinone **149** for BV oxidation and rearrangement, while the methoxy group also serves as a better leaving group than hydroxyl, and hence it is essential for the formation of xanthone.[4] For XanO4R45A, the formation of **183** breaks the aromaticity of rings B and C and permits the opening of the epoxy ring, removing the C17 methoxy as methanol (**180**) (Fig. 30II). This was an unprecedented case in which direct oxidative replacement of a carbonyl group in anthraquinone led to the formation of the xanthone ring. Although similar chemical oxidative replacement of a carbonyl group[124–127] has been reported, this reaction requires a more complex substrate structure and multi-step synthesis.

The genetic and biochemical characterization of *xanO4* homologs (*ax30* (ref. 122) and *llpOVIII*[52]) confirmed the transformation of anthraquinone to xanthone in the biosynthesis of related BPXNPs.[4] Therefore, XanO4-mediated xanthone formation can be a common mechanism for BPXNPs. This means XanO4 and its homologues provide a potentially green alternative chemical or chemoenzymatic route for the synthesis of the xanthone intermediate, which may be beneficial in addressing the growing demand for novel chemotherapeutic agents.

However, it remains unknown whether there are other possible mechanisms for the formation of the xanthone ring. The isotopic oxygen atom insertion in **157** and **82** confirmed the proposal that BV oxidation is involved in the formation of xanthone. Meanwhile, in lysolipin I (**81**), simaomicin α (**57**) and MS 901809 (**73**), the arrangement consistency of the two-carbon unit of ring A with that of rings B–F suggests the previous proposal of direct cyclization without ring A rotation (Fig. 31, pathway a). Alternatively, in citreamicin α (**46**), the xanthone oxygen atoms arise from the building block unit, and the orientation of the two-carbon unit of ring A is different from that of rings B–F. The same type can be found in FD-594 (**75**). It can be hypothesized that rotation of the aromatic ring A is involved in the formation of the xanthone ring in **46** and **75** (Fig. 31, pathway b). These findings suggest a different mechanism from that of XanO4. Future enzymatic study of PnxO4 will provide direct proof and improve the understanding of the biosynthesis of BPXNPs.

4.3.2 Methylations essential for xantholipin biosynthesis. Besides the construction of the xanthone ring, the second contribution by You's group is the unveiling of the cryptic remethylation on the newly formed C17 hydroxyl group, resulting from demethoxylation. Considering the presence of a methylene carbon atom between C17 and C19 in **33**, remethylation of the hydroxyl group at C17 occurs after xanthone formation undoubtedly. An *O*-methyl group at the position corresponding to C17 in **33** can be found in the intermediates or final products of lysolipins (**81** and **82**), arixanthomycin B (**39**), FD-594 (**75**) and other structurally-related BPXNPs such as turbinmicin (**77**). Moreover, the isolation and structural characterization of the dechlorinated naphthaxanthone intermediate **179** from *ΔxanH* mutant confirmed the remethylation at C17.[4] Three OMTs, *i.e.*, XanM1–M3, are

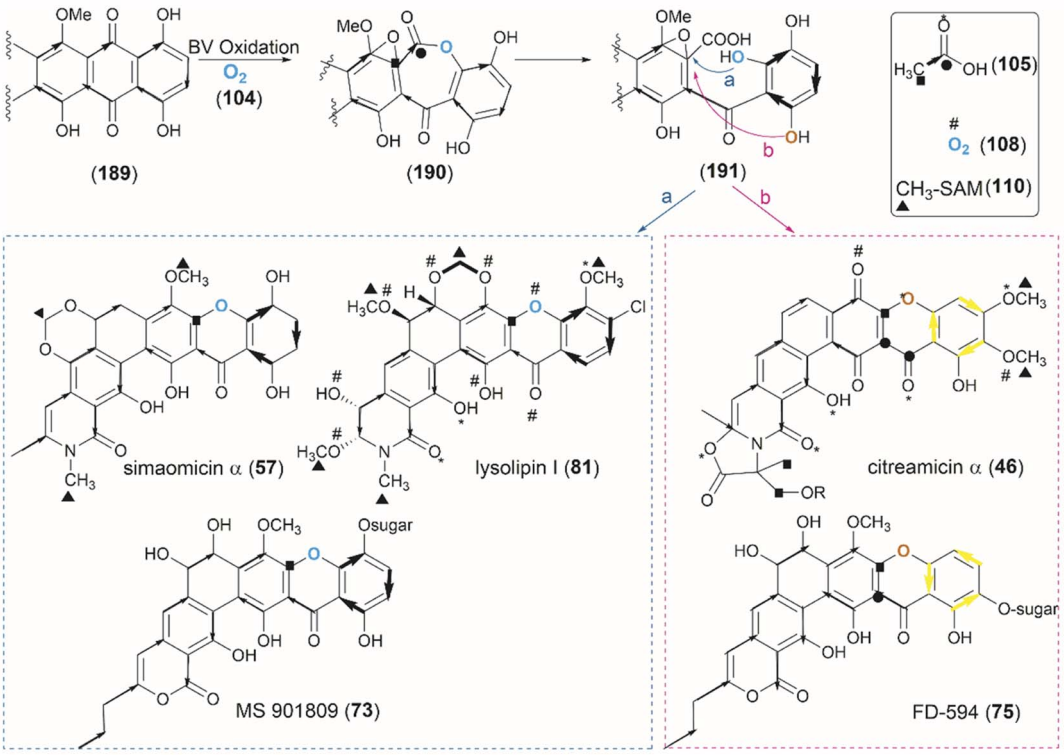

Fig. 31 Divergent biosynthetic routes of BPXNPs.

Published on 09 September 2022. Downloaded by Shanghai Jiaotong University on 10/24/2022 5:38:16 AM.

encoded in the *xan* cluster. To unveil the functions of XanM1–M3, You's group performed genetic interruptions of *xanM1–M3* and *in vitro* enzymatic assays of XanM1–M3.[128] They found that XanM1–M3 catalyze three specific regiospecific methylations, modulating the biosynthesis of **33** from the beginning to end (Fig. 32). Initially, it appeared that without XanM1, the nascent polyketide could not be released from the PKS given that neither **33** nor any intermediate could be detected in the *ΔxanM1* mutant. The oxidative formation of the xanthone ring by XanO4 is dependent on a cryptic demethylation step at C17-OMe, which is most likely added by XanM1 during the maturation of the nascent polyketide intermediate **148** into **149**. The demethylated C17-OH on xanthone **179** is immediately remethylated by XanM3, hence making the demethylation cryptic in the biosynthetic pathway. It was also observed that the demethylated anthraquinone **181** resulting from partial conversion by XanO4 could be recycled back into the pathway *via* remethylation of the C17-OH by XanM3 and partially by XanM2. Finally, after the formation of the pyridine *via* lactamization followed by hydroxylation at C19, XanM2 is the major OMT that methylates the C13-OH of **192** to form **152**. However, this C13-OH-methylation activity can also be partially complimented by XanM1 and XanM3. This C13-methoxyl group is likely necessary for the formation of the methylene dioxygen bridge catalyzed by cytochrome P450 XanO2 as the gene disruption resulted in the accumulation of compound **152** without the production of **33**. Taken together, each of the three multifunctional OMTs, XanM1–M3, possesses minor catalytic activities that overlap with the other OMTs besides their major function. However, despite their catalytic overlap, XanM1–M3 exhibited high substrate-dependent regiospecificity. Substrate-dependent regioselectivity has not been reported for OMTs but appears to be more commonly reported for multifunctional oxygenases, especially P450s such as MycG,[129] AurH,[130] TamI[131] and GfsF.[132] These enzymes catalyze multiple reactions in a highly ordered fashion at separate sites, starting with a single substrate molecule. Moreover, the substrate-dependent regioselectivity of these P450s can be attributed to the conformation variation and binding pockets changes when reacted with different substrates.[128] It is worth discovering whether the multifunctional OMTs XanM1–M3 use similar strategies to alter the regioselectivity. Nevertheless, multiple methylations have already been reported in the biosynthesis of gentamicin[133] and spinosyn.[134] With the complicated methylations, early biosynthetic intermediates are ectopically modified by the major activities of OMTs and minor activities of these OMTs contribute to the branched methylation network. However, only one productive methylation route has been found for the rhamnose moiety.[134] Possibly, the functional redundancy of the three OMTs, XanM1–M3, may serve as a mechanism to ensure that all biosynthetic intermediates in the pathway are directed toward **33**.[128]

Another interesting finding accompanying the methylation modification by You's group was the exploration on the origin of

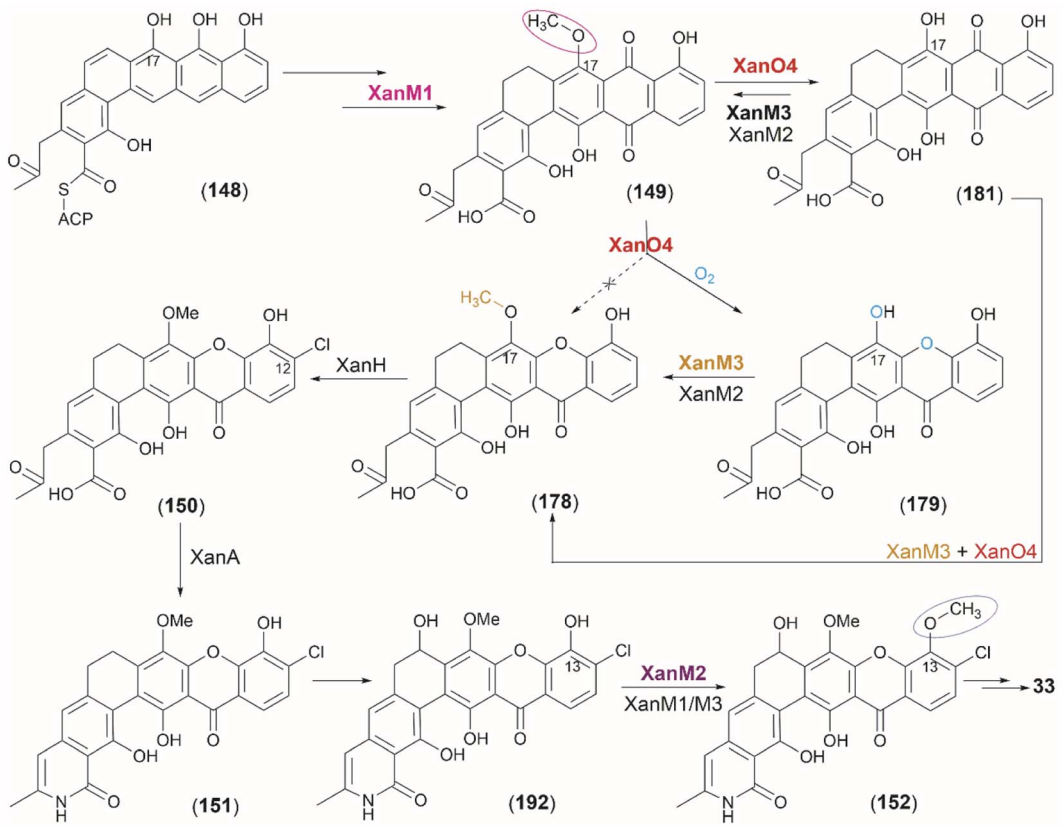

Fig. 32 Methylations involved in the biosynthesis of xantholipin.

 This journal is © The Royal Society of Chemistry 2022

Published on 09 September 2022. Downloaded by Shanghai Jiaotong University on 10/24/2022 5:38:16 AM.

the three homologous OMTs. The origin of new genes is a fundamental biological question. Gene duplication provides a source for genetic evolution. Also, a new gene is proposed to be derived from a new secondary minor function of ancestral gene with selective advantages (innovation); subsequent selection favoring the minor function resulted in duplications of the genes (amplification), and the increased copy number provides multiple targets for beneficial mutations. During continuous growth under continuous selection, new gene with beneficial mutations will accumulate (divergence).[135] This innovation–amplification–divergence (IAD) model allows the study of gene evolution in real time. Methylation is a common modification in BPXNPs and OMTs encoding genes have been identified in other BGCs of BPXNPs. XanM1–M3 share moderate sequence identity and form a small clade with the homologous OMTs LlpMII, LlpMIII, LlpMIV, and LlpMVI in the *llp* cluster.[128] All these OMTs were proposed to evolve from a common multifunctional ancestor shared with Arx34 from the *arx* cluster encoding arixanthomycins (**21–23**). To support this proposal, the four most possible ancestral proteins for XanM1–M3 were reconstructed, expressed, purified and characterized.[128] One versatile ancestral protein possessing all the activities of XanM1–M3 was identified. Therefore, it was proposed that the promiscuous common ancestor of homologous OMTs from the *xan* and *llp* clusters obtained new catalytic activities before divergence, possibly following the innovation-amplification-divergence (IAD) model.[135,136] Meanwhile, the nonhomologous OMTs encoded by the *llp*, *arx* and *pnx* clusters could be responsible for the structure differences among the corresponding BPXNPs. These studies provided new insights into the directed evolution for diversifying natural product pathways to generate chemical diversity.

4.3.3 Halogenation involved in xantholipin biosynthesis. Besides redox and methylation, chlorination is also a prevalent reaction acting on the aromatic phenolic ring of BPXNPs. For natural products, most of the halogen substituents have been proven to play important roles in tuning new or improved activities and enhancing their pharmacological efficacy.[137] Nature has evolved six families of halogenases with diverse elegant mechanisms to regioselectively halogenate a diverse range of active natural compounds.[137] Enzymatic halogenations exhibit good selectivity and are environmentally friendly processes, setting an important stage for the development of biocatalysts to biosynthesize active substances and construct new synthetic routes.[138] However, the research in halogenating enzymes is still in its infancy.

Many BPXNPs are halogenated, such as xantholipin (**33**), lysolipins (**81** and **82**), kibdelones (**59–61**), and isokibdelones (**75–77**). These halogenated compounds exhibited potent and selective cytotoxicity against cancer cells. However, the role of chlorine atoms in their biological activities has not been systematically illustrated to date. To explore the chlorination mechanism and provide insight into the future recombinatorial biosynthesis of halogenated BPXNPs, You's group demonstrated the function of a candidate halogenase XanH.[128] XanH possesses the typical GXGXXG motif and the conserved WxWxIP catalytic motif of FAD-dependent halogenase (FDHs).[137] The *in vitro* assay proved that XanH is a bifunctional FDH that reduces FAD by the oxidation of NADH and chlorinated methylated anthraxanthone **178** (Fig. 32).[128] Therefore, XanH is definitely an FDH that can accept freely diffusing substrates with aromatic scaffolds different from the exclusively studied tryptophan halogenases such as PrnA.[139,140] This finding suggests that XanH can be a potential material for the development of biocatalysts with different molecular skeletons. However, the increased k_{cat}/K_m of XanH with the addition of extra flavin reductase (FDR) proposed a tedious problem for future engineering development. To facilitate the engineering construction of XanH derivative proteins, self-sufficient FDR-XanH fusion proteins were successfully constructed.[128] The successful identification of one fusion protein E1 with comparable activities may be a good alternative for future protein engineering. These findings can further improve the understanding of the biosynthesis of BPXNPs.

4.4 Xanthone biosynthesis in fungi and plants

Owing to the "privileged structure" and various activities of xanthones, they have attracted immense attention regarding their structures, biological functions, chemical synthesis, and biosynthetic pathways.[141] Xanthones from fungi are biosynthesized by distinct pathways but all fungal xanthones are considered to be derived from the common anthraquinone precursors emodin (**195**), questin (**196**) and chrysophanol (**197**)[142–144] (Fig. 33). **195** was synthesized by a nonreducing PKS and could be transformed into **196** and **197** (Fig. 33). Bioinformatic analysis and genetic manipulations of the genes in the *nsr* cluster contributed to the proposal of xanthone formation in neosartorin.[144] The xanthones were proposed to be derived from a single acetate-derived polyketide precursor and the polyketide chain was then cyclized to form **197**. Three enzymes, including BVMO NsrF, methyltransferase NsrG and FMO NsrK, were proposed involved in the formation of xanthone. NsrF catalyzed the BV-type oxidative insertion of one oxygen atom in **197** at two different positions, giving rise to two lactones (**198** and **199**). After the hydrolysis of lactones, NsrG catalyzed the methylesterification of the carboxyl group, giving **198** and **199**. NsrK served as an epoxidase and facilitated the addition of phenol to the electrophilic A-ring and gave tricyclic xanthones **204** and **205** (Fig. 33).[143] The insertion of an oxygen atom at two different positions indicated the promiscuous activity of NsrF toward aromatic rings A and C. This promiscuity diverged the formation of different xanthones. However, AacuH, a homologous BVMO of NsrF, selectively oxidized **197** and altered the metabolic profile for the production of **206** (Fig. 33).[143]

In chemoenzymatic assays, MdpC involved in the biosynthesis of monodictyphenone was proven to catalyze the reduction of **195**, giving two tautomeric forms of emodin hydroquinones (**208** and **209**) (Fig. 34I).[142] Four proteins, *i.e.*, AgnL8, AgnL6, AgnL4 and AgnL3, were found to be homologous proteins of MdpB, MdpC, MdpK and MdpL, respectively. In the biosynthetic machinery of agnestins, AgnL4 firstly reduces emodin (**195**) to its hydroquinone (**208**), which is then reduced

Published on 09 September 2022. Downloaded by Shanghai Jiaotong University on 10/24/2022 5:38:16 AM.

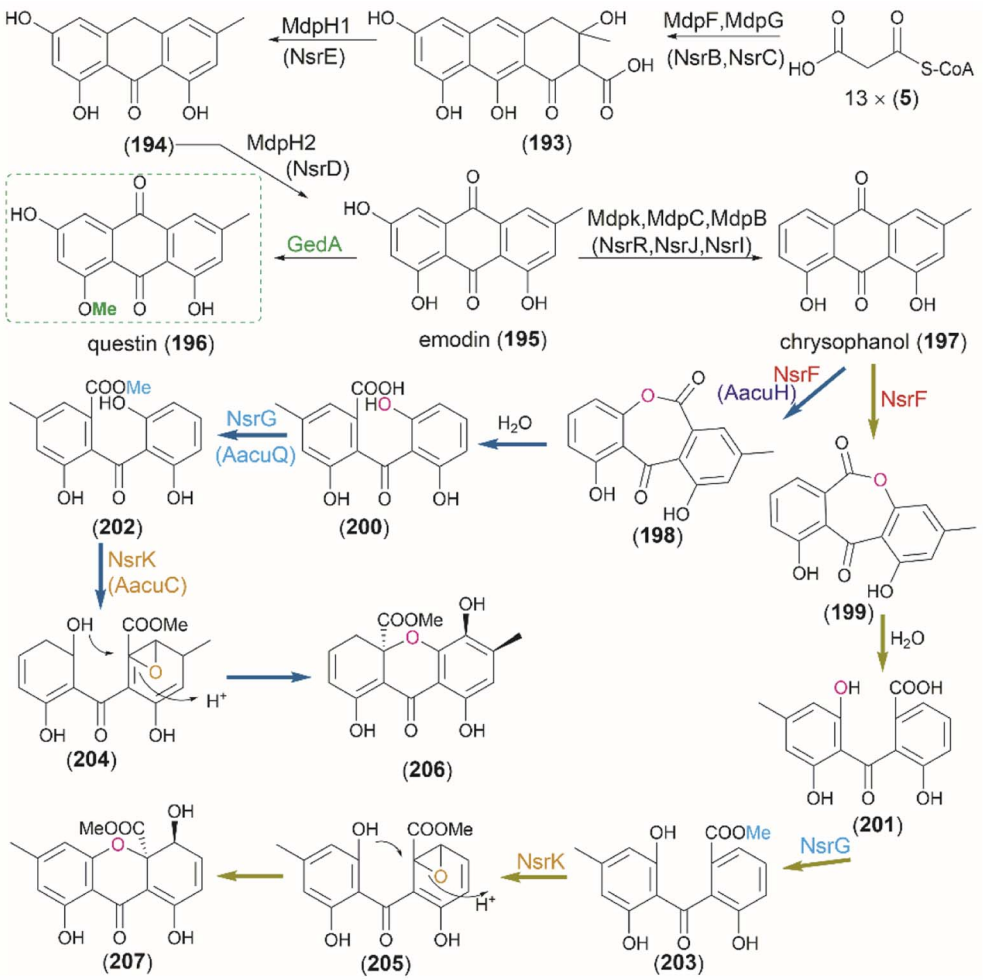

Fig. 33 Formation of xanthone catalyzed by NsrF.

to hydroxyketone (**212**). Subsequently, AgnL8 mediates dehydration, giving **197**. BV oxidation catalyzed by AgnL3 combined with the subsequent hydrolysis of monodictylactone (**198**) results in the formation of monodictyphenone (**213**).[145] Comparative analysis of homologous BGCs suggested the generality of the successive reactions for fungal xanthones, such as cryptosporioptide.[146] The identification of reductases AgnL4 (MdpK, DmxR7 (ref. 145) and PhoK[147]) responsible for *in vivo* anthraquinone reduction confirmed the previously postulated essential step in the aromatic deoxygenation of **195** to **197** (Fig. 34II)[142] and phomoxanthones.[147] Similarly, data from genetic manipulation, enzymatic assays and ^{18}O chasing experiments confirmed that reductase GedF was responsible for the reduction of questin (**197**) into questin hydroquinone (**220**), and the dioxygenase GedK catalyzed the intramolecular cleavage, giving rise to desmethylsulochrin (**221**) (Fig. 34III). Based on the phylogenetic analysis and successful broad substrate specificity assay of GedK, this bienzyme-catalytic and dioxygenation-mediated anthraquinone ring-opening mechanism seemed to be general in the biosynthesis of diverse fungal secoanthraquinone.[148] GedF and GedK provide a new ring cleavage mechanism for the construction of xanthone and will contribute to completely solving the long mystery of key steps in the fungal biosynthesis of xanthone.

The xanthones of plant origin are simple xanthones, glycosylated xanthones and prenylated xanthones. Their biosynthesis pathway involves the mixed shikimate pathway and type III PKS (called benzophenone synthase (BPS)) routes. The former pathway provides L-phenylalanine (**222**), while the latter catalyzes polyketide chain formation for the construction of two central 2,3′,4,6-tetrahydroxybenzophenones (2,3′,4,6-tetraHBP) (**232** and **233**, Fig. 35). Based on feeding studies with isotope-labeled precursors, two parallel pathways for the formation of **232** and **233** were proposed (Fig. 35). In the *Hypericaceae* family, **222** was transformed to **224**, which was then activated by benzoate-CoA ligase (BZL). The resultant benzoyl-CoA (**225**) was used to produce 2,4,6-trihydroxybenzophenone (2,4,6-triHBP, **226**).[149] In the *Gentianaceae* family, **227** was activated in the form of 3-hydroxybenzoate-CoA (**228**) and involved in the biosynthesis of **232** and **233**. Benzophenone 3′-hydroxylase (B3′H), HpCYP81AA1 and HpCYP81AA2 could catalyze the transformation of **226** to **232** and **233** (Fig. 35).[150] Meanwhile, HpCYP81AA1 and HpCYP81AA2 also catalyzed the subsequent C–O phenol coupling to form 1,3,7-trihydroxyxanthone (1,3,7-

 This journal is © The Royal Society of Chemistry 2022

Published on 09 September 2022. Downloaded by Shanghai Jiaotong University on 10/24/2022 5:38:16 AM.

THX, **236**) and 1,3,5-trihydroxyxanthone (1,3,5-THX, **237**) (Fig. 35).[150] The bifunctional HpCYP81AA1 and HpCYP81AA2 serve as regioselective phenol coupling mechanisms in the biosynthesis of plant xanthone. Moreover, 2,4,5′,6-tetrahydroxybenzophenone-2′-*O*-glucoside (**238**) and the subsequent acid or unknown enzymatic hydrolysis directly lead to the formation of **236**.[151]

Taken together, the tricyclic xanthone formation approaches involving multiple enzymes in fungi and plants are more complex than the multifunctional XanO4-mediated strategy in bacteria. Different xanthone construction approaches suggest the chemoenzymatic diversities utilized by bacteria, fungi and plants. These findings provide alternative candidates for the future engineering development of biocatalysts for the construction of xanthone derivatives.

4.5 Biosynthetic perspectives

The biosynthetic studies of xantholipin (**33**) provide vital clues for the future machinery proposal of recently discovered BPXNPs (Fig. 36). Considering the structural similarity and existence of homologous genes in BGCs, xantholipin B (**54**), dehydroxantholipin (**35**), sattahipmycin (**37**), actinomadurone (**76**) and turbinmicin (**77**) may share partial biosynthetic machinery with **33**. Even with a halogenase SatZ (81% sequence identity to XanH), C12 is not chlorinated in **37**. The absence of chlorination may have resulted from the inactivation of SatZ or

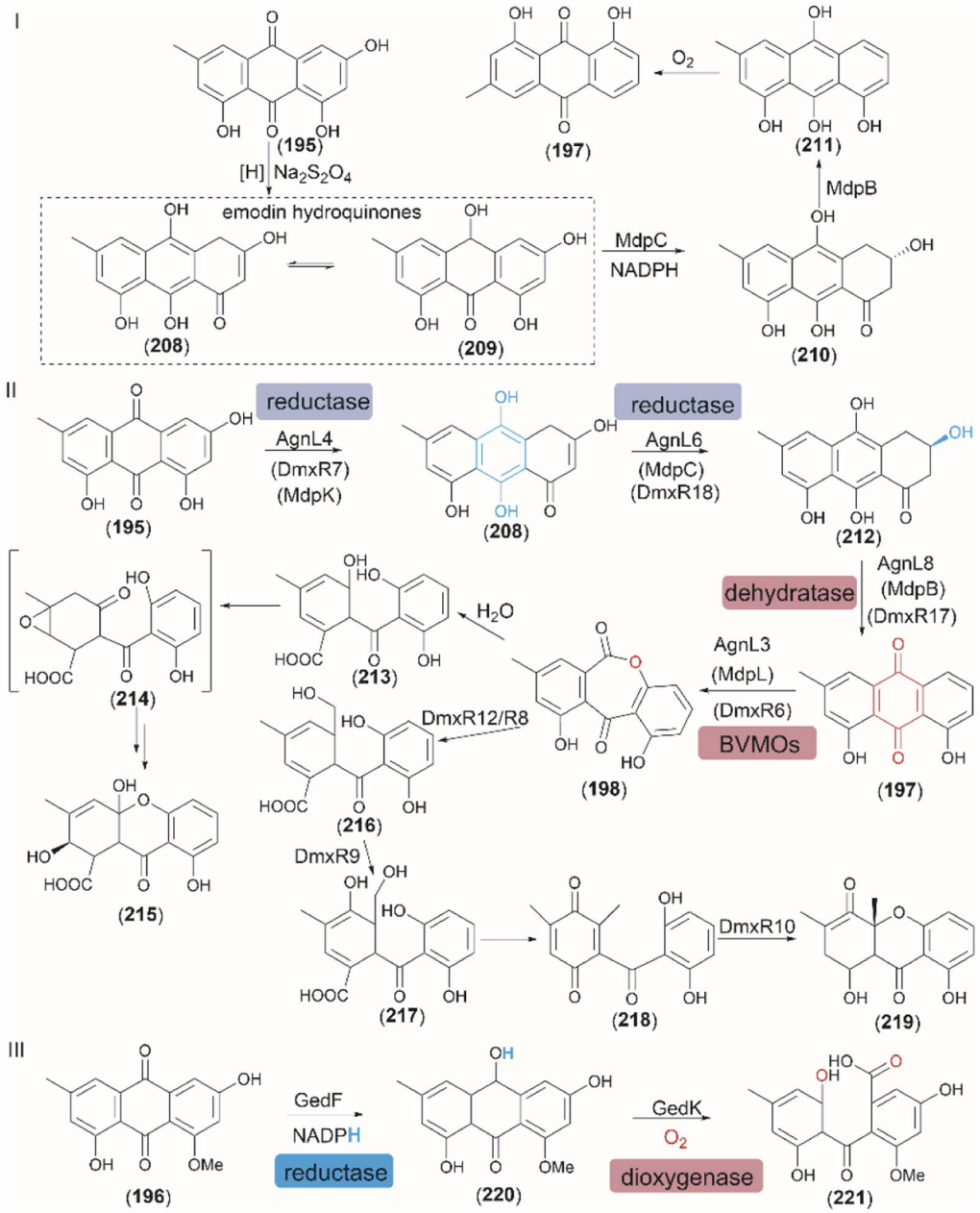

Fig. 34 Xanthone formation initiated by indispensable reductases.

Published on 09 September 2022. Downloaded by Shanghai Jiaotong University on 10/24/2022 5:38:16 AM.

silencing of the *satZ* gene. For the biosynthesis of **76** and **77**, two possible acyltransferases will catalyze the acylation at C11 in ring A. Given that the acylation was reported to enhance the antifungal activity of **77**, future characterization of the acyltransferase will benefit the engineering biosynthesis of new BPXNP derivatives against fungal pathogens. Meanwhile, **76** and **77** are two BPXNPs with tetrahydrooxygen xanthone, their future studies will extend our understanding of the biosynthesis of BPXNPs.

Future biosynthetic research of BPXNPs will have to address four major goals. Firstly, many BPXNPs possess nitrogen-containing heterocycles (ring F). These nitrogen heterocyclic structures have been proven to be vital for the biological activities of nitrogen heterocyclic natural products.[152] Among the BPXNPs possessing nitrogen heterocycles, cervinomycin C_2 (**17**) was about 80-fold more active against HCT116 cell than cervinomycin C_4 (**25**),[19] and the only structural difference is the substituents in the nitrogen-hetero cycle (ring F). Similarly, without the nitrogen atom in ring F, citreamicin θ analogues showed no obvious activities against *Staphylococcus aureus* ATCC 43300 and no cytotoxicity against even HeLa cells.[20] Another similar case is that biosynthetic intermediates **178** and **150** involved in the biosynthesis of xantholipin (**33**) were about 10^2- to 10^3-fold less potent against a lung cancer cell line, a colon cancer cell line, and a leukemia cell line.[113] These findings suggest the essentiality of the five-membered nitrogen-containing heterocycle for biological activity. Several BPXNPs contain both a nitrogen heterocycle (ring F) and oxazolidine ring (ring G). In arixanthomycins (**38–40**), the oxazolidine ring likely arises from the coupling of a serine to the terminal polyketide carboxylic acid and a spontaneous intramolecular cyclization (Fig. 24). In kigamicins (**41–45**), the oxazolidine ring G may arise from the incorporation of an ethanolamine or alanine. In cervinomycins (**16–25**), the selectivities on nitrogen donors of aminotransferases may contribute to the molecular diversity of cervinomycins (Fig. 27). The known BGCs for BPXNPs with ring F (with or without ring G) encode homologous aminotransferases XanA, LlpA, Arx5, Cer2/4/33 and SatK. Future identification of these enzymes will improve our understanding of the construction of nitrogen-containing heterocycle BPXNPs and may guide the recombinational biosynthesis of "unnatural" BPXNPs.

Secondly, additional focus must be directed towards studying the redox reactions (occurring in ring A, ring C and ring E) involved in the biosynthesis of BPXNPs. The oxidation state of ring A is directly correlated with the nature of tricyclic xanthone. For the BPXNPs with known BGCs to date, only albofungins (**78** and **79**) and turbinmicin (**77**) are

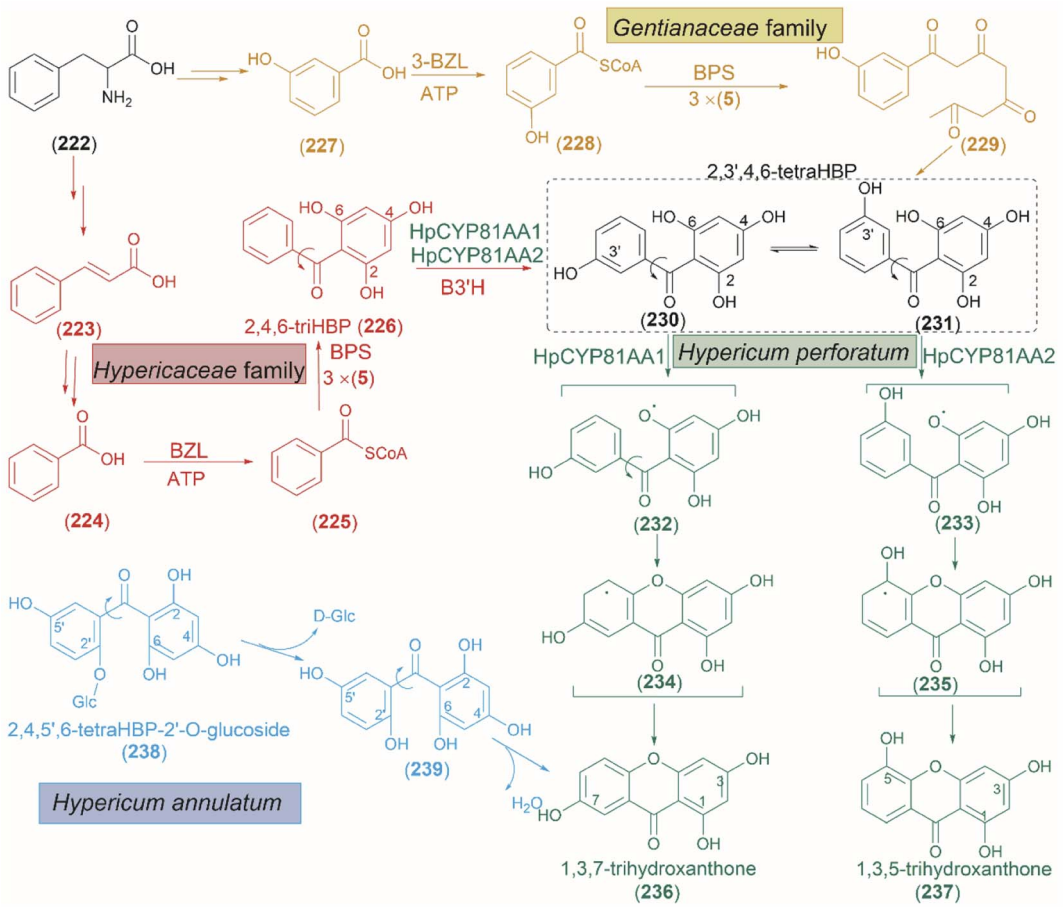

Fig. 35 Xanthone biosynthesis of plant origin.

 This journal is © The Royal Society of Chemistry 2022

Published on 09 September 2022. Downloaded by Shanghai Jiaotong University on 10/24/2022 5:38:16 AM.

tetrahydroxanthone. For **77**, the reduction of ring A may occur at either early stage prior to the formation of aromatic xanthone or late stage before acylation (Fig. 36). Future biosynthetic studies would definitely give a clear answer. Ring C in the form of hydroquinone and benzoquinone can be found in different cervinomycins. This difference affects their biological activities to a certain degree. Thus, enzymatic illustrations of ring C formation will be beneficial for the construction of BPXNP analogues with higher activity. BPXNPs including **33** are highly oxidized molecules and the known BGCs contain many redox genes. Multiple redox reactions still remain to be discovered. For **33**, the inactivation study of the only P450 monooxygenase XanO2 in the *xan* BGC suggested that it may be responsible for catalyzing the reaction between the C19 hydroxyl group and C17 methoxyl group in **152** to form the methylenedioxy bridge (ring H),[153] but further studies are still needed for a clear answer. Subsequent oxygenases responsible for the hydroxylation and oxidation for ring E in **153** can be identified among the remaining redox genes, such as *xanO1* and *xanO3*. However, the reduction of the double bond in ring E of **35** was suggested to be catalyzed by XanZ2, which was supported by the comparative analysis of the molecular structures of dehydroxantholipin (**35**)[59] and sattahipmycin (**37**) to their corresponding BGCs.

Thirdly, biochemical mechanism of the acylations in BPXNPs still need to be discovered. To date, citreamicins (**46–50**), actinomadurone (**76**) and turbinmicin (**77**) are acylated BPXNPs. In **46–50**, the acyl groups vary in the structure and length of the carbon chain. **76** and **77** with a polyene chain were identified. The docking of **77** in the phospholipid binding pocket of Sec14p discovered that its polyene tail extends into a hydrophobic cleft. In **77**, acylation was needed for the remarkable activity against drug-resistant fungi. The responsible acyltransferases for acylations need to be identified and the mechanistic characterization of acylations will contribute to the engineering construction of new BPXNPs.

Finally, two major obstacles for the future large-scale production and drug development of BPXNPs should be settled. One is the low productivity of original producers and the other is their low solubility in most solvents. Each BGC encodes candidate biosynthetic regulators of BPXNPs. The demonstration of biosynthetic regulatory networks will benefit the construction of engineering strains with higher productivity. In the case of the low solubility of BPXNPs, glycosylation is an

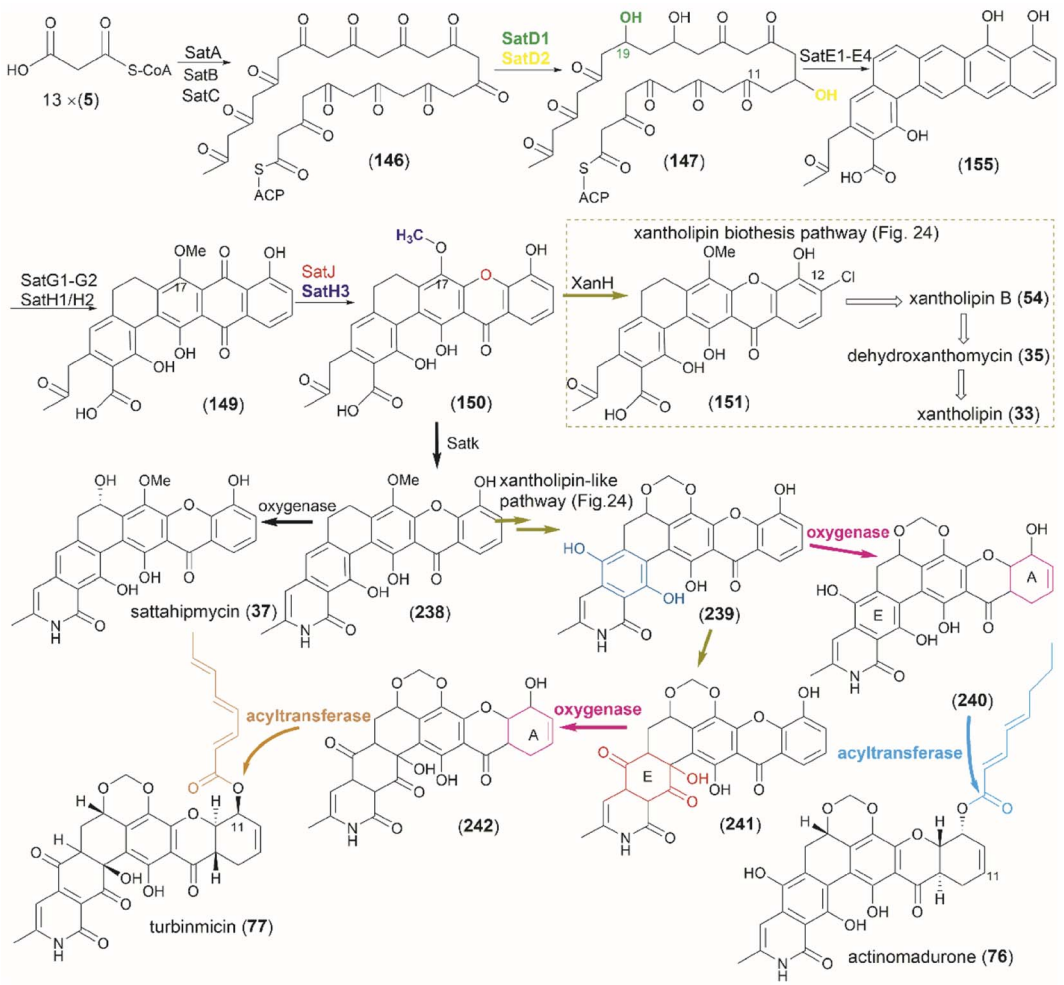

Fig. 36 Proposed biosynthesis of xantholipin-related BPXNPs.

Published on 09 September 2022. Downloaded by Shanghai Jiaotong University on 10/24/2022 5:38:16 AM.

Table 4 Representative total synthesis of BPXNPs[a]

Classification	Academic group	Main starting materials	Steps	Yield (%)	Main methods involved	End product	Ref.
BPXNPs with tetrahydrobenzene ring A	Porco	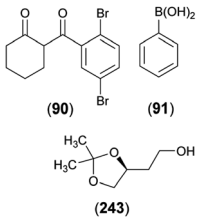 (90) (91) (243)	[I]15 [II]18	[a]3.7 [b]2.6	Pt(IV)-mediated arylation, intramolecular iodo halo-Michael aldol reaction	**12**	89 and 154
	Ready	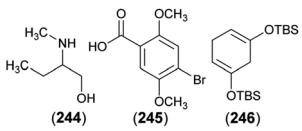 (244) (245) (246)	28	0.5	Sonogashira coupling, Shi epoxidation, acid-catalyzed cyclization	**12**	91
	Gao	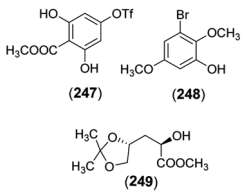 (247) (248) (249)	33	0.07	6π-electrocyclization, InBr3-promoted lactonization, DMAP-mediated oxa-Michael/aldol cascade reaction	**12**	143
	Kelly	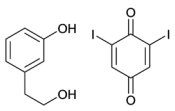 (250) (251)	16	5.97	Heck coupling, 6π photocyclization	**16,17**	65
BPXNPs with hydroquinone ring C	Gao	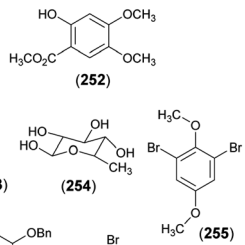 (252) (253) (254) (255) (256) (257)	26	2.68	Intramolecular Friedel–Crafts acylation, palladium-catalyzed Sonogashira cross-coupling, Cu-mediated oxidative phenol coupling	**72**	41
	Martin	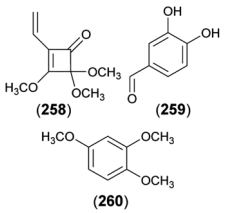 (258) (259) (260)	11	4.6	Moore rearrangement, cyclization, regioselective bromination, coupling of acetylides with hindered ketones	Pentacycle of **50**	163
BPXNPs with oxazolidine ring G	Ready	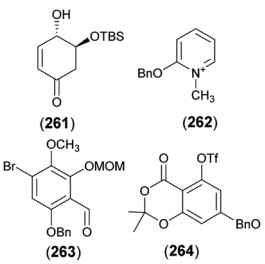 (261) (262) (263) (264)	27	Trace	Oxidative cyclization, Sonogashira coupling	Kigamicin aglycon	161

This journal is © The Royal Society of Chemistry 2022

Published on 09 September 2022. Downloaded by Shanghai Jiaotong University on 10/24/2022 5:38:16 AM.

Table 4 (*Contd.*)

Classification	Academic group	Main starting materials	Steps	Yield (%)	Main methods involved	End product	Ref.
BPXNPs with methylene dioxygen bridge ring H	Ready	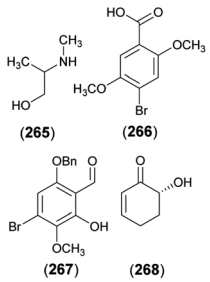 (265) (266) (267) (268)	28	3.7	Asymmetric reduction, C–E biaryl linkage, dehydrogenative coupling, dual C–H functionalization	**57**	160
	Suzuki	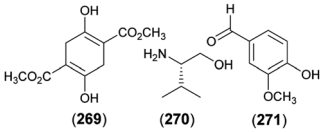 (269) (270) (271)	46	6.3	Heck coupling, SmI2-mediated pinacol cyclization, chirality transfer	**75** aglycon	159
	Martin	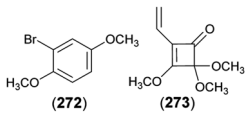 (272) (273)	22	3.1	Direct Moore rearrangement	**66** aglycon	158
Glycosylated BPXNPs	Gao	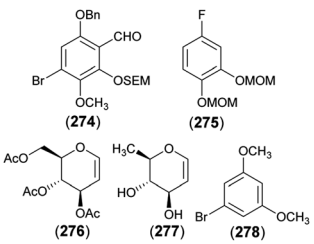 (274) (275) (276) (277) (278)	[III]24 [IV]23 [V]6	[c]12.2 [d]0.45 [e]19.5	Oxidative cyclization, Suzuki–Miyaura coupling, Sonogashira coupling, asymmetric dihydroxylation, Bennett's reliable glycosylation	**75**	162

[a] [a]3.7 and [b]2.6 for **93** synthesis and coupling reaction, respectively. [c]12.2, [d]0.45 and [e]19.5 for fragment synthesis and coupling reaction for **75** synthesis; [I]15 steps for **93** synthesis and [II]18 steps for **12** synthesis by coupling. [III]24, [IV]23 and [V]6 steps for fragments synthesis and coupling reaction.

efficient strategy to improve their solubility. Among the glycosylated BPXNPs, glycosylation occurs at different positions with various types of sugars in different numbers. Therefore, the *O*-glycosylation mechanism of BPXNPs seems to be an attractive field for future research.

In summary, the diverse structures of BPXNPs indicates that bacteria exploit various chemical reactions to construct structural diversity. With the increasing available BGCs for BPXNPs, comparative analysis between BGCs correlated with the structures of BPXNPs will be an effective approach for identifying candidate genes (enzymes). Thorough and detailed information on the enzymatic mechanism will be important for unveiling interesting and useful reactions involved in the biosynthetic machinery of BPXNPs.

5. Chemical synthesis

The unique structural features and compelling biological activities of BPXNPs have sparked academic interest in their total synthesis. However, the establishment of viable synthetic routes is a challenge for the synthetic community, not only due to the partially saturated polycyclic rings but also owing to the chirality on the polycyclic skeleton.[9] Previously, the total synthesis of BPXNPs has mostly been limited to fully aromatic BPXNPs (such as kibdelone C (**12**)[89,91,154–156] and the aglycon of IB-00208 (ref. 157 and 158)). To date, the synthesis of the more challenging BPXNPs with tetrahydroxanthone carrying more than one hydroxyl groups in a ring (such as the asymmetric synthesis of the FD-594 aglycon,[159] simaomicin α (**57**),[160] and aglycon of kigamicin[161,162]) and glycosylated BPXNPs (such as kigamicin[162] and calixanthomycin A (**72**)[41]). Three main strategies are involved in the synthesis of BPXNPs, including the linear strategy, modular strategy and convergent strategy. The methods implied recently during the chemical synthesis of BPXNPs are summarized and tabulated in Table 4, which will hold promise for future endeavors in flexible and efficient approach innovation.

6. Conclusion

Microbial natural products are specialized metabolites endowed with diverse biological activities, and thus are of great

Published on 09 September 2022. Downloaded by Shanghai Jiaotong University on 10/24/2022 5:38:16 AM.

value to society. The diverse biological activities of BPXNPs have inspired both the biological and synthetic communities. Considering the potent biological activities of BPXNPs, they are a group of potential candidates for future clinical trials. However, before that, their industrial large-scale availability is prerequisite. Accordingly, synthetic chemists have made great efforts to construct synthetic routes for BPXNPs. However, chemical synthesis has significant disadvantages, including multiple steps, low yield, and poor regio- and stereo-specificity in the case of the structures of BPXNPs. Synthetic biology can afford a unique opportunity to decipher how biology functions and synthetic biology allows us to intervene in the machinery and modify natural systems to install new functionalities with better physical and chemical properties.[164] The biosynthesis of BPXNPs has the advantages of high efficiency and rigid specificity. The availability and development of modern and advanced genomic sequencing technologies, bioinformatics and biostatistics methods,[165] transcriptomics,[166] proteomics and metabolomics approaches[167] will help in the elucidation of Nature's synthetic machineries for BPXNPs. This review shed light on both the biosynthetic breakthroughs and recent development in the chemical synthesis of BPXNPs. Further progress towards the uncovering of the biosynthetic and biological mechanisms will facilitate a greater understanding of BPXNPs, and ultimately allow the use of synthetic biology approaches to overcome the limitations and address the growing demand for novel chemotherapeutic agents.

7. Author contributions

LXK: conceptualization, data curation, formal analysis, writing-original draft; XZD: conceptualization, formal analysis, funding acquisition; DLY: writing-review & editing, supervision.

8. Conflicts of interest

There are no conflicts to declare.

9. Acknowledgements

This work was supported by a grant from the National Key research and development Program of China (2021YFC2100100, 2021YFA0909500, 2021YFC2100600, 2018YFA0900400), and National Natural Science Foundation of China (32170077, 32170075) and the Startup Fund for Young Faculty at Shanghai Jiao Tong University (SFYF at SJTU) 21X010500720.

10. References

1 M. M. M. Pinto, M. E. Sousa and M. S. J. Nascimento, *Curr. Med. Chem.*, 2005, **12**, 2517–2538.
2 K.-S. Masters and S. Bräse, *Chem. Rev.*, 2012, **112**, 3717–3776.
3 B. Lesch and S. Bräse, *Angew. Chem., Int. Ed. Engl.*, 2004, **43**, 115–118.
4 L. Kong, W. Zhang, Y.-H. Chooi, L. Wang, B. Cao, Z. Deng, Y. Chu and D. You, *Cell Chem. Biol.*, 2016, **23**, 508–516.
5 G. T. Carter, J. J. Goodman, M. J. Torrey, D. B. Borders and S. J. Gould, *J. Org. Chem.*, 1989, **54**, 4321–4323.
6 G. T. Carter, D. B. Borders, J. J. Goodman, J. Ashcroft, M. Greenstein, W. M. Maiese and C. J. Pearce, *J. Chem. Soc., Perkin Trans. 1*, 1991, 2215–2219.
7 H. Bockholt, G. Udvarnoki, J. Rohr, U. Mocek, J. M. Beale and H. G. Floss, *J. Org. Chem.*, 1994, **59**, 2064–2069.
8 K. Kondo, T. Eguchi, K. Kakinuma, K. Mizoue and Y. F. Qiao, *J. Antibiot.*, 1998, **51**, 288–295.
9 D. K. Winter, D. L. Sloman and J. A. Porco Jr, *Nat. Prod. Rep.*, 2013, **30**, 382–391.
10 L. Gales and A. M. Damas, *Curr. Med. Chem.*, 2005, **12**, 2499–2515.
11 F. Jean and D. S. Bohle, *Anti-Infect. Agents Med. Chem.*, 2006, **5**, 15–31.
12 H. Q. Yu, G. Li and H. X. Lou, *Front. Microbiol.*, 2022, **13**, 922089.
13 R. Ratnayake, E. Lacey, S. Tennant, J. H. Gill and R. J. Capon, *Chemistry*, 2007, **13**, 1610–1619.
14 R. Ratnayake, E. Lacey, S. Tennant, J. H. Gill and R. J. Capon, *Org. Lett.*, 2006, **8**, 5267–5270.
15 S. Omura, Y. Iwai, K. Hinotozawa, Y. Takahashi, J. Kato, A. Nakagawa, A. Hirano, H. Shimizu and K. Haneda, *J. Antibiot.*, 1982, **35**, 645–652.
16 S. Omura, A. Nakagawa, K. Kushida and G. Lukacs, *J. Am. Chem. Soc.*, 1986, **108**, 6088–6089.
17 A. Nakagawa, S. Omura, K. Kushida, H. Shimizu and G. Lukacs, *J. Antibiot.*, 1987, **40**, 301–308.
18 X. Hu, X. Hu, X. Hu, S. Li, L. Li, L. Yu, H. Liu, X. You, Z. Wang, L. Li, B. Yang, B. Jiang and L. Wu, *J. Nat. Prod.*, 2019, **82**, 2337–2342.
19 X. Hu, W. Sun, S. Li, L. Li, L. Yu, H. Liu, X. You, B. Jiang and L. Wu, *J. Antibiot.*, 2020, **73**, 812–817.
20 L.-L. Liu, Y. Xu, Z. Han, Y.-X. Li, L. Lu, P.-Y. Lai, J.-L. Zhong, X.-R. Guo, X.-X. Zhang and P.-Y. Qian, *Mar. Drugs*, 2012, **10**, 2571–2573.
21 M. Chu, I. Truumees, R. Mierzwa, J. Terracciano, M. Patel, P. R. Das, M. S. Puar and T.-M. Chan, *Tetrahedron Lett.*, 1998, **39**, 7649–7652.
22 Y. Terui, C. Yiwen, L. Jun-ying, T. Ando, H. Yamamoto, Y. Kawamura, Y. Tomishima, S. Uchida, T. Okazaki, E. Munetomo, T. Seki, K. Yamamoto, S. Murakami and A. Kawashima, *Tetrahedron Lett.*, 2003, **44**, 5427–5430.
23 F. Annang, I. Pérez-Victoria, G. Pérez-Moreno, E. Domingo, I. González, J. R. Tormo, J. Martín, L. M. Ruiz-Pérez, O. Genilloud, D. González-Pacanowska, F. Vicente and F. Reyes, *J. Nat. Prod.*, 2018, **81**, 1687–1691.
24 Y. Koyanagi, T. Kawahara, Y. Hitora and S. Tsukamoto, *Heterocycles*, 2020, **100**, 1686–1693.
25 K. Leetanasaksakul, W. Koomsiri, T. Suga, H. Matsuo, R. Hokari, P. Wattana-Amorn, Y. k. Takahashi, K. Shiomi, T. Nakashima, Y. Inahashi and A. Thamchaipenet, *J. Nat. Prod.*, 2022, **85**, 1211–1217.
26 H. S. Kang and S. F. Brady, *ACS Chem. Biol.*, 2014, **9**, 1267–1272.
27 S. Kunimoto, T. Someno, Y. Yamazaki, J. Lu, H. Esumi and H. Naganawa, *J. Antibiot.*, 2003, **56**, 1012–1017.

 This journal is © The Royal Society of Chemistry 2022

Published on 09 September 2022. Downloaded by Shanghai Jiaotong University on 10/24/2022 5:38:16 AM.

28 T. Someno, S. Kunimoto, H. Nakamura, H. Naganawa and D. Ikeda, *J. Antibiot.*, 2005, **58**, 56–60.
29 G. T. Carter, J. A. Nietsche, D. R. Williams and D. B. Borders, *J. Antibiot.*, 1990, **43**, 504–512.
30 L. Huo, J. J. Hug, C. Fu, X. Bian, Y. Zhang and R. Müller, *Nat. Prod. Rep.*, 2019, **36**, 1412–1436.
31 S. Wu, T. Huang, D. Xie, J. Wo, X. Wang, Z. Deng and S. Lin, *J. Antibiot.*, 2017, **70**, 90–95.
32 R. Cooper, I. Truumees, I. Gunnarsson, D. Loebenberg, A. Horan, J. Marquez, M. Patel, V. Gullo, M. Puar, P. Das and S. Mittelman, *J. Antibiot.*, 1992, **45**, 444–453.
33 A. Hornung, M. Bertazzo, A. Dziarnowski, K. Schneider, K. Welzel, S.-E. Wohlert, M. Holzenkämpfer, G. J. Nicholson, A. Bechthold, R. D. Süssmuth, A. Vente and S. Pelzer, *ChemBioChem*, 2007, **8**, 757–766.
34 T. M. Lee, G. T. Carter and D. B. Borders, *J. Chem. Soc., Chem. Commun.*, 1989, 1771–1772.
35 K. Kobayashi, C. Nishino, J. Ohya, S. Sato, T. Mikawa, Y. Shiobara and M. Kodama, *J. Antibiot.*, 1988, **41**, 502–511.
36 K. Kobayashi, C. Nishino, J. Ohya, S. Sato, T. Mikawa, Y. Shiobara and M. Kodama, *J. Antibiot.*, 1988, **41**, 741–750.
37 A. J. Peoples, Q. B. Zhang, W. P. Millett, M. T. Rothfeder, B. C. Pescatore, A. A. Madden, a. L. L. Ling and C. M. Moore, *J. Antibiot.*, 2008, **61**, 457–463.
38 L. Malet-Cascón, F. Romero, F. Espliego-Vázquez, D. Grávalos and J. L. Fernández-Puentes, *J. Antibiot.*, 2003, **56**, 219–225.
39 K. Ojiri, H. Nishioka, K. Torigoe, S. Nakajima, K. Kawamura and H. Suda, *Jpn. Kokai Tokkyo Koho*, 1995, **JP 07**(258, 93.
40 K. Herbert, H. W. Fehlhaber, C. M. Mather, D. J. Upadhyay, L. E. L. Coutinho, B. N. Ganguli and J. Blumbach, *Eur. Pat. Appl.*, 1992, **EP 512**, 522.
41 K. Chen, T. Xie, Y. Shen, H. He, X. Zhao and S. Gao, *Org. Lett.*, 2021, **23**, 1769–1774.
42 F. Zhang, M. Zhao, D. R. Braun, S. S. Ericksen, J. S. Piotrowski, J. Nelson, J. Peng, G. E. Ananiev, S. Chanana, K. Barns, J. Fossen, H. Sanchez, M. G. Chevrette, I. A. Guzei, C. Zhao, L. Guo, W. Tang, C. R. Currie, S. R. Rajski, A. Audhya, D. R. Andes and T. S. Bugni, *Science*, 2020, **370**, 974–978.
43 T. Bunyapaiboonsri, S. Yoiprommarat, C. Suriyachadkun, S. Supothina, R. Chanthaket, C. Chutrakul and V. Vichai, *Tetrahedron Lett.*, 2017, **58**, 3223–3225.
44 A. I. Gurevich, M. G. Karapetyan, M. N. Kolosov, V. N. Omelchenko, V. V. Onoprienko, G. I. Petrenko and S. A. Popravko, *Tetrahedron Lett.*, 1972, **13**, 1751–1754.
45 A. I. Gurevich, T. I. Deshko, G. A. Kogan, M. N. Kolosov, V. V. Kudryashova and V. V. Onoprienko, *Tetrahedron Lett.*, 1974, **15**, 2801–2804.
46 T. Bunyapaiboonsri, S. Lapanun, S. Supothina, P. Rachtawee, S. Chunhametha, C. Suriyachadkun, T. Boonruangprapa, P. Auncharoen, C. Chutrakul and V. Vichai, *Tetrahedron*, 2016, **72**, 775–778.
47 W. Ye, W. She, H. H. Y. Sung, P. Qian and I. D. Williams, *Acta Crystallogr., Sect. C: Struct. Chem.*, 2020, **76**, 1100–1107.
48 M. Chu, I. Truumees, R. Mierzwa, J. Terracciano, M. Patel, D. Loebenberg, J. J. Kaminski, P. Das and M. S. Puar, *J. Nat. Prod.*, 1997, **60**, 525–528.
49 H. Drautz, W. Keller-Schierlein and H. Zähner, *Arch. Microbiol.*, 1975, **106**, 175–190.
50 M. Dobler and W. Keller-Schierlein, *Helv. Chim. Acta*, 1977, **60**, 178–185.
51 H. Zähner, H. Drautz, W. Keller, *US Pat.*, US 4, 277, 478, 1981.
52 P. Lopez, A. Hornung, K. Welzel, C. Unsin, W. Wohlleben, T. Weber and S. Pelzer, *Gene*, 2010, **461**, 5–14.
53 G. A. Kogan, T. N. Deshko, A. I. Gurevich, V. V. Onoprienko and M. N. Kolosov, *J. Struct. Chem.*, 1975, **15**, 700–704.
54 Z. H. Zhao, J. Y. Li, X. Y. Yang and Y. W. Chu, *Chin. J. Antibiot.*, 2003, **28**, 627–632.
55 D. C. Hopp, D. J. Milanowski, J. Rhea, D. Jacobsen, J. Rabenstein, C. Smith, K. Romari, M. Clarke, L. Francis, M. Irigoyen, M. Luche, G. J. Carr and U. Mocek, *J. Nat. Prod.*, 2008, **71**, 2032–2035.
56 A. J. Peoples, Q. Zhang, W. P. Millett, M. T. Rothfeder, B. C. Pescatore, A. A. Madden, L. L. Ling and C. M. Moore, *J. Antibiot.*, 2008, **61**, 457–463.
57 J. C. Rodríguez, J. L. Fernández Puentes, J. P. Baz and L. M. Cañedo, *J. Antibiot.*, 2003, **56**, 318–321.
58 T. Eguchi, K. Kondo, K. Kakinuma, H. Uekusa, Y. Ohashi, K. Mizoue and Y.-F. Qiao, *J. Org. Chem.*, 1999, **64**, 5371–5376.
59 D. Xu, E. Tian, F. Kong and K. Hong, *Mar. Drugs*, 2020, **18**(255.
60 X. Zhang and S. Li, *Nat. Prod. Rep.*, 2017, **34**, 1061–1089.
61 H.-S. Kang and S. F. Brady, *J. Am. Chem. Soc.*, 2014, **136**, 18111–18119.
62 W. She, W. Ye, A. Cheng, X. Liu, J. Tang, Y. Lan, F. Chen and P. Y. Qian, *Front. Microbiol.*, 2021, **12**, 635268.
63 Y.-M. Chiang, M. Ahuja, C. E. Oakley, R. Entwistle, A. Asokan, C. Zutz, C. C. C. Wang and B. R. Oakley, *Angew. Chem., Int. Ed. Engl.*, 2016, **55**, 1662–1665.
64 Z. Hu, Y. Ye and Y. Zhang, *Nat. Prod. Rep.*, 2021, **38**, 1775–1793.
65 T. R. Kelly, C. T. Jagoe and Q. Li, *J. Am. Chem. Soc.*, 1989, **111**, 4522–4524.
66 K. Christoph, R. Ulrich, S. Frank, L. Ernest, G. J. Helen and H. Kirstin, *PCT Int. Appl.*, 2001, **WO 01**, 95909.
67 W. M. Maiese, J. Korshalla, J. Goodman, M. J. Torrey, S. Kantor, D. P. Labeda and M. Greenstein, *J. Antibiot.*, 1990, **43**, 1059–1063.
68 H. Ui, A. Ishiyama, H. Sekiguchi, M. Namatame, A. Nishihara, Y. Takahashi, K. Shiomi, K. Otoguro and S. Omura, *J. Antibiot.*, 2007, **60**, 220–222.
69 A. L. Nichols, P. Zhang and S. F. Martin, *Tetrahedron*, 2012, **68**, 7591–7597.
70 L.-L. Liu, L.-S. He, Y. Xu, Z. Han, Y.-X. Li, J.-L. Zhong, X.-R. Guo, X.-X. Zhang, K. M. Ko and P.-Y. Qian, *Chem. Res. Toxicol.*, 2013, **26**, 1055–1063.
71 K. Izuishi, K. Kato, T. Ogura, T. Kinoshita and H. Esumi, *Cancer Res.*, 2000, **60**, 6201–6207.

Published on 09 September 2022. Downloaded by Shanghai Jiaotong University on 10/24/2022 5:38:16 AM.

72 H. Esumi, K. Izuishi, K. Kato, K. Hashimoto, Y. Kurashima, A. Kishimoto, T. Ogura and T. Ozawa, *J. Biol. Chem.*, 2002, **277**, 32791–32798.
73 I. Filipuzzi, S. Cotesta, F. Perruccio, B. Knapp, Y. Fu, C. Studer, V. Pries, R. Riedl, S. B. Helliwell, K. T. Petrovic, N. R. Movva, D. Sanglard, J. Tao and D. Hoepfner, *PLoS Genet.*, 2016, **12**, e1006374.
74 D. Ang, K. Liberek, D. Skowyra, M. Zylicz and C. Georgopoulos, *J. Biol. Chem.*, 1991, **266**, 24233–24236.
75 M. S. Razzaque and T. Taguchi, *Histol. Histopathol.*, 1999, **14**, 1199–1212.
76 P.-S. Bellaye, O. Burgy, P. Bonniaud and M. Kolb, *Expert Opin. Ther. Targets*, 2021, **25**, 49–62.
77 M. Sunamoto, K. Kuze, H. Tsuji, N. Ohishi, K. Yagi, K. Nagata, T. Kita and T. Doi, *Lab. Invest.*, 1998, **78**, 967–972.
78 E. Firouzi Niaki, T. Van Acker, L. Imre, P. Nánási Jr, S. Tarapcsák, Z. Bacsó, F. Vanhaecke and G. Szabó, *Sci. Rep.*, 2020, **10**, 1107.
79 G. J. Quigley, A. H. Wang, G. Ughetto, G. van der Marel, J. H. van Boom and A. Rich, *Proc. Natl. Acad. Sci. U. S. A.*, 1980, **77**, 7204–7208.
80 M. Arai, H. Sato, H. Kobayashi, M. Suganuma, T. Kawabe, H. Tomoda and S. Ōmura, *Biochem. Biophys. Res. Commun.*, 2004, **317**, 817–822.
81 A. Ishiyama, K. Otoguro, M. Namatame, A. Nishihara, T. Furusawa, Y. Takahashi, R. Masuma, K. Shiomi and S. Omura, *J. Antibiot.*, 2008, **61**, 254–257.
82 Y. Koizumi, H. Tomoda, A. Kumagai, X.-p. Zhou, S. Koyota and T. Sugiyama, *Cancer Sci.*, 2009, **100**, 322–326.
83 C. J. Sherr, *Cell*, 1994, **79**, 551–555.
84 Y. Fuchs and H. Steller, *Cell*, 2011, **147**, 742–758.
85 S. Elmore, *Toxicol. Pathol.*, 2007, **35**, 495–516.
86 S. H. Inayat-Hussain and D. Ross, *Chem. Res. Toxicol.*, 2005, **18**, 420–427.
87 D. Shinabarger, *Expert Opin. Invest. Drugs*, 1999, **8**, 1195–1202.
88 P. A. Turner, E. M. Griffin, J. L. Whatmore and M. Shipman, *Org. Lett.*, 2011, **13**, 1056–1059.
89 D. L. Sloman, B. Mitasev, S. S. Scully, J. A. Beutler and J. A. Porco, *Angew. Chem., Int. Ed. Engl.*, 2011, **50**, 2511–2515.
90 J. Rujirawanich, S. Kim, A.-J. Ma, J. R. Butler, Y. Wang, C. Wang, M. Rosen, B. Posner, D. Nijhawan and J. M. Ready, *J. Am. Chem. Soc.*, 2016, **138**, 10561–10570.
91 J. R. Butler, C. Wang, J. Bian and J. M. Ready, *J. Am. Chem. Soc.*, 2011, **133**, 9956–9959.
92 C. Hertweck, A. Luzhetskyy, Y. Rebets and A. Bechthold, *Nat. Prod. Rep.*, 2007, **24**, 162–190.
93 J. Jiang, C. N. Tetzlaff, S. Takamatsu, M. Iwatsuki, M. Komatsu, H. Ikeda and D. E. Cane, *Biochemistry*, 2009, **48**, 6431–6440.
94 M. C. Tang, H. Y. He, F. Zhang and G. L. Tang, *ACS Catal.*, 2013, **3**, 444–447.
95 J. Gubbens, H. Zhu, G. Girard, L. Song, B. I. Florea, P. Aston, K. Ichinose, D. V. Filippov, Y. H. Choi, H. S. Overkleeft, G. L. Challis and G. P. van Wezel, *Chem. Biol.*, 2014, **21**, 707–718.
96 N. M. Kamerbeek, D. B. Janssen, W. J. H. van Berkel and M. W. Fraaije, *Adv. Synth. Catal.*, 2003, **345**, 667–678.
97 G. J. ten Brink, I. W. C. E. Arends and R. A. Sheldon, *Chem. Rev.*, 2004, **104**, 4105–4124.
98 D. E. Torres Pazmiño, H. M. Dudek and M. W. Fraaije, *Curr. Opin. Chem. Biol.*, 2010, **14**, 138–144.
99 F. Kudo, T. Yonezawa, A. Komatsubara, K. Mizoue and T. Eguchi, *J. Antibiot.*, 2011, **64**, 123–132.
100 W. Zhang, B. D. Ames, S. C. Tsai and Y. Tang, *Appl. Environ. Microbiol.*, 2006, **72**, 2573–2580.
101 Y. Chen, E. Wendt-Pienkowski, J. Ju, S. Lin, S. R. Rajski and B. Shen, *J. Biol. Chem.*, 2010, **285**, 38853–38860.
102 W. Bauer and M. H. Zenk, *Phytochemistry*, 1991, **30**, 2953–2961.
103 M. Rueffer and M. H. Zenk, *Phytochemistry*, 1994, **36**, 1219–1223.
104 S. Clemens and W. Barz, *Phytochemistry*, 1996, **41**, 457–460.
105 N. Ikezawa, M. Tanaka, M. Nagayoshi, R. Shinkyo, T. Sakaki, K. Inouye and F. Sato, *J. Biol. Chem.*, 2003, **278**, 38557–38565.
106 E. Ono, M. Nakai, Y. Fukui., N. Tomimori, M. Fukuchimizutani, M. Saito, H. Satake., T. Tanaka., M. Katsuta., T. Umezawa and Y. Tanaka, *Proc. Natl. Acad. Sci. U. S. A.*, 2006, **103**, 10116–10121.
107 N. Ikezawa, K. Iwasa and F. Sato, *FEBS J.*, 2007, **274**, 1019–1035.
108 A. Das and C. Khosla, *Acc. Chem. Res.*, 2009, **42**, 631–639.
109 M. Daum, I. Peintner, A. Linnenbrink, A. Frerich, M. Weber, T. Paululat and A. Bechthold, *ChemBioChem*, 2009, **10**, 1073–1083.
110 M. S. Abdelfattah and R. Jürgen, *Angew. Chem., Int. Ed. Engl.*, 2006, **45**, 5685–5689.
111 Z. Yunt, K. Reinhardt, A. Li, M. Engeser, H.-M. Dahse, M. Gütschow, T. Bruhn, G. Bringmann and J. Piel, *J. Am. Chem. Soc.*, 2009, **131**, 2297–2305.
112 E. R. Rafanan, C. R. Hutchinson and B. Shen, *Org. Lett.*, 2000, **2**, 3225–3227.
113 W. Zhang, L. Wang, L. Kong, T. Wang, Y. Chu, Z. Deng and D. You, *Chem. Biol.*, 2012, **19**, 422–432.
114 Z. Feng, D. Kallifidas and S. F. Brady, *Proc. Natl. Acad. Sci. U. S. A.*, 2011, **108**, 12629–12634.
115 T. R. Valentic, D. R. Jackson, S. F. Brady and S.-C. Tsai, *ACS Chem. Biol.*, 2016, **11**, 3421–3430.
116 E. J. Culp, G. Yim, N. Waglechner, W. Wang, A. C. Pawlowski and G. D. Wright, *Nat. Biotechnol.*, 2019, **37**, 1149–1154.
117 M. Gibson, M. Nur-e-alam., F. Lipata, M. A. Oliveira and J. Rohr, *J. Am. Chem. Soc.*, 2005, **127**, 17594–17595.
118 H. Leisch, K. Morley and P. C. K. Lau, *Chem. Rev.*, 2011, **111**, 4165–4222.
119 R. J. Klose, E. M. Kallin and Y. Zhang, *Nat. Rev. Genet.*, 2006, **7**, 715–727.
120 W. Jiang, M. A. Wilson and D. P. Weeks, *ACS Chem. Biol.*, 2013, **8**, 1687–1691.
121 M. P. Beam, M. A. Bosserman, N. Noinaj, M. Wehenkel and J. Rohr, *Biochemistry*, 2009, **48**, 4476–4487.

 This journal is © The Royal Society of Chemistry 2022

Published on 09 September 2022. Downloaded by Shanghai Jiaotong University on 10/24/2022 5:38:16 AM.

122 Y. Hu, D. Dietrich, W. Xu, A. Patel, J. A. Justin, J. Wang, W.-B. Yin, K. Qiao, K. N. Houk, J. C. Vederas and Y. Tang, *Nat. Chem. Biol.*, 2014, **10**, 552–554.
123 K. M. Henry and C. A. Townsend, *J. Am. Chem. Soc.*, 2005, **127**, 3724–3733.
124 W. F. Bailey and M.-J. Shih, *J. Am. Chem. Soc.*, 1982, **104**, 1769–1771.
125 H. Suginome and S. Yamada, *Tetrahedron Lett.*, 1984, **25**, 3995–3998.
126 W. F. Bailey and J. J. Bischoff, *J. Org. Chem.*, 1985, **50**, 3009–3010.
127 H. Suginome and S. Yamada, *Bull. Chem. Soc. Jpn.*, 1985, **58**, 3055–3056.
128 L. Kong, Q. Wang, W. Yang, J. Shen, Y. Li, X. Zheng, L. Wang, Y. Chu, Z. Deng, Y. H. Chooi and D. You, *ACS Chem. Biol.*, 2020, **15**, 2107–2115.
129 Y. Anzai, S.-i. Tsukada, A. Sakai, R. Masuda, C. Harada, A. Domeki, S. Li, K. Kinoshita, D. H. Sherman and F. Kato, *Antimicrob. Agents Chemother.*, 2012, **56**, 3648–3656.
130 G. Zocher, M. E. A. Richter, U. Mueller and C. Hertweck, *J. Am. Chem. Soc.*, 2011, **133**, 2292–2302.
131 J. C. Carlson, S. Li, S. S. Gunatilleke, Y. Anzai, D. A. Burr, L. M. Podust and D. H. Sherman, *Nat. Chem.*, 2011, **3**, 628–633.
132 A. Miyanaga, R. Takayanagi, T. Furuya, A. Kawamata, T. Itagaki, Y. Iwabuchi, N. Kanoh, F. Kudo and T. Eguchi, *ChemBioChem*, 2017, **18**, 2179–2187.
133 S. Li, J. Guo, A. Reva, F. Huang, B. Xiong, Y. Liu, Z. Deng, P. F. Leadlay and Y. Sun, *Proc. Natl. Acad. Sci. U. S. A.*, 2018, **115**, 1340–1345.
134 H. J. Kim, J. A. White-Phillip, Y. Ogasawara, N. Shin, E. A. Isiorho and H. W. Liu, *J. Am. Chem. Soc.*, 2010, **132**, 2901–2903.
135 J. Näsvall, L. Sun, J. R. Roth and D. I. Andersson, *Science*, 2012, **338**, 384–387.
136 U. Bergthorsson, D. I. Andersson and J. R. Roth, *Proc. Natl. Acad. Sci. U. S. A.*, 2007, **104**, 17004–17009.
137 J. Latham, E. Brandenburger, S. A. Shepherd, B. R. K. Menon and J. Micklefield, *Chem. Rev.*, 2018, **118**, 232–269.
138 A. H. P. S. Mori, T. N. Chandrika, S. Garneau-Tsodikova and O. V. Tsodikov, *Nat. Commun.*, 2019, **10**, 1–11.
139 S. A. Shepherd, C. Karthikeyan, J. Latham, A.-W. Struck, M. L. Thompson, B. R. K. Menon, M. Q. Styles, C. Levy, D. Leys and J. Micklefield, *Chem. Sci.*, 2015, **6**, 3454–3460.
140 A. Lang, S. Polnick, T. Nicke, P. William, E. P. Patallo, J. H. Naismith and K.-H. van Pée, *Angew. Chem., Int. Ed. Engl.*, 2011, **50**, 2951–2953.
141 X. Wei and Y. Matsuda, *Org. Lett.*, 2020, **22**, 1919–1923.
142 M. A. Schätzle, S. M. Husain, S. Ferlaino and M. Müller, *J. Am. Chem. Soc.*, 2012, **134**, 14742–14745.
143 Y. Matsuda, C. H. Gotfredsen and T. O. Larsen, *Org. Lett.*, 2018, **20**, 7197–7200.
144 J. F. Sanchez, R. Entwistle, J.-H. Hung, J. Yaegashi, S. Jain, Y.-M. Chiang, C. C. C. Wang and B. R. Oakley, *J. Am. Chem. Soc.*, 2011, **133**, 4010–4017.
145 C. Greco, K. de Mattos-Shipley, A. M. Bailey, N. P. Mulholland, J. L. Vincent, C. L. Willis, R. J. Cox and T. J. Simpson, *Chem. Sci.*, 2019, **10**, 2930–2939.
146 A. J. Szwalbe, K. Williams, Z. Song, K. de Mattos-Shipley, J. L. Vincent, A. M. Bailey, C. L. Willis, R. J. Cox and T. J. Simpson, *Chem. Sci.*, 2018, **10**, 233–238.
147 S.-W. Yuan, S.-H. Chen, H. Guo, L.-T. Chen, H.-J. Shen, L. Liu and Z.-Z. Gao, *Org. Lett.*, 2022, **24**, 3069–3074.
148 F. Qi, W. Zhang, Y. Xue, C. Geng, X. Huang, J. Sun and X. Lu, *J. Am. Chem. Soc.*, 2021, **143**, 16326–16331.
149 C. Songsiriritthigul, N. Nualkaew, J. Ketudat-Cairns and C. J. Chen, *Acta Crystallogr., Sect. F: Struct. Biol. Commun.*, 2020, **76**, 597–603.
150 I. El-Awaad, M. Bocola, T. Beuerle, B. Liu and L. Beerhues, *Nat. Commun.*, 2016, **7**, 11472.
151 G. M. Kitanov and P. T. Nedialkov, *Phytochemistry*, 2001, **57**, 1237–1243.
152 A. J. Waldman, T. L. Ng, P. Wang and E. P. Balskus, *Chem. Rev.*, 2017, **117**, 5784–5863.
153 G. Sun, C. Hu, Q. Mei, M. Luo, X. Chen, Z. Li, Y. Liu, Z. Deng, Z. Zhang and Y. Sun, *Nat. Commun.*, 2020, **11**, 4501.
154 D. L. Sloman, J. W. Bacon and J. A. Porco, *J. Am. Chem. Soc.*, 2011, **133**, 9952–9955.
155 D. K. Winter, M. A. Endoma-Arias, T. Hudlicky, J. A. Beutler and J. A. Porco, *J. Org. Chem.*, 2013, **78**, 7617–7626.
156 Y. Dai, F. Ma, Y. Shen, T. Xie and S. Gao, *Org. Lett.*, 2018, **20**, 2872–2875.
157 D. Knueppel, J. Yang, B. Cheng, D. Mans and S. F. Martin, *Tetrahedron*, 2015, **71**, 5741–5757.
158 J. Yang, D. Knueppel, B. Cheng, D. Mans and S. F. Martin, *Org. Lett.*, 2015, **17**, 114–117.
159 R. Masuo, K. Ohmori, L. Hintermann, S. Yoshida and K. Suzuki, *Angew. Chem., Int. Ed. Engl.*, 2009, **48**, 3462–3465.
160 Y. Wang, C. Wang, J. R. Butler and J. M. Ready, *Angew. Chem., Int. Ed. Engl.*, 2013, **52**, 10796–10799.
161 A.-J. Ma and J. M. Ready, *Org. Lett.*, 2019, **21**, 1148–1151.
162 T. Xie, C. Zheng, K. Chen, H. He and S. Gao, *Angew. Chem., Int. Ed. Engl.*, 2020, **59**, 4360–4364.
163 S. Blumberg and S. F. Martin, *Org. Lett.*, 2017, **19**, 790–793.
164 B. Zakeri and T. K. Lu, *ACS Synth. Biol.*, 2013, **2**, 358–372.
165 F. Hemmerling and J. Piel, *Nat. Rev. Drug Discovery*, 2022, **21**, 359–378.
166 G. C. A. Amos, T. Awakawa, R. N. Tuttle, A.-C. Letzel, M. C. Kim, Y. Kudo, W. Fenical, B. Moore and P. R. Jensen, *Proc. Natl. Acad. Sci. U. S. A.*, 2017, **114**, E11121–E11130.
167 L. K. Caesar, R. Montaser, N. P. Keller and N. L. Kelleher, *Nat. Prod. Rep.*, 2021, **38**, 2041–2065.